Disentangling *Arctica islandica's* environmental archive

Ecological drivers of its feeding behaviour and growth

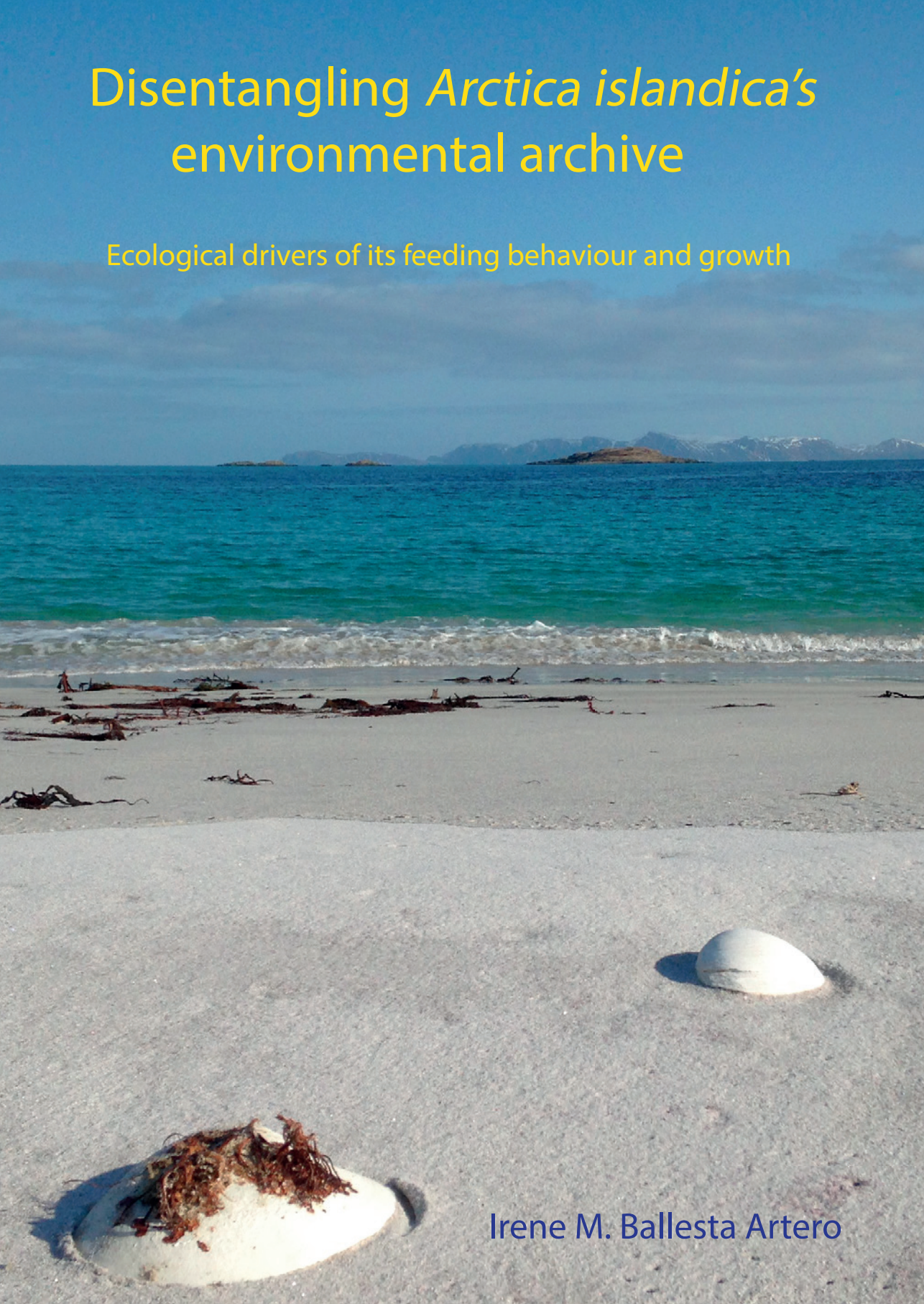

Irene M. Ballesta Artero

Disentangling *Arctica islandica*'s environmental archive

Ecological drivers of its feeding behavior and growth

The research presented in this thesis was conducted at the Department of Coastal Systems at the NIOZ Royal Netherlands Institute for Sea Research,'t Hornje (Texel), The Netherlands, according to the requirements of the Faculty of Science (Animal Ecology, Free University of Amsterdam).

This work was funded by the EU within the framework (FP7) of the Marie Curie International Training Network ARAMACC "Annually Resolved Archives of MArine Climate Change" (grant number: 604802). The printing was supported by NIOZ.

The preferred citation for this thesis is:
Ballesta-Artero, I.M. 2018. Disentangling *Arctica islandica*'s environmental archive: Ecological drivers of its feeding behavior and growth. PhD thesis, VU University Amsterdam, The Netherlands.

Layout: I.M. Ballesta Artero
Cover design: I.M. Ballesta Artero (Sanden Bay and Ingøya map)
Photographs: pages 6, 31, 77, 133, 159, 203, Irene Ballesta Artero; 11, 17 Madelyn Mette; 105, Dan Frost; 189, Randall Hyman; 199, Alan Wanamaker.
Printed by: Ipskamp Printing.
ISBN: 978-94-028-1159-9

© I.M. Ballesta Artero (ballestartero@gmail.com)

VRIJE UNIVERSITEIT

Disentangling *Arctica islandica's* environmental archive

Ecological drivers of its feeding behavior and growth

ACADEMISCH PROEFSCHRIFT

ter verkrijging van de graad Doctor aan

de Vrije Unversiteit Amsterdam,

op gezag van de rector magnificus

prof.dr. V. Subramaniam,

in het openbaar te verdedigen

ten overstaan van de promotiecommissie

van de Faculteit der Bètawetenschappen

op maandag 15 oktober 2018 om 9.45 uur

in het auditorium van de universiteit,

De Boelelaan 1105

door

Irene María Ballesta Artero

geboren te Huércal-Overa, Spanje

promotor: prof.dr. J.van der Meer

copromotor: dr. R. Witbaard

Contents

Summary

In these times of global and fast climate change, there is a need to further develop the research field of sclerochronology. This relatively new discipline uses the annual banding in the shells of long-lived mollusks to develop long timelines or chronologies. These chronologies can be coupled with local environmental records, in the same way as growth rings of trees are used in dendrochronology (Jones, 1980; Witbaard et al., 1994; Karney et al., 2011). As such they provide insight into past and present ocean climatic conditions (Schöne et al., 2003; Witbaard et al., 2003; Butler et al., 2013; Mette et al., 2016). Continuous long-term (>50 years) instrumental records of environmental conditions are sparse in the marine environment. Thus, proxy-based environmental reconstructions are needed to improve regional and temporal coverage and to understand past marine climate variability (Jones et al. 2009; Wanamaker et al., 2011; Mette et al., 2016; Steinhardt et al., 2016).

The boreal species *Arctica islandica* (Mollusca, Bivalvia) is an example of a great marine bioarchive due to its wide distribution and extreme long-life (up to five centuries). This species' shell presents annual growth increments (or growth bands) which provides dated environmental information by way of variable growth increments, and microstructural and geochemical properties. However, the duration, timing, and main environmental forces regulating *A. islandica*'s growing season still needed further study. The combined role of temperature and food in regulating activity patterns and shell growth of this bivalve had to be disentangled.

Chapter 1 of this thesis describes the main characteristics of the species and the aim of my research. Chapter 2 reports about a fieldwork *in situ* experiment where we discovered that *A. islandica* gaping activity in northern Norway has an eight months long active season in which valve movements are mainly regulated by food availability. Active gaping periods appear to coincide with periods of growth, indicating that *A. islandica* records their environment when its valves are open.

A series of food and temperature experiments (Chapter 3 and Chapter 4), where the microstructural properties of *A. islandica* shells were studied, showed that temperature, but not food, induced a change in the crystallographic orientation of the biomineral units, indicating that this microstructural property may be a potential proxy for seawater temperature. This change in crystallographic orientation was only detected by confocal Raman microscopy (CRM), not by scanning electron microscopy (SEM).

Chapter 4 explores the combined effects of temperature and food availability on the shell and tissue growth of *A. islandica* under laboratory conditions. It appeared that the concentration of algal food is

the main factor driving siphon activity and with that shell and tissue growth. Thus, these experimental outcomes support the results from Chapter 2, where *in situ* gaping activity was most closely correlated with the concentration of chlorophyll-a and to a lesser degree with the seawater temperature.

We used a subsample of specimens from above laboratory growth experiment (Chapter 4) to study the role of environmental and biological controls on trace elemental incorporation of *A. islandica* shells (Chapter 5). We found that all trace element-to-calcium ratios (Mg, Sr, Na, and Ba) were significantly affected by growth rate. This indicates that physiological processes seem to dominate the controls of element incorporation into *A. islandica* shells.

Chapter 6 describes the energy use of *A. islandica* based on a Dynamic Energy Budget model. Our results indicate that *A. islandica*'s extreme longevity arises from its low somatic maintenance cost $[\dot{p}_M]$ and low ageing acceleration $\ddot{h}_a$. We could not find a direct relationship between food availability and lifespan (theory of caloric restriction) in the eight North Atlantic populations studied. Nevertheless, food estimates based on the DEB's scaled functional response can be a good food indicator, sometimes the only one, of the benthic food conditions at *A. islandica* localities.

The main conclusions of this thesis are that (1) *A. islandica* gaping and growing season seems to be limited to 8 months of the year, and that food availability and not temperature is the main driver of this gaping and growth behavior, (2) some microstructural and geochemical properties of *A. islandica* shell contain environmental information, but further study still need to be done to use them as a reliable environmental proxy, and (3) the extreme longevity of the species is due to its low somatic maintenance cost and low accumulation of waste that provokes ageing.

Resumen

Para entender mejor el cambio climático a nivel global, es necesario seguir desarrollando campos de investigación como la esclerocronología. Esta disciplina, relativamente nueva, utiliza las bandas anuales presentes en las valvas o conchas de moluscos de gran longevidad para desarrollar cronologías. Cronologías que se enlazan con registros ambientales locales, de la misma manera que los anillos de crecimiento de los árboles se utilizan en dendrocronología (Jones, 1980; Witbaard et al, 1994; Karney et al., 2011), para proporcionar información sobre las condiciones climáticas pasadas y presentes del océano (Schöne et al., 2003; Witbaard et al., 2003; Butler et al., 2013; Mette et al., 2016). Ya que los registros instrumentales continuos de las condiciones ambientales son escasos en el entorno marino, sobre todo por periodos largos de tiempo (> 50 años), se necesitan reconstrucciones ambientales basadas en proxis (indicadores indirectos) que mejoren la cobertura regional y temporal, y hagan entender la variabilidad del clima marino (Jones et al., 2009; Wanamaker et al., 2011; Mette et al., 2016; Steinhardt et al., 2016).

La especie boreal *Arctica islandica* (Mollusca, Bivalvia) es un ejemplo de gran bio-archivo marino debido a su amplia distribución y extrema longevidad (hasta cinco siglos). La concha de esta especie presenta incrementos anuales de crecimiento (o bandas de crecimiento) que proporcionan información ambiental datada a través de variables tasas de crecimiento y propiedades micro-estructurales y geoquímicas. Sin embargo, la longevidad, el periodo y las principales fuerzas ambientales que regulan la temporada de crecimiento de *A. islandica* necesitaban seguir investigándose. El papel combinado de la temperatura y la alimentación en la regulación de los patrones de actividad y crecimiento de este bivalvo aún no se han esclarecido, y algunos pretenden ser explicados en esta tesis.

El Capítulo 1 describe las principales características de la especie y el objetivo de mi investigación. El Capítulo 2 informa sobre un experimento de campo *in situ* donde descubrimos que la actividad de apertura de las valvas de *A. islandica* en el norte de Noruega tiene una temporada activa de ocho meses, en la cual sus movimientos están regulados principalmente por la disponibilidad de alimento. Este movimiento parece coincidir con el crecimiento de estas, lo que indica que *A. islandica* registra su entorno cuando sus valvas están abiertas.

Una serie de experimentos con diversas temperaturas y fuentes de alimento (Capítulo 3 y Capítulo 4), donde se estudiaron las propiedades microestructurales de la concha de *A. islandica*, mostró que la temperatura, no el alimento, induce un cambio en la orientación cristalográfica de las unidades biominerales, indicando que esta propiedad microestructural puede ser un proxy potencial para la

temperatura marina. Pese a haber utilizado también microscopía electrónica de barrido (SEM) para el análisis, este cambio en la orientación cristalográfica solo se detectó a través de espectroscopía Raman (CRM).

El Capítulo 4 explora los efectos combinados de la temperatura y el alimento en el crecimiento del tejido y la concha de *A. islándica* en condiciones de laboratorio. Parece que la concentración de fitoplancton es el factor principal que impulsa la actividad de los sifones y en consecuencia, el crecimiento del tejido y de la concha. Por lo tanto, estos resultados experimentales respaldan los resultados del Capítulo 2, donde la actividad de apertura *in situ* se correlacionó estrechamente con la concentración de clorofila-a y en menor grado con la temperatura marina.

En el Capítulo 5, utilizamos una submuestra de especímenes del experimento anterior de crecimiento en laboratorio (Capítulo 4) para estudiar el papel del control ambiental y biológico en la incorporación de elementos traza en las conchas de *A. islandica*. Encontramos que todas las proporciones de elementos (Mg, Sr, Na y Ba) respecto al calcio se vieron significativamente afectadas por la tasa de crecimiento. Esto indica que los procesos fisiológicos contribuyen al control sobre la incorporación de estos elementos en la concha de *A. islandica*.

El Capítulo 6 describe el uso de energía de *A. islandica* basado en un modelo de balance energético dinámico, DEB (por sus siglas en inglés, Dynamic Energy Budget). Nuestros resultados indican que la extrema longevidad de *A. islandica* se debe a su bajo coste de mantenimiento $[\dot{p}_M]$ y baja aceleración de envejecimiento $\ddot{h}_a$. No pudimos encontrar una relación directa entre la disponibilidad de alimento y la esperanza de vida (teoría de la restricción calórica) en las ocho poblaciones estudiadas en el Atlántico Norte. Sin embargo, las estimaciones de alimento basadas en la respuesta funcional escalada del DEB pueden ser un buen indicador, a veces el único, de la disponibilidad de alimento en la zona bentónica donde se encuentre *A. islandica*.

Las principales conclusiones que se recogen esta tesis son: (1) la apertura de *A. islandica* y su temporada de crecimiento parecen estar limitadas a ocho meses del año, y están impulsadas por la disponibilidad de alimento y no por la temperatura, (2) algunas propiedades microestructurales y geoquímicas de la concha de *A. islandica* contienen información ambiental, pero aún se necesitan estudios adicionales para utilizarlas como un proxy ambiental confiable, y (3) la extrema longevidad de la especie se debe a su bajo coste de mantenimiento somático y a la baja acumulación de desechos que provocan el envejecimiento.

Chapter 1

Introduction

Sclerochronology, *Arctica islandica*, and the ARAMACC project

The research field called "Sclerochronology" is a relatively new discipline that uses the annual banding in the shells of long-lived mollusks to develop long-timelines or chronologies. These chronologies can be coupled with local environmental records, in the same way as growth rings of trees are used in dendrochronology (Jones, 1980; Witbaard et al., 1994; Karney et al., 2011), and hence might provide insight into past and present ocean conditions (Schöne et al., 2003; Witbaard et al., 2003; Butler et al., 2013; Mette et al., 2016).

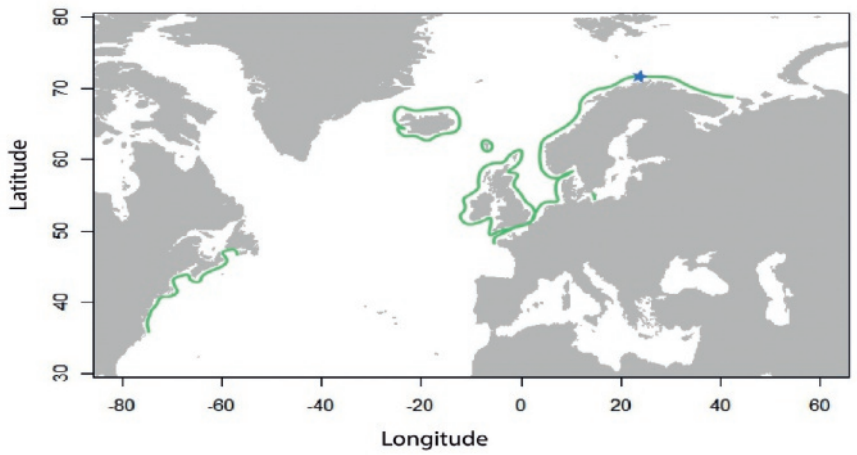

Fig. 1. 1: Actual distribution of *Arctica islandica* (green line). The blue star points out Ingøya, our fieldwork location in northern Norway.

The bivalve *Arctica islandica* (Mollusca, Bivalvia), also known as the ocean quahog, is one of the longest-living organisms on Earth, with a life span of up to five centuries (Wanamaker et al., 2008a; Butler et al., 2013). Due to its extreme long-life and wide distribution (Fig. 1.1), it is a perfect organism to be used as a bio-chronicle. *Arctica islandica* secretes annual shell growth increments (or growth bands) which provide basic biological information such as age and growth rate. Moreover, the width of these bands and the composition and structure of the shell material therein can reflect the environmental conditions when the carbonate was deposited.

It was not until the 1980's, that *A. islandica* shell growth increments were confirmed as annual (Ropes, 1984; Witbaard et al., 1994), and its development as a proxy species began.

From this moment onwards, the number of studies greatly increased (e.g. Schöne et al., 2003; Witbaard et al., 2003; Wanamaker et al., 2008a; Butler et al., 2013; Mette et al., 2016; Marali et al., 2017a, b; Wanamaker and Gillikin 2018). Nowadays, there are two main lines of investigation: a) the study of the cellular mechanisms which allow for its extreme longevity (Abele et al., 2008; Begum et al., 2009, 2010; Strahl et al., 2007, 2011), and b) the study of its shell properties as environmental proxies. This thesis mainly focuses on the second line of investigation (Chapter 2 - 5), but Chapter 6 also reports about the energetics of the species within a Dynamic Energy Budget (DEB) theory framework.

Even though the number of *A. islandica* studies considerably increased over the last decades, some of the underlying growth mechanisms of the species are still poorly understood. Diverse experiments have demonstrated the role of temperature and food on the shell and tissue growth of the species (Witbaard et al., 1997a; Hiebenthal et al., 2012, 2013), but the combined role of these two variables still need to be disentangled. Usually the assumption has been made that the specimens have a constant growth rate within the growth season. But in most environments, food supply is strongly pulsed. This means that energy supply and consumption, activity and metabolism, and potential growth rate are likely to vary over time.

This thesis attempts to clarify the effects of environmental factors on the feeding behavior, growth, and energetics of the species. Ingøya, an island from the Arctic region in Northern Norway (71° N, Fig. 1. 1), was chosen as the fieldwork location. This place has almost complete darkness from October to mid-February, and due to rapidly increasing light levels in spring, phytoplankton growth starts at the end of March when sea water temperatures are still at their coldest (Carroll et al., 2009; Chapter 2 and Box 8. A1). Therefore, the roles of these two environmental factors regulating activity patterns and shell growth can be disentangled most effectively. In this population near the biogeographical limit of the species, small variations in environmental conditions can have large impacts on physiological functions and performance. We complete our investigation on the effects of food and temperature with controlled laboratory experiments performed at NIOZ (Royal Netherlands Institute for Sea Research; Texel, the Netherlands).

This PhD research was part of the project ARAMACC (Annually Resolved Archives of Marine Climate Change 604802), an EU-funded international collaboration (Marie Curie Initial

Training Network) whose scientific goal was to use the shells of very long-lived mollusks as a record of environmental change over the past thousand years (www.aramacc.com). ARAMACC mainly concentrated its effort on the northeast Atlantic Ocean, although long-lived Mediterranean bivalve species as *Glycymeris glycymeris, Glycymeris pilosa,* and *Callista chione* were also studied as promising sclerochronological species (Peharda et al., 2016; Purroy et al., 2017, 2018; Featherstone et al., 2017). As a Marie Curie Initial Training Network, ARAMACC focused on training the next generation of specialist researchers in the field of sclerochronology. Ten PhD students, including me, were trained in specific aspects of this relative new science discipline. ARAMACC science aimed at developing a network of these shell-based chronologies in the northeast Atlantic Ocean, and at the same time to advance the applications of this kind of research in the fields of biology, climate modelling, proxy development, and environmental monitoring (see e.g., Steinhardt et al., 2016; Milano et al., 2017a, b; Zhao et al., 2017a, b, c; Pyrina et al., 2017; Ballesta-Artero et al., 2017, 2018; Featherstone et al., 2017; Bonitz et al., 2018; Purroy et al., 2017, 2018; Trofimova et al., 2018).

Outline of the chapters

The aim of this research was to link the biology of *Arctica islandica* (the animal as a whole) to the geochemical properties and microstructure of its shell. Most studies about *A. islandica* only focused on its shell growth lines and did not consider the animals as a living organism that interact with its environment. However, the relationship between the metabolism of this species and its growth in specific environmental conditions is key to better understand the information enclosed in its shell.

In Chapter 2, the population from Ingøya was firstly investigated during 20 months (February 2014 –September 2015). We simultaneously studied the gaping activity of up to 16 specimens and the local environmental conditions (temperature, salinity, chlorophyll-a, turbidity, and light), gaining insight into the environmental factors controlling the species' seasonal changes. Then, to identify the main factors driving *A. islandica* growth biology, various laboratory experiments were set up. First, *A. islandica* specimens were reared in a couple of experiments under three different dietary regimes and two different temperatures. We explored shell microstructure properties of these experimentally grown shells as potential proxies (Chapter 3). On basis of these first experiments, a multispecies-microalgae diet

appeared to be the best food to promote growth and was used to test the interactive effect of temperature and food availability on the growth of *A. islandica*. Chapter 4 reports the shell and tissue growth in a multi-factorial experiment with four food levels (no food, low, medium, and high) and three different temperatures (3, 8, 13 °C). In this experiment, observations on the opening state of the siphons were used as indication of feeding activities which links the results to *in situ* measured valve gape as reported in Chapter 2. A subset of these experimental animals was used to investigate the effect of environmental and biological factors on trace elemental incorporation and microstructural properties of *A. islandica* shells (Chapter 5). Finally, all relevant field and laboratory data were used to construct a Dynamic Energy Budget (DEB) model for *A. islandica* (Chapter 6). This model combined tissue and shell growth data of the species to understand the meaning of the observed growth line patterns in terms of environmental temperature and food supply.

Chapter 7 summarizes the general conclusions of above research. The knowledge gained from this thesis will contribute to the understanding of how *A. islandica* responds to environmental variability, and will thus provide insight into past North Atlantic climate (Witbaard et al., 2003; Wanamaker et al., 2008a; Mette et al., 2016).

Chapter 2

Environmental factors regulating gaping activity of the bivalve *Arctica islandica* in Northern Norway

Ballesta-Artero, Irene; Witbaard, Rob; Carroll, Michael L.; van der Meer, Jaap

Published in Marine biology 164(5): 116 (2017)

Abstract

Arctica islandica is the longest-living non-colonial animal known at present. It inhabits coastal waters in the North Atlantic and its annual shell increments are widely used for paleoclimatic reconstructions. There is no consensus, however, about the intra-annual timing of its feeding activity and growth. This research aims to identify the main environmental drivers of *A. islandica* valve gape in order to clarify the ambiguity surrounding its seasonal activity. A lander was deployed from February 2014 to September 2015 on the sea bottom at Ingøya, Norway (71° 03' N, 24° 05' E) containing living *A. islandica* specimens (70.17 ± 0.95 mm SE) in individual containers. Each individual was attached to an electrode unit that measured the distance between their valves (valve gape) every minute. Individuals were followed for various lengths of time, and in some cases replaced by smaller individuals (54.34 ± 0.63 mm SE). The lander was also equipped with instruments to simultaneously monitor temperature, salinity, [Chl-a], turbidity, and light. There was a significant difference in the average monthly valve gape (P-value < 0.01), with monthly means of 19–84 % of the total valve gape magnitude. The experimental population was largely inactive October–January, with an average daily gape < 23%. During this period the clams opened at high amplitude once or twice a month for 1–3 days. Seasonal cycles of sea water temperature and [Chl-a] were temporally offset from each other, with temperature lagging [Chl-a] by about 2 months. Multiple regression analyses showed that bivalve gaping activity was most closely correlated with variable [Chl-a], and to a much smaller degree with photoperiod and temperature.

Keywords

Benthic lander, ocean quahog, valve gape*, growing season, food availability,* seasonality

INTRODUCTION

The bivalve *Arctica islandica*, also known as the ocean quahog, inhabits coastal waters in the North Atlantic (Jones, 1980; Dahlgren et al., 2000). The species is the longest-living non-colonial animal yet known, with a longevity of > 500 years (Butler et al., 2013). As in other bivalves, a history of their growth is retained in their shells. Shell growth increments (or growth bands) can provide basic biological information on the species including age and growth rate. Moreover, the pattern of these bands and the composition of the shell material therein can reflect environmental conditions when the shell was deposited.

Annual synchronization of band widths among individuals in a population has been identified in numerous studies (Jones, 1980; Witbaard et al., 1997a; Butler et al., 2009; Mette et al., 2016), suggesting that synchronous shell growth is influenced by a common environmental signal (Marchitto et al., 2000; Schöne et al., 2003; Dunca et al., 2009; Marali and Schöne, 2015). Temperature alone does not always fully explain variations in growth performance (Witbaard, 1996). Food availability is considered important in explaining the various reports on its growing season (Witbaard, 1996; Schöne et al., 2003; Witbaard et al., 2003). In the Fladen Ground (North Sea), for instance, an eddy system led to the import and accumulation of organic matter into that area (Witbaard, 1996), and this hydrodynamic feature was identified as the factor responsible for the growth variation of *A. islandica* there.

Likewise, high synchrony in valve gape, i.e., the distance between a valve pair, has been observed in various bivalve species, also suggesting that a common external force with a periodicity similar to gaping drives the response (Thorin, 2000; Borcherding, 2006; Mat et al., 2012; García-March et al., 2016). Based on those studies, food, temperature, and light conditions are considered key drivers of valve activity. Earlier studies on *A. islandica* (Winter, 1969) and other bivalves (Higgins, 1980; Williams and Pilditch, 1997; Riisgård et al., 2006) identified the presence of Chl-a as the main driver for a sustained opening of their valves. Other studies, however, demonstrated that light conditions can directly trigger valve gape activity of species such as *Pinna nobilis* and *Hippopus hippopus* (García-March et al., 2008; Schwartzmann et al., 2011).

The confounded roles of temperature, light and food in regulating activity patterns and shell growth in *A. islandica* can be disentangled most effectively in populations occurring near

their biogeographical limits, where small variations in environmental conditions can have large impacts on physiological functions and performance. In the present study, we analyzed *A. islandica* gaping activity patterns in relation to key environmental factors in an Arctic region in Northern Norway. The light cycle at this latitude (71°N) exhibits extreme seasonal variations in light intensity and day length (Kaartvedt, 2008), and could have a major influence on the seasonal gaping activity *of A. islandica*.

Filter-feeding bivalves must open their valves and extend their siphons to filter water, to respire and feed. Thus, wide open valves indicate periods of feeding and respiration (Møhlenberg and Riisgård, 1979; Newell et al., 2001; Riisgård and Larsen, 2015). In contrast, the reduction of the opening distance or total closure of valves implies a retraction of the mantle edges and siphons, resulting in a reduction and eventually in a cessation of filtration (Møhlenberg and Riisgård, 1979; Riisgård and Larsen, 2015). Witbaard et al. (1997b) measured siphon activity in *A. islandica* juveniles as the number of times an individual had the mantle extended with open siphons. It was expressed as the percentage of the total number of observations per specimen and then they calculated an average of siphon activity for multiple individuals per treatment. Siphon activity varied from 12% in a treatment with no food to 76% in the highest food concentration. This study thus also demonstrated a positive relationship between high siphon activity and growth in all treatments (Witbaard et al., 1997b). These results suggest that valve opening and closing of *A. islandica* can be used as a proxy for active feeding and as an indicator of periods of potential growth.

Based on those earlier lab experiments (Møhlenberg and Riisgård, 1979; Witbaard et al., 1997b; Newell et al., 2001; Riisgård and Larsen, 2015), we designed an in situ experiment to link gaping activity to environmental factors. We set up a field study of *A. islandica* at its northern geographical limit (Dahlgren et al., 2000; Mette et al., 2016) to examine environmental regulation of shell gaping activity. Locally collected living individuals of *A. islandica* with an electrode array attached to their valves were deployed on the sea bottom for various lengths of time in the period February 2014–September 2015. Valve gaping activity was measured together with environmental conditions (temperature, salinity, [Chl-a], turbidity, and light) to provide insight into environmental factors controlling seasonal changes in *A. islandica*.

METHODS

Site description

The in situ experiment took place at a 10-m deep site in Sanden Bay (71° 03' N, 24° 05' E), on the east side of Ingøya (Finnmark, northern Norway; Fig. A1, Appendix A). Ingøya is located ~ 15 km northwest of the Norwegian mainland and 60 km west of North Cape. Sanden Bay is exposed to the open Barents Sea from the northeast but protected from the full oceanic swell by a series of islets at its mouth. The seafloor in the bay is a mosaic of rocky outcrops covered with kelp, intermixed with patches of shell sand and maerl-like soft sediments with a median grain size of 400 µm (silt < 1%). *Arctica islandica* densities of ~ 10 m^{-2} occur within these patches of soft sediments. This Sanden Bay population appears to be the northern most known (Dahlgren et al., 2000; Mette et al., 2016).

Ingøya is located ~ 480km north of the Arctic Circle, where there is almost complete darkness, October–mid-February. Due to rapidly increasing light levels in the spring, phytoplankton growth starts at the end of March when sea water temperatures are still at their coldest (Carroll et al. 2009). In temperate zones, temporal patterns of temperature and phytoplankton growth are usually strongly linked and distinguishing their impacts on activity or growth is not easy. However, in northern Norway, sea temperature lags primary productivity by ~ two months.

Lander description

For the in situ experiment, we used a benthic lander constructed at the Royal Netherlands Institute for Sea Research (Texel, Netherlands) (Fig. 2. 1). The lander weighs around ~ 150 kg, with lead-weighted legs to ensure stability on the sea bottom. It consists of a triangular aluminum frame (Al 50St) with sides of 1.6 m and height of 1 m. This structure was used as a platform for the various instruments. We used two valve gape monitors with 8 specimen cups each and an array of environmental sensors including a CT (conductivity and temperature sensor), a turbidity/fluorescence and a light sensor (Fig. 2. 1). The lander was placed on the seafloor by slowly lowering it with a line from the ship. A buoy marked the position for later retrieval.

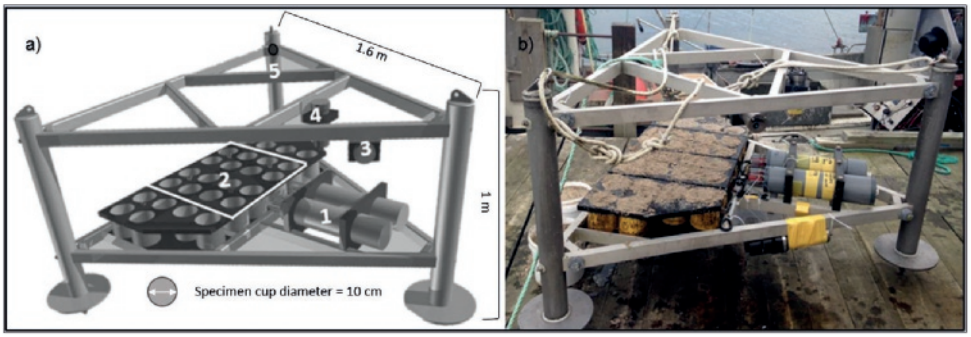

Fig. 2. 1: a) Benthic lander details (triangular aluminum frame): 1. Valve gape recorders, 2. Specimen cups: 16 for valve gape the experiment (within white rectangle), and 12 controls for future growth studies, 3. ALEC fluorimeter, 4. ALEC PAR sensor, 5. Conductivity and Temperature. b) Benthic lander before deployment.

Valve gape monitors

Two valve gape monitor control units were attached to the lower triangular part of the lander frame (Fig. 2. 1), 30 cm above the seafloor when deployed. Each valve gape monitor consists of a waterproof PVC housing with eight pairs of electro-coils coated by plastic tubing (1mH coils with self-extinguishing polyolefin sleeve; http://www.te.com/usa-en/home.html). The electro-coils are connected to an electronic circuit board with 0.6-mm coaxial cable. The electrical circuit board contains a 2-GB SD memory card to store the data. The system is powered by a 5-V battery pack.

Each valve gape monitor unit simultaneously records the valve gape, or distance between the two valves, of eight individual *A. islandica* specimens. Valve distance is defined as the space between the two paired valves at the siphon end. The distance is measured by the electro-coils based on electromagnetic theory. The electro-coils were glued on the siphon side of each valve with light-curing dental resin cement (3M ESPE RelyX Unicem 2Clicker).

Each clam was placed in an individual PVC cylinder, or specimen cup, filled with local sand. The specimen cups were 15 cm high with a diameter of 10 cm. The largest specimen had a shell height of 7.8 cm and length of 8.8 cm. Thus the specimens had enough space to maneuver in their cups and orient themselves. Each cup had a perforated bottom to allow

entry of the wires with coils from the PVC valve gape monitor housing. The wires were long enough to allow movement of the individuals within the cup.

The valve gape monitors were programmed so that once a minute the active coil generated an electromagnetic field which resulted in a current in the second responsive coil. The strength of the measured electromagnetic field (electrical signal) depends on the distance between the two coils and thus the distance between the valves (valve gape).

The raw electrical signal data were amplified and stored on the internal memory card for later conversion into a distance measurement. A calibration indicated that the distance between the two coils could be determined by the following linear relationship:

$$D_t \propto \sqrt{(\frac{1}{S_t})}$$

where D_t equals the distance in mm between the coils at time(t), and S_t is the electrical signal strength at time (t).

The coils could not be fixed to the shell at exactly the same distance from the valve edge or from each other in each specimen. To make the results comparable between individuals and periods, the measured distance was recalculated for each individual separately and expressed as a relative valve gape, hereafter called valve gape (G_t):

$$G_t = \frac{D_t - \min(D_t)}{\max(D_t) - \min(D_t)}$$

With this convention, (G_t) varies between 0 (fully closed) and 1 (fully open valves).

We made measurements over 592 d, February 2014–September 2015, excluding short periods of 1–3d when the lander was recovered for servicing (Table 2.1). A total of 21 individuals were monitored during four periods, including one for the entire time, ten for the first three periods, and seven for at least two consecutive periods. The resulting time series of valve gape data thus spanned 20 months with a maximum of 1440 data points day^{-1} specimen^{-1}.

Table 2. 1: Deployment periods with specimen identity number by channel. Asterisk* indicates the specimen that died (B665). B677–B684 (n=6) were the smaller replacements collected later in the experimental period (Fig. A1.A2, A3 Appendix A). Gaps indicate that the channel malfunctioned during that period.

Deployments	**D1 (110d)**	**D2 (82d)**	**D3 (233d)**	**D4 (161d)**
Starting day	7/Feb/2014	29/May/2014	22/Aug/2014	15/Apr/2015
Ending day	28/May/2014	19/Aug/2014	12/Apr/2015	22/Sep/2015
Channel 1	B649	B649	B649	
Channel 2	B655	B655	B655	
Channel 3	B658	B658	B658	
Channel 4	B660	B660	B660	
Channel 5	B661	B661	B661	
Channel 6	B665	B665	B665*	
Channel 7	B666	B666	B666	
Channel 8	B667	B667	B667	
Channel 9	B668	B668	B668	B682
Channel 10	B669	B669	B669	B683
Channel 11	B670		B670	B684
Channel 12	B671	B671	B671	B671
Channel 13	B672	B672		
Channel 14			B677	B677
Channel 15	B674	B674	B678	B678
Channel 16	B675	B675	B680	B680

Long term environmental measurements

Self-logging sensors for temperature (°C), salinity (PSU: Practical salinity unit), turbidity (FTU: Formazine Turbidity Unit), [Chl-a] (ug L^{-1}), and light conditions (PAR: Photosynthetic Available Radiation measured as µmol m^{-2} s^{-1}), were mounted on the lander over the entire deployment period.

Temperature and salinity were measured by a DST CT system (STAR-ODDI Data Storage Tag Conductivity and Temperature logger; http://www.star-oddi.com/) attached to the upper triangle part of the lander, 90 cm above the seabed. The CT system recorded temperature and salinity every 30 min.

Turbidity, [Chl-a], and light conditions were measured using two versions of JFE ocean instruments (http://ocean.jfe-advantech.co.jp). Wipers cleaned the sensor surface every 30

minutes immediately before a burst of 10 measurements. Light conditions were recorded with an upwards facing COMPACT-LW-ALW-CMP. Turbidity and [Chl-a] were measured with an Infinity-CLW-ACLW2-USB which was oriented parallel to the seabed 90 cm above the bottom.

Sea level records (in cm; reference Lowest Astronomical Tide) from the nearest tidal station (Hammerfest; http://www.kartverket.no/sehavniva/) were examined for the possible influences of tides on valve gape activity.

Experimental specimens

In February 2014, adult specimens of *A. islandica* were collected with a 30-cm clam dredge in Sanden Bay, Ingøya (Fig. A1, Appendix A). Sixteen specimens were selected for the valve gape monitoring experiment. Another 12 specimens were collected and placed in additional cups on the lander next to the valve gape monitors for future studies (Fig. 2. 1). Shell heights were 63.7–78.5 mm (±0.1 mm) at the beginning of the experiment. Each specimen was labeled with a shellfish tag (Glue-On shellfish tags FPN 8x4mm; http://www.hallprint.com/). For this, a small portion of the periostracum in the umbonal region was abraded away, after which the label was adhered with cyanoacrylate glue.

During the entire experimental period, a total of 21 individuals were used (Table 2. 1). One specimen died (*A. islandica* B665) and seven of the larger specimens were replaced with smaller ones (SH 50.7–56.6 mm) collected from the same population. Some of these individuals were used in continuing growth studies.

The lander was deployed for the first time on 7 February 2014 using a traditional coastal Norwegian fishing boat (sjark) “Fjord Strup”. Since this first deployment, the benthic lander was retrieved for maintenance and data collection twice per year (see Table 2.1). In the laboratory, all shells were measured, the data were downloaded from all instruments, and the instruments were cleaned, serviced and reprogrammed. Before redeployment, the aluminum lander frame was cleaned to remove overgrowth by fouling organisms. The time period from lander retrieval to redeployment was 1–3 d depending on weather conditions (Table 2. 1). During these days, specimens were kept in their cups within 80L baths of aerated sea water and at ambient temperature, but were not fed.

Statistical analysis

First, the synchrony among individuals was tested by calculating the pairwise correlation factor between all individuals and then between each of them and the average valve gape d^{-1} of all specimens ($mean(G_{t\ 1-n})$). The number of individuals (n) per time (t) varied among periods due to technical problems in some recorder channels (Table 2. 1).

Second, we applied a standard multiple-regression to identify which environmental factors were related to the average valve gape of the specimens in the experimental setup. A logit transformation of the average valve gape d^{-1} ($logit(mean(G_{t\ 1-n}))$) was applied to fulfill linear modelling assumptions (Warton and Hui 2011). To avoid collinearity, explanatory variables were included in the analyses only when they had a (Pearson) correlation coefficient ≤ ±0.5 (Graham, 2003; Duncan, 2011; Ieno and Zuur, 2015).

Third, an alternative approach was employed to address possible collinearity among the explanatory variables. PCA (Principal Component Analysis) was conducted on the environmental explanatory variables and the scores of the principal components were used as new explanatory variables in a subsequent multiple regression analysis (Graham, 2003). This method allowed us to include all the original variables in the regression model, avoiding the subjective process of variable dropping (Graham, 2003).

Finally, the two statistical approaches were compared. All analyses were done in R version 3.2.2 (www.r-project.org) and PAST3 (http://folk.uio.no/ohammer/past/).

RESULTS

Sea level

Sea level variation was ± 0.5 m for all the experimental periods, except one day in May 2014 when a single 1-m variation occurred (Fig. 2. 2a). This indicates that storms have an additional effect on sea level in the bay beyond the tidal influence (http://www.kartverket.no/sehavniva/).

Temperature

The daily average water temperature in Sanden Bay over the deployment period was 2.4–10.1 °C (Fig. 2. 2b). In both 2014 and 2015, August was the warmest month with an average

monthly temperature of 9.0 °C. In 2014, the coldest month was March with an average temperature of 3.7 °C, while in 2015 the coldest month was February with an average temperature of 3.3 °C. There were, however, individual measurements with recorded temperatures < 1.6 °C in the first half of February 2015 and > 10 °C in August 2014 and 2015. The lowest individual temperature record of 0.8 °C was recorded on February 3, 2015, and the maximum temperature of 10.3 °C occurred on August 9, 2014 and August 27, 2015.

Salinity

The daily average salinity range was 30.8–34.4 (Fig. 2. 2c). The minimum average daily value (30.8) was observed on February 10, 2015. However, there were occasional values < 30 between January 28 and February 16, 2015. A large, sustained decrease in salinity occurred in both summers following the spring melt. In the summer of 2015, salinity decreased from 33.4 on June 21 to 32.3 on September 21(Fig. 2. 2c). We observed not only a seasonal change in salinity but also a gradual decrease over the entire experimental period.

Light

Because Ingøya is ~ 500km north of Arctic Circle, there are immense seasonal changes in light. Light levels rapidly decrease in October and November, while in December and early January there is no appreciable daylight at all. Light levels increase again in late January and February (Fig. 2. 2d). The rapidly increasing light levels in February are accompanied by high levels of [Chl-a] in Sanden Bay by mid-March (Figs. 2d, 2e), when sea temperatures still are at or near their lowest for the year (Fig. 2. 2b). From mid-May to mid-July the sun does not set, providing perpetual daylight. In May 2014, however, we recorded an artificial light reduction due to algal overgrowth on the JFE sensor screen (Fig. 2. 2d).

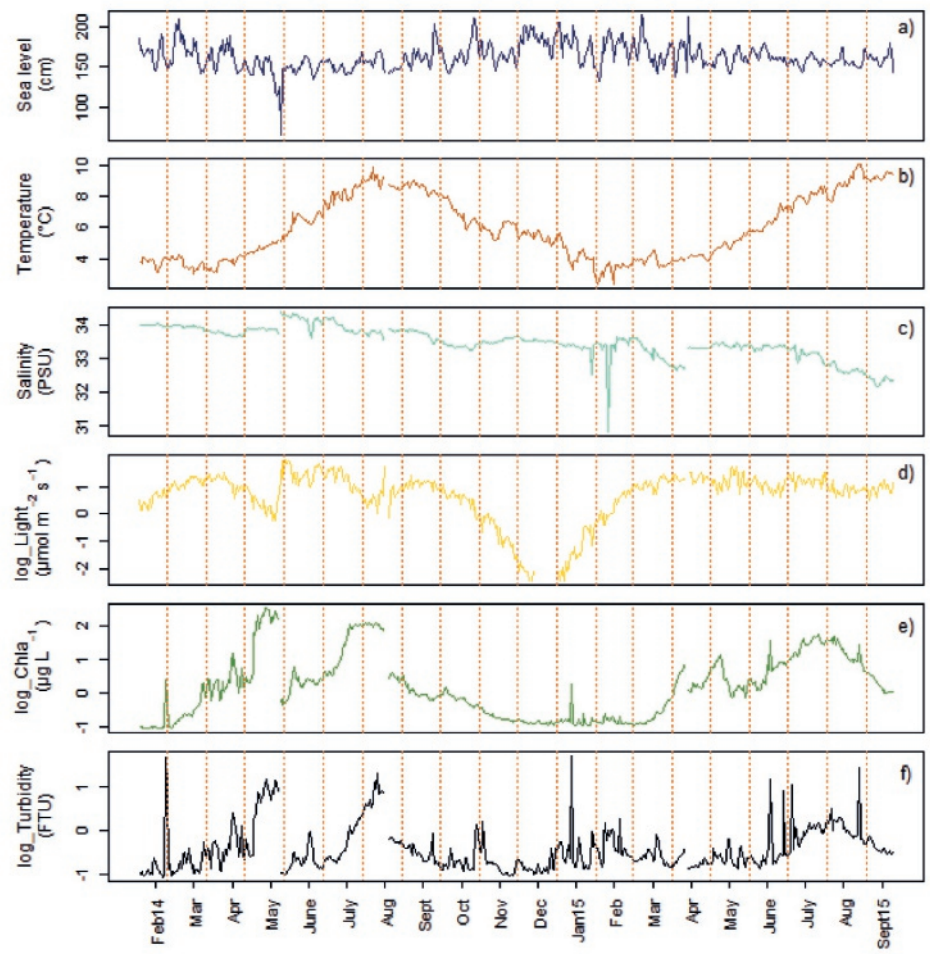

Fig. 2. 2: Daily averaged time series of the measured environmental variables by month. a) Sea level (cm); b) Temperature (°C); c) Salinity (PSU); d) Light conditions (log_µmol m^{-2} s^{1}); e) [Chl-a] (log_µg L^{-1}); f) Turbidity (log_FTU). Calendar years and months are indicated along horizontal axis (14= year 2014, and 15= year 2015). Some sensors were fouled prior to lander retrieval in May 2014.

[Chl-a] and Turbidity

Turbidity ([FTU]) values were measured by optical backscatter (OBS) to estimate water transparency, and [Chl-a] (ug L^{-1}) by fluorescence as an indication of primary productivity in

Sanden Bay. There were well defined, but episodic [Chl-a] peaks in mid-February 2014 and inmid-January in 2015 (Fig. 2. 2e). These transient peaks during winter, each lasting only 1–2 d, were likely due to the effect of winter storms leading to sediment resuspension releasing buried [Chl-a]. This is supported by turbidity values, which also showed transient spikes in February 2014 and January 2015, with maximum values of 44 and 48 FTU respectively (Fig. 2. 2f). More sustained [Chl-a] peaks occurred during spring and summer, reaching the highest values in May and August respectively (Fig. 2. 2e). In 2014, [Chl-a] varied from 0.1–348.1 µg L^{-1}. The extremely high values measured in spring were due to algal overgrowth on the JFE sensor screen. In 2015, the sensor problem was solved by covering the sensor with a PVC cylinder to exclude light and therefore eliminate the algae on the sensor. The [Chl-a] in 2015 were 0.1–57.1 µg L^{-1}.

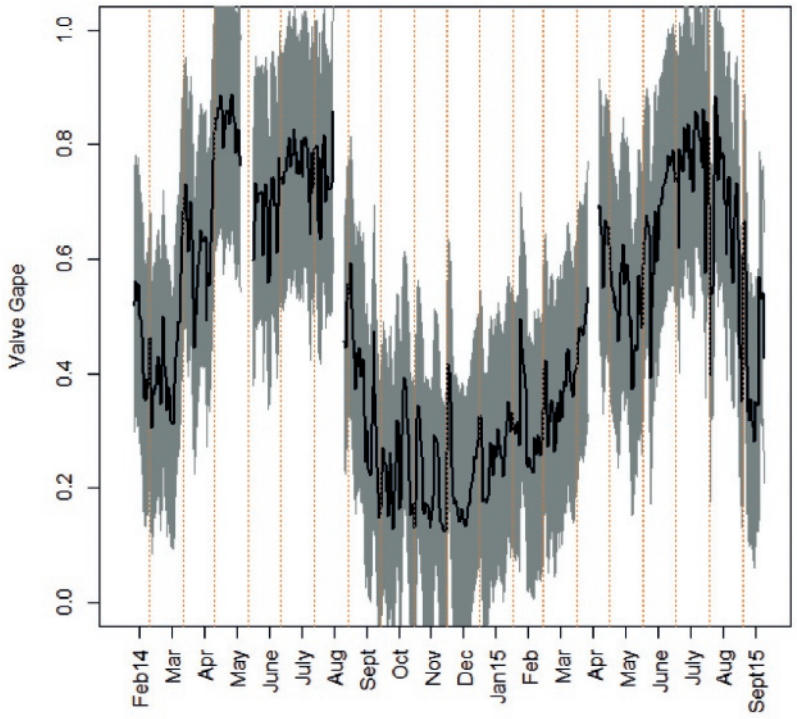

Fig. 2. 3: Valve gape daily mean (black line) and SD (grey shadow) by month from all available specimens per unit of time (n=7–15).

Valve gape monitors

There were significant differences in monthly valve gape activity (P< 0.01; one-way ANOVA), with monthly means of 0.19–0.84 (19–84% of the valve gape total magnitude respectively; Fig. 2. 3). Valve gape measurements over the two calendar years showed a well-defined activity cycle in *A. islandica* (Fig. 2.3). There were distinct types of gaping activity levels that were consistent between years as well as among individuals. We discerned two levels of activity, i.e. "active" with an average valve gape > 0.2, and "inactive" with an average valve gape ≤ 0.2 (Fig. 2. 3 and Fig. A1, A2, A3, Appendix A). Values < ~20% represent >95% probability of valves being closed in bivalves (Jou et al., 2013).

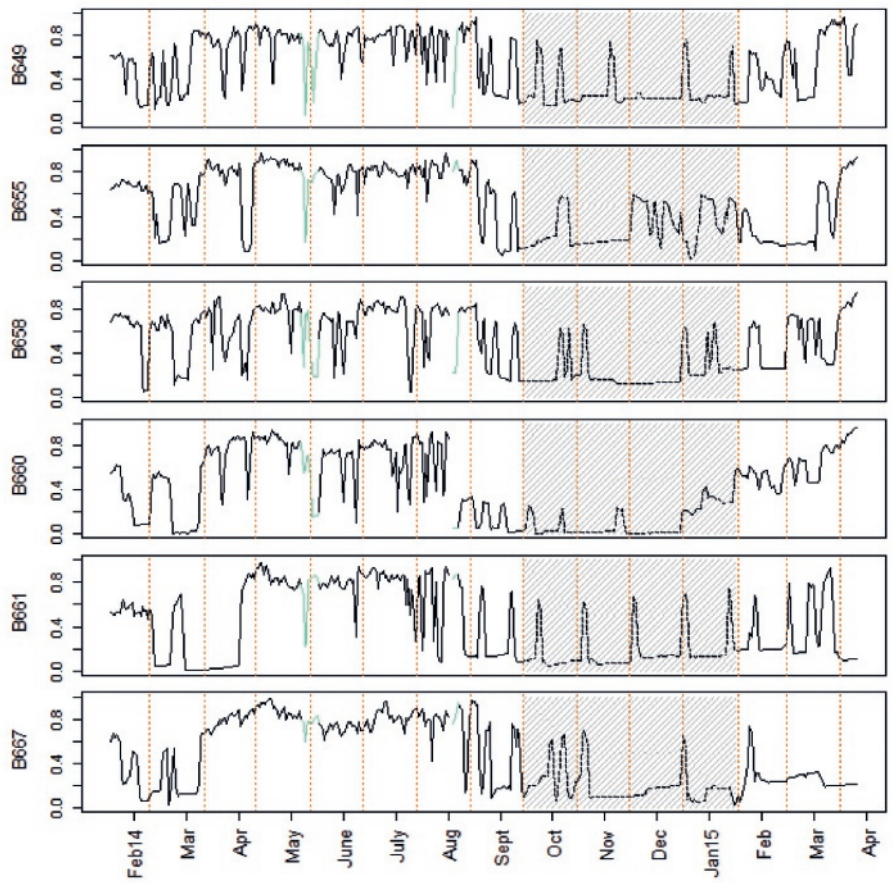

Fig. 2. 4: Gaping activity of six *A. islandica* specimens (Table 2.1) February 2014–April 2015. Green line highlights a week of valve gape data after the lander was deployed (excluded from analyses; May and August). Grey hashed background highlights common inactive period for all the specimens (average valve gape <0.2), which includes periodic gaping lasting 1–3 d.

On average, the sample population of *A. islandica* individuals was inactive from the beginning of October to the end of January (with an average daily gape < 23%; Fig. 2.3). That inactivity period, however, started earlier (mid-September) and/or finished later (end February/early March) in some specimens (Figs. 4 and Fig. A1, A2, A3, Appendix A). During that time, they opened widely once or twice a month for 1–3 days (Fig. 2. 4 and Fig. A1, A2, A3, Appendix A). Furthermore, we observed that all specimens required around a week to recover their normal activity after lander redeployment (Fig. 2. 4, green line). Consequently, those data were not considered in the statistical analysis.

In both 2014 and 2015, a consistent transition from low valve gape to high started between February and March. The daily mean valve gape then increased considerably between the months of March and April, from 0.41 to 0.63 in 2014, and from 0.36 to 0.56 in 2015 (Fig. 2. 3). During summer 2014 (June 21–September 21), the daily average valve gape was 0.65 and ranged from a maximum of 0.86 in mid-August to 0.22 in September. In summer 2015 the results were quite similar, with a daily average valve gape of 0.66, ranging from 0.88 in early August to 0.28 in September. During both years, the highest, continuous level of activity occurred in late spring to early summer. Valve gape monthly means reached their maximum in May 2014 (0.84) and in July 2015 (0.78; Fig. 2. 3).

Valve gape activity vs. environmental records

When average valve gape activity was compared with daily means of the different environmental variables, [Chl-a] was the variable with the highest correlation (r=0.8; P-value <0.01; Fig. 2. 5a), followed by turbidity (Fig. 2. 5b), sea level, light (Fig. 2. 5c), temperature (Fig. 2. 5d), and salinity (Table 2. 2). The periods with the highest valve gape coincided with the highest levels of [Chl-a] (Fig. 2. 5a). It is also apparent that the seasonal change in valve gape activity was temporally offset from temperature, with higher valve gape values leading the temperature pattern by 2–3 months (Fig. 2. 5d).

Turbidity was highly correlated with [Chl-a] values (r=0.71; P-value<0.01). When primary production increased in the bay, water transparency was reduced (Figs. 2d, 2e). Because of the correlation with [Chl-a], this variable was removed from the standard multiple regression analysis but included in the PCA regression.

Sea level had a negative relationship with gaping activity due to its influence on other environmental factors (Table 2. 2). When sea level increased, there was less [Chl-a] available (r=-0.47; P-value<0.01) and less light at the sea bottom (r=-0.28; P-value<0.01). An increase in sea level was furthermore associated with a decrease in water temperature (r=-0.24; P-value<0.01) and salinity(r= -0.08; P-value<0.01). This illustrates the influence of tides and storms on water exchange within Sanden Bay and seems to indicate that local primary production drives the bay's productivity.

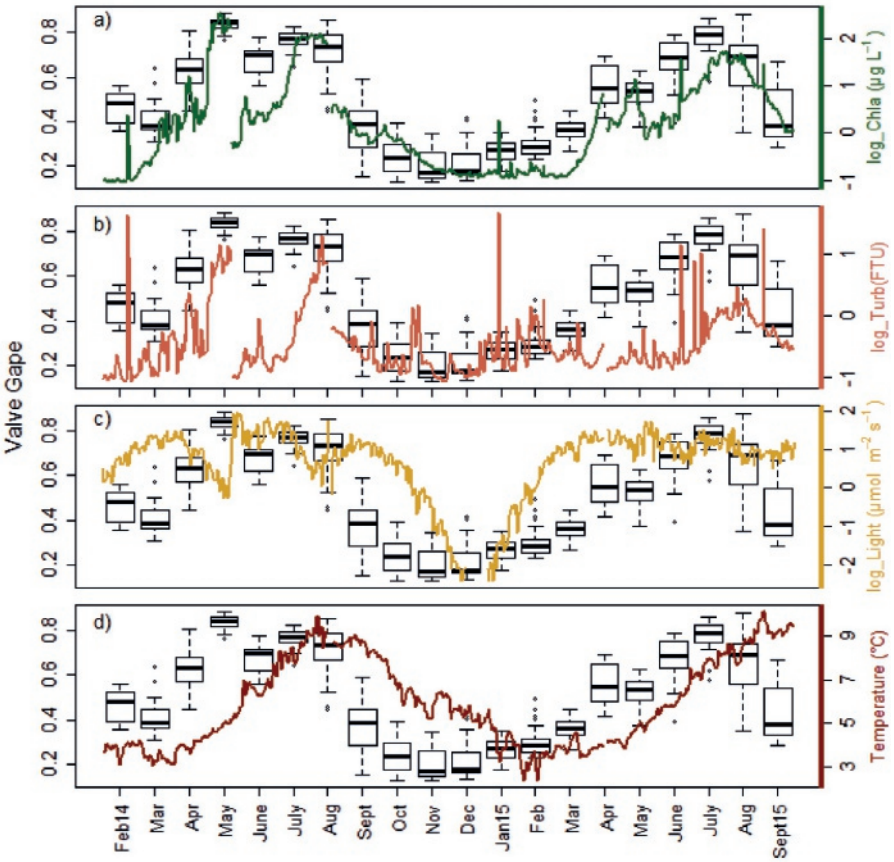

Fig. 2. 5: Boxplox per month of daily average valve gape of all the specimens *vs.* key environmental variables: a) [Chl-a] b) Turbidity, c) Light, d)Temperature.

Synchrony among individuals

There was high synchrony in daily gaping activity among all specimens. Further, there was also high synchrony between individuals and the average gape of all specimens (Fig. 2. 3 and Figs. A4, A5, A6, Appendix A). Correlation factors ranged 0.5–0.9. Specimen B665 was the only one which died (end of August 2014), and which correlated poorly with the rest of the population (Fig. A4, Appendix A).

Multiple-Regression

After linearity exploration of the environmental variables with the dependent variable, we log-transformed the variables [Chl-a] and Turbidity. Turbidity was removed from the analysis due to high correlation with [Chl-a] (r=0.7; Fig. A7, Appendix A). A stepwise variable selection procedure (both directions) did not lead to exclusion of any other measured explanatory variables. Consequently, we modeled the logit of the average daily valve gape with a dependency on Temperature, Salinity, log [Chl-a], Light, and Sea level:

M1: $y_i = \beta_0 + \beta_1 \times Temperature_i + \beta_2 \times Salinity_i + \beta_3 \times \log\_[Chla_i] + +\beta_4 \times Light_i + \beta_5 \times Sea\ level_i + \varepsilon_i$

Where y_i was the logit of the average valve gape on day i (i range 1–592), and ε_i the model error on day i ($\varepsilon_i \sim N(0,1)$).

Model M1 explained 75% of the variation in the average daily valve gape of *A. islandica* (adjusted R^2=0.75, $F_{1,66}$=328; Table 2. 3). All the variables were statistically significant (P-value <0.05). Residual plots showed a good fit of the model (Fig. A8, Appendix A). We then explored the contribution of each variable to the total model (M1.1–M1.4; Table A1, Appendix A). [Chl-a] was the main contributor to M1, individually explaining 66% of the gaping activity variance. When the variable light was added to the single variable [Chl-a] model, the two variables explained 72% of the variability in valve gape through time. This is roughly equivalent to the full M1 model (75%; Table A1, Appendix A). Thus [Chl-a] and light were the most important explanatory variables for the seasonal cycle in valve gape.

Table 2. 3: Regression table for model M1.

M1 logit(AvgGape) ~	Coefficient	Std.Error	t-value	P-value
(Intercept)	-4.041	1.793	-2.253	0.0246
Salinity	0.143	0.052	2.760	0.0059
Temperature	-0.088	0.013	-6.720	4.63E-11
Light	0.021	0.002	9.745	<2E-16
Sea level	-0.004	0.002	-2.335	0.0199
log_[Chl-a]	0.903	0.030	29.942	<2E-16
			R^2-adjusted	**= 0.75**

PCA regression

First, a PCA was conducted on the observations of the explanatory variables to extract the common signal from all of them (PCA; Table 2. 4). This approach prevents the loss of explanatory power resulting from exclusion of variables (Carnes and Slade 1988; James and McCulloch 1990). PC1 accounted for 38.7% of the variability among the variables (λ= 2.32), with log [Chl-a] driving the loadings positively (with a correlation with PC1 = 0.6; Fig. 2.6 and Table 2. 4). PC2 explained 22.8% of the remaining variability among the variables (λ= 1.37), and was best represented by light conditions (correlation with PC2= 0.7; Fig. 2. 6 and Table 2. 4). See Table 2. 4 for principal components with Eigenvalue < 1.

Ultimately, multiple regression analysis was conducted using the scores of the principal components as explanatory variables and the logit of average daily valve gape as response variable (Graham 2003):

M2: $y_i = \beta_0 + \beta_1 \times PC1_i + \beta_2 \times PC2_i + \beta_3 \times PC3_i + +\beta_4 PC4_i + \beta_5 \times PC5_i + \beta_5 \times PC6_i + \varepsilon_i$

Where y_i was the logit of the average valve gape on day i (i range 1–592), and ε_i the model error on day i ($\varepsilon_i \sim N(0,1)$). This regression model (M2) explained 75% of the valve gape variance (adjusted R^2=0.75, $F_{1,66}$ =273; Table 2. 4 and Table A2, Appendix A), with significant values for all the variables (P-value < 0.05; Table 2. 4). Thus the M2 results were identical to

those yielded by M1, where 75% of the gaping activity variance was also explained. Therefore, excluding turbidity from M1, did not influence our results.

In summary, the standard multiple regression results (M1) were supported by the PCA regression model (M2). These two statistical approaches and the consistency in the results from them, clearly suggest that [Chl-a], followed by light conditions, are the main environmental drivers of *A. islandica* gaping activity. While other variables may have some relevance and have a relationship at a particular time, these were generally far less influential in relation to the valve gape of this northern Norwegian population (Table 2.1, Appendix A).

Table 2. 4: Correlation table between key variables and principal components (top) and multiple regression model M2 summary (bottom). x*** = significant variable with P-value = 0, x** = significant variable with P-value < 0.01, x* = significant variable with P-value < 0.05 and, x = not significant variable. Numbers in bold indicate the two main environmental factors driving the principal component (PC).

	PC1	**PC2**	**PC3**	**PC4**	**PC5**	**PC6**
Variance explained	(38.7%)	(22.8%)	(16.3%)	(10.4%)	(9.1%)	(2.7%)
Temperature	0.45	-0.17	-0.43	**0.48**	**-0.55**	0.23
Salinity	-0.09	**0.57**	**0.61**	0.41	-0.35	0.02
Light	0.13	**0.66**	**-0.44**	0.18	0.50	0.25
Sea level	-0.41	-0.37	0.01	**0.74**	**0.38**	-0.09
log_[Chl-a]	**0.61**	0.02	0.11	0.15	0.22	**-0.74**
log_Turbidity	**0.49**	-0.26	0.49	0.02	0.36	**0.57**
M2 (R^2-adjusted= 0.75)	x***	x***	x***	x*	x***	x***

DISCUSSION

Our field experiment addresses the critical need to study *A. islandica* biological activity at several temporal scales. We documented the in situ daily and seasonal gaping activity of this bivalve in relation to environmental factors that drive their rhythms. Valve gape in *A. islandica* exhibits a well-defined seasonal pattern which is mainly driven by [Chl-a].

Although the experimental organisms had electro-coils attached to the outside of their shells and were each kept in individual cups, there is no indication that this experimental setup

impacted the study results or considerably modified the valve gape behavior. Over the study period only one specimen died and we furthermore observed that the specimens buried themselves deep into the cups. Moreover an analysis of the body mass index (BMI = Dry Weight-Ash Weight/ Height^3) showed that individuals from the experiment had the same or even slightly higher BMI than individuals freshly collected from the field at the time the lander was recovered. Results from other species show that electro-coils attached to the external shell surface had no influence on their behavior (Tran et al., 2011; Jou et al., 2013).

Valve gape vs. growth

Valve gape activity in bivalves is related to important physiological processes including feeding and respiration (Bayne, 1998; Markich, 2003; Riisgård et al., 2003; García-March et al., 2008). Filter-feeding bivalves open their valves to extend their siphons and filter the surrounding water. Witbaard et al., (1997b) demonstrated in a laboratory experiment that a large proportion of the inter-specimen variation in shell growth of *A. islandica* could be explained by differences in individual feeding activities. This suggests a link between valve gape, open siphons, and shell growth, i.e. that valve gape is indicative of shell growth. Unfortunately, we were unable to collect small specimens at the start of the experiment which might have enabled a posteriori determination of this relationship. The specimens used were too large and too slow-growing to measure shell growth with calipers, given the measurement error (Thompson et al., 1980a). We used an alternative method to determine whether the seasons with wide open valves (≥50% gape April–September) and closed valves (≤20% October–end of January) coincided with periods of shell growth and non-growth. These thresholds (20 and 50%) are based on Jou et al., (2013), representing > 95% probability of valves being closed or, alternately, siphons extended, respectively, in *Corbicula fluminea*. We used the change in monthly maximum (raw) valve gape signal, i.e. the minimum measured distance of completely closed valves. A progressively decreasing signal strength (or drift) indicated that the valves and the electro-coils became progressively further apart when closed. The growing shell margin pushes the sensors away from each other, directly indicating shell growth (Schwartzmann et al., 2011; Massabuau et al., 2015). Six out of seven specimens exhibited a strong trend of decreasing signal (maximal) strength between April and September 2014 (Fig.

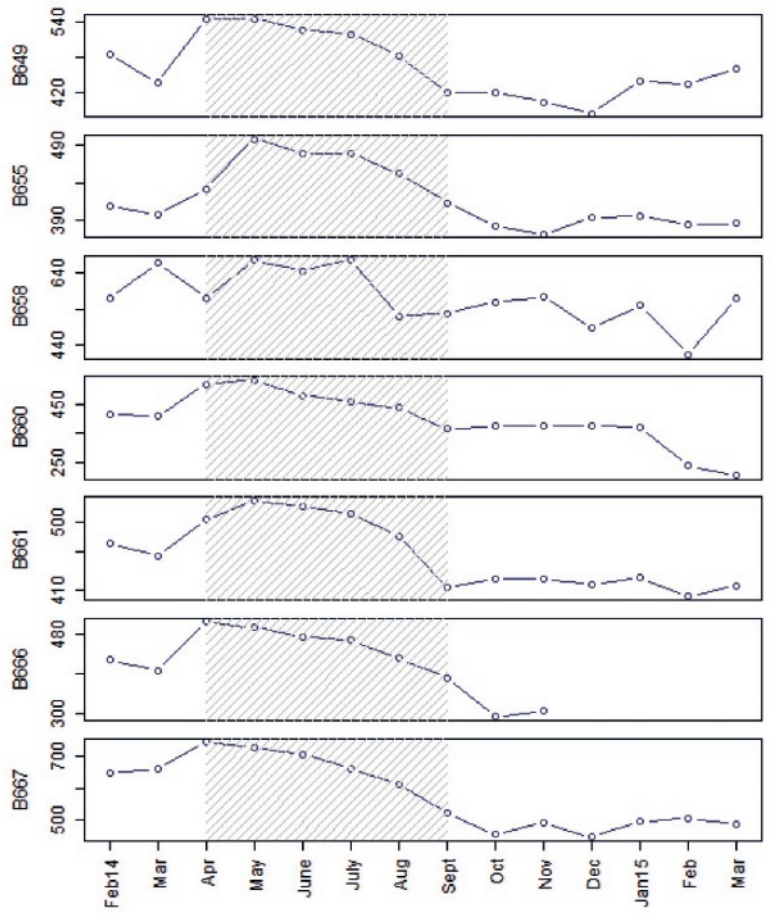

Fig. 2. 6: Maximum signal per month of *A. islandica* specimens from recorder 1(except specimen B665 which died). Grey dashed background highlights months with higher average gape valve (>0.5). There are different scales on the y-axis to better illustrate the change in the monthly maximum signal per specimen. NOTE: Recorder 2 specimens are not shown because R2 was adjusted in August 2014, so raw data were not comparable.

2.,6) followed by a more stationary period without a clear trend in the maximum signal. These periods coincided with the periods of high and low valve gape values, respectively. This suggests that periods with high valve gape activity and high [Chl-a] corresponded to a progressive decline in maximum signal strength (increase in minimum valve gape) and

therefore shell growth. These results are supported by earlier studies that found the highest shell growth rates for this species in spring and early summer (Thompson et al., 1980a; Schöne et al., 2005b; Witbaard and Hippler, 2009), and provide a link between food availability ([Chl-a]), high valve gape activity, and shell growth.

The valve gape data presented here thus suggest an 'active' growth season of about eight months for this location in northern Norway. Some studies have previously correlated their *A. islandica* growth chronologies with Sea Surface Temperature (SST) or salinity data from February–September (northeast Iceland; Marali and Schöne, 2015). Our study clarifies the ecological and biological basis for using this period.

In contrast to our findings, Mette et al., (2016) described a growing season of 12 months from the same population in Sanden Bay (from April to March/April of the following year). Their results, however, were based on shell oxygen isotopes values from only two subsampled annual increments. Our results are based on daily averages of gaping activity from a minimum of 7 simultaneously measured specimens. Although oxygen isotopes are excellent tools for reconstructing long time series of environmental annual variability, more replication (of individuals and years) and/or fine scaler sampling of the shell increments is needed when addressing sub-annual resolution (DeLong et al., 2013; Schöne and Gillikin, 2013).

Valve gape vs. environment

Average daily valve gape was highly synchronized ($r_{\text{all animals}}$ >0.5) and showed clear seasonal differences. High synchrony in valve gape has also been observed in other bivalves such as *Mya arenaria*, *Dreissena polymorpha*, *Crassostrea gigas*, and *Pinna nobilis* suggesting that a common external force with a periodicity similar to the activity drives such a response (Thorin, 2000; Borcherding, 2006; Mat et al., 2012; García-March et al., 2016).

We measured various environmental variables of which [Chl-a], light, and temperature are the most likely to explain the seasonal pattern in shell gape. *Arctica islandica* is a poikilotherm and its activity and growth is directly dependent on ambient temperature (Winter, 1969; Clarke, 2003; Hiebenthal et al., 2012). There are, however, conflicting results on the significance of temperature on *A. islandica* growth and gape activity. In laboratory growth experiments, faster growth at higher temperatures was reported (Witbaard et al., 1997b),

with an added effect of salinity (Hiebenthal et al., 2012). Field studies were however not always conclusive about the role of temperature in shell growth. Some found significant correlation between SST and shell growth rate of *A. islandica* (Wanamaker et al., 2008a; Butler et al., 2010; Marali and Schöne, 2015), while others did not find such a strong relationship (Witbaard, 1996; Marchitto et al., 2000; Epplé et al., 2006; Stott et al., 2010). In a temperate environment, food and temperature are hard to separate as explanatory variables for activity or growth. The difficulty in disentangling these two variables in a field setting was one of the reasons we conducted this study at this northern location (71 °N). Our results were consistent with other bivalve growth studies at high latitudes, which also found growth cessation at elevated temperatures coincident with low food availability (Carroll et al., 2009; Carroll et al., 2011; Ambrose et al., 2012).

In this study, we observed that the population started to consistently open their valves and become active near the coldest period of the year (around March) and conversely closed their valves and started to become inactive by mid-September when temperatures were near their annual maximum (Fig. 2. 5d). The valve gape records however show that they were not completely inactive in this winter period. All clams opened their valves widely once or twice a month for 1–3 d, and then closed again. A similar pattern has previously been observed in experiments and in the field (Taylor, 1976; Strahl et al., 2011). While the reason for this behavior is not clear, it could be related to respiration and/or might be a type of probing behavior to test whether the environment is favorable. Our results showed that once there is food enough, the bivalves do not return to a dormant state but start feeding continuously with fully open valves. These results agree with earlier studies in *A. islandica* (Winter, 1969) and other bivalves (Higgins, 1980; Williams and Pilditch, 1997; Riisgård et al., 2006) where the presence of Chl-a appears to be the main driver for sustained opening of their valves.

Next to [Chl-a], there was a relatively strong positive correlation between valve gape and light conditions. In some bivalve species valve gape behavior is directly triggered by light conditions (García-March et al., 2008; Schwartzmann et al., 2011), whereby variations in sun or moon irradiance immediately provoke a response. *Arctica islandica* is known to have a shadow reaction to light (Morton, 2011), but our results did not indicate an immediate response of valve gape to moon phase, day length or hourly variations in light intensity (unpubl data). Light could have an indirect effect on *A. islandica* through modulation of food

availability (Kaartvedt, 2008). There is indeed evidence that for some species of bivalves, valve gape responds to the presence of algal food (Higgins, 1980; Williams and Pilditch, 1997; Riisgård et al., 2003; Riisgård et al., 2006. In laboratory conditions under continuous light exposure, *A. islandica* exhibited a 3–7 min periodicity in valve and mantle activity, which could be related to intrinsic drivers such as a biological clock (Rodland et al. ,2006). The exact role of light as driving factor for valve gape of *A. islandica* remains unresolved, and the effect of photoperiod at different algal concentrations should be studied to clarify this issue.

In summary, our research found that: (1) gaping activity of *A. islandica* is highly synchronized among individuals in the studied population (2) [Chl-a] is the main driver of valve gaping activity in northern Norway, (3) the clams had a period of active gaping of eight months between (February–September). These results suggest the length of growing season in northern Norway is likely limited to about eight months (Weidman et al., 1994; Schöne et al., 2005b; Dunca et al., 2009) starting very early in the spring and ending in late summer/early fall (Witbaard et al., 2003; Dunca et al., 2009).

Compliance with ethical standards

The authors declare that they have no conflict of interest. All applicable international, national, and/or institutional guidelines for the care and use of animals were followed.

Acknowledgments

Thanks to Captain Thorleif Hansen for his indispensable help at the field location at Ingøya, Norway. Thanks to the NIOZ workshop for their construction work of field equipment. Special thanks to William Ambrose Jr, Dmitri Barjitski, Odd Fjelde, Aubrey Foulk, Dan Frost, Ann Hansen, Erlend Hesten, Randall Hyman, Maddie Mette, Julie and Michael Retelle, and Alan Wanamaker for their assistance during the fieldwork.

This work was funded by the EU within the framework (FP7) of the Marie Curie International Training Network ARAMACC (604802). Support for MLC was provided by the Research Council of Norway (Project: #227046).

Appendix A

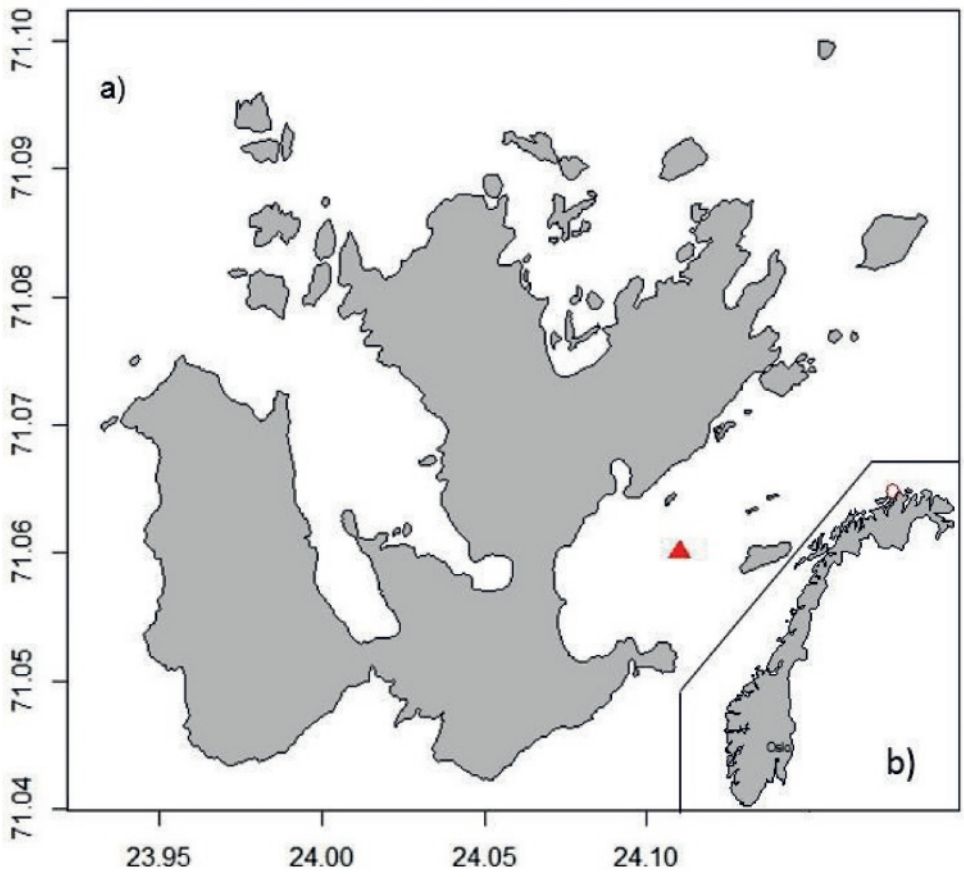

Fig. A1: a) Ingøya Island with triangle marking lander position and b) Norway map with circle highlighting fieldwork location.

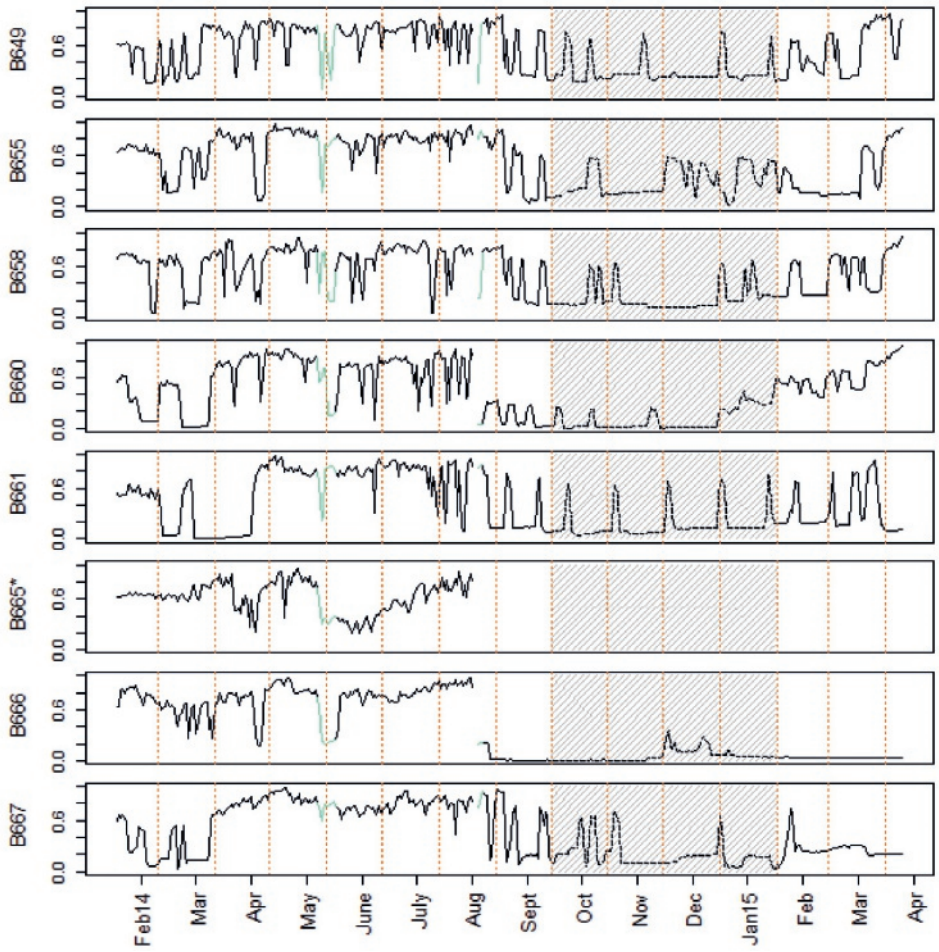

Fig. A2: All data from the eight *A. islandica* specimens in recorder 1. No data from April 2015 to September 2015, recorder was flooded. B665* died at the end of August 2014. Grey background highlights winter period.

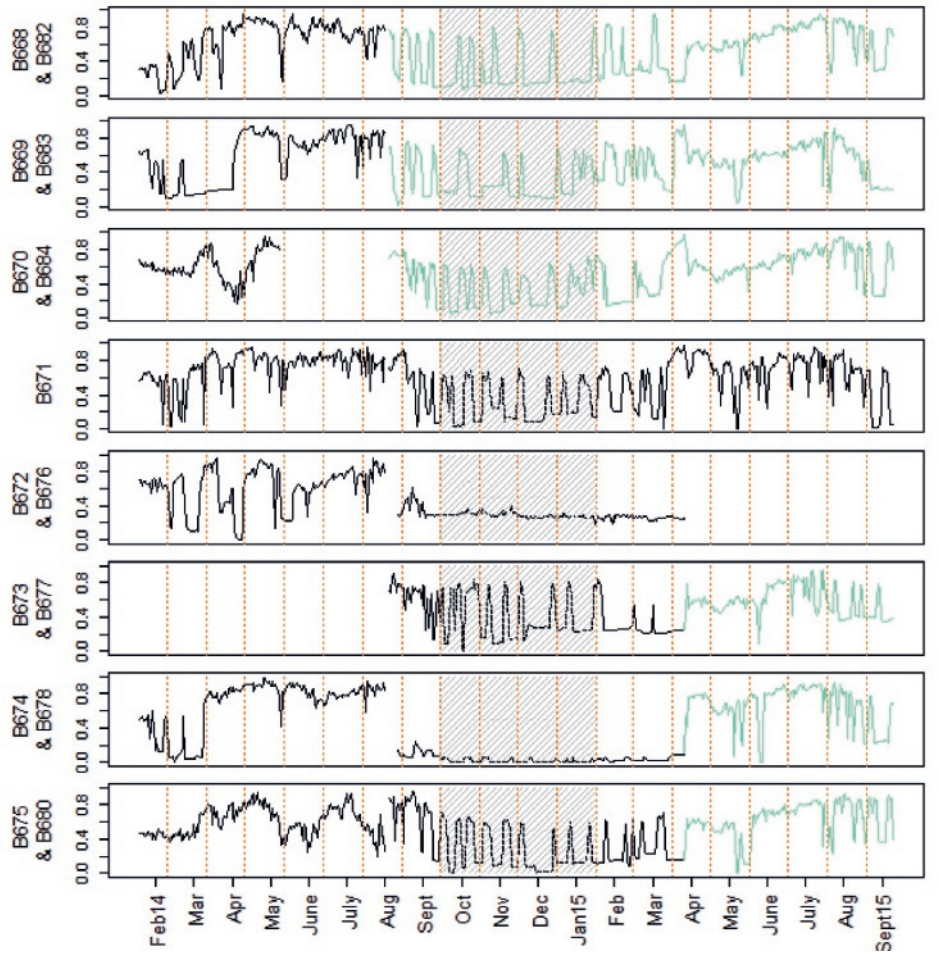

Fig. A3: All data from the 15 *A. islandica* specimens in recorder 2. Different line color indicates specimen change. Grey background highlights winter period.

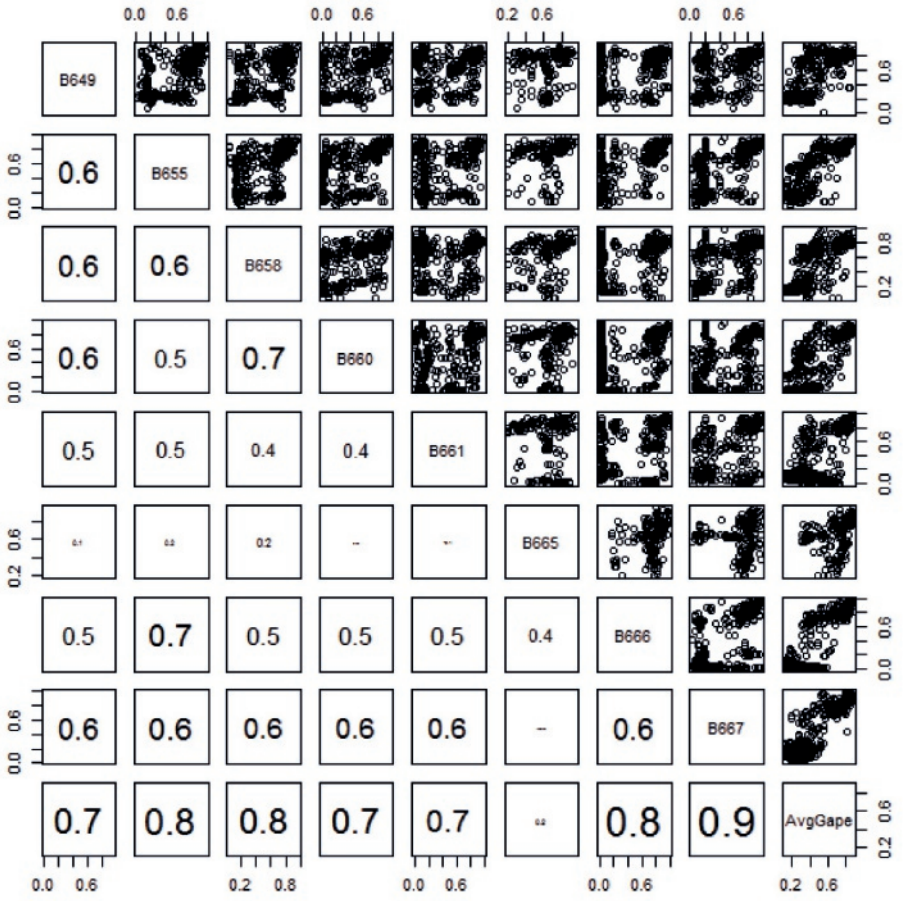

Fig. A4: Correlation plot between original specimens' recorder 1 and the average valve gape of all the specimens (AvgGape). *A. islandica* B665 died at the end of August 2014. No data for replacement specimen B681, channel did not work for that period.

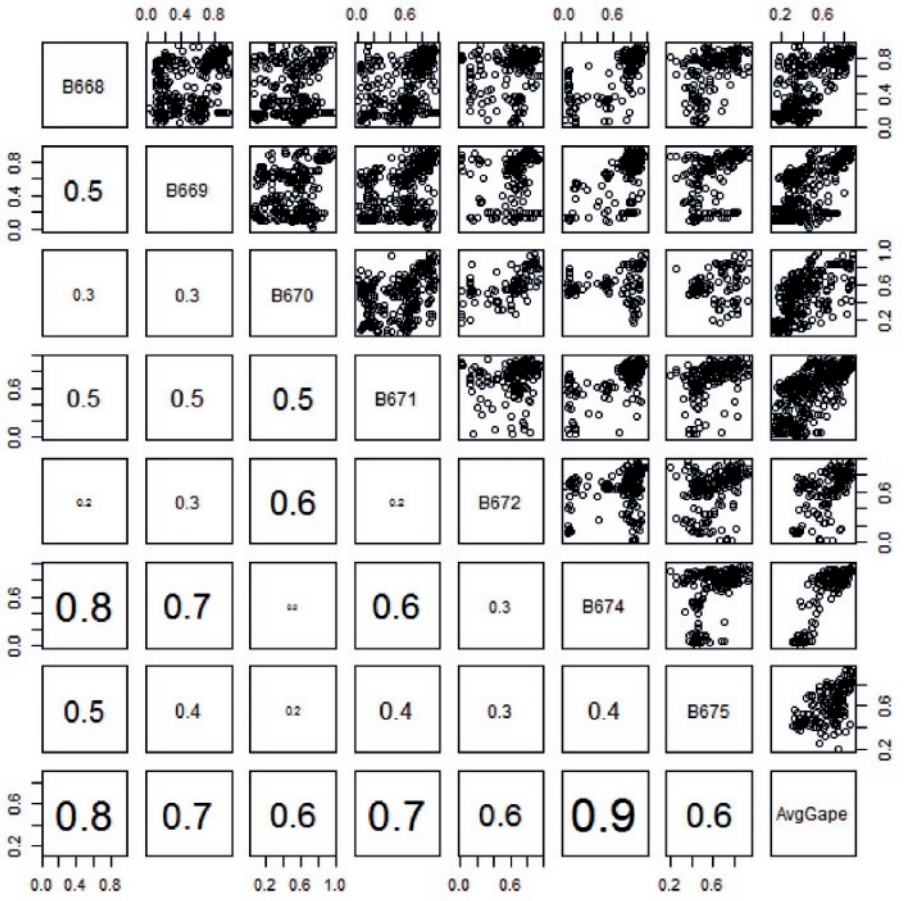

Fig. A5: Correlation plot between original specimens' recorder 2 and AvgGape. No data for *Arctica islandica* B673, channel did not work.

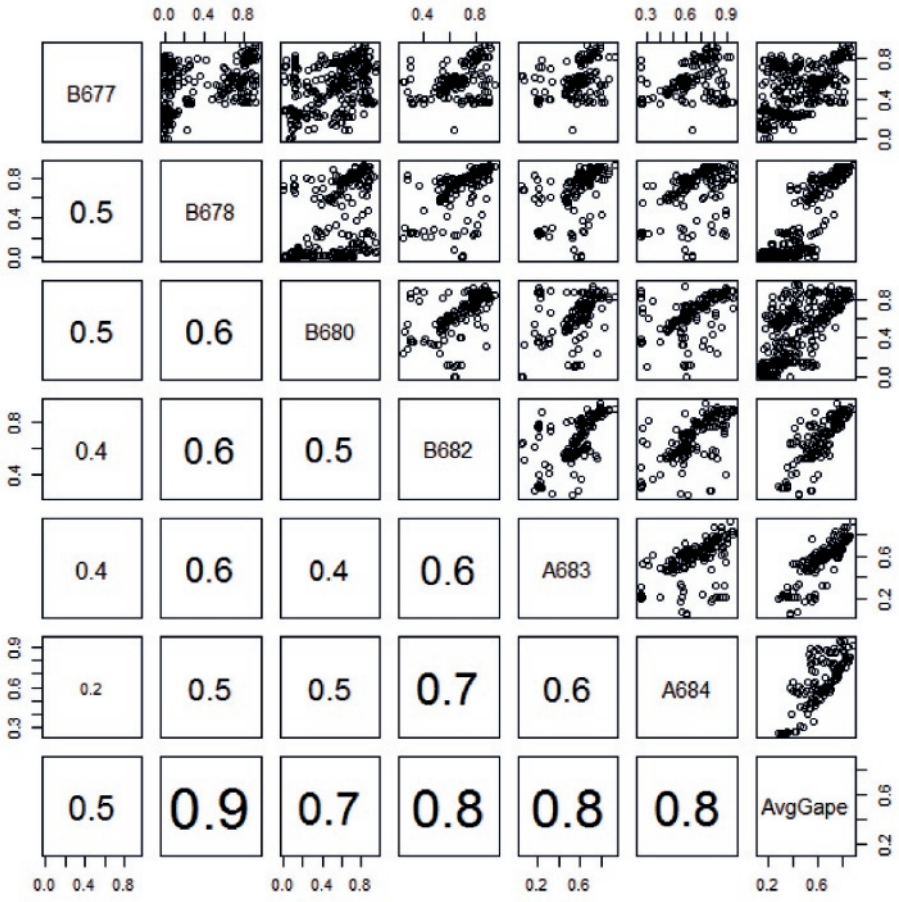

Fig. A6: Correlation plot between new specimens' recorder 2 and AvgGape. No data for *Arctica islandica* B676, channel did not work.

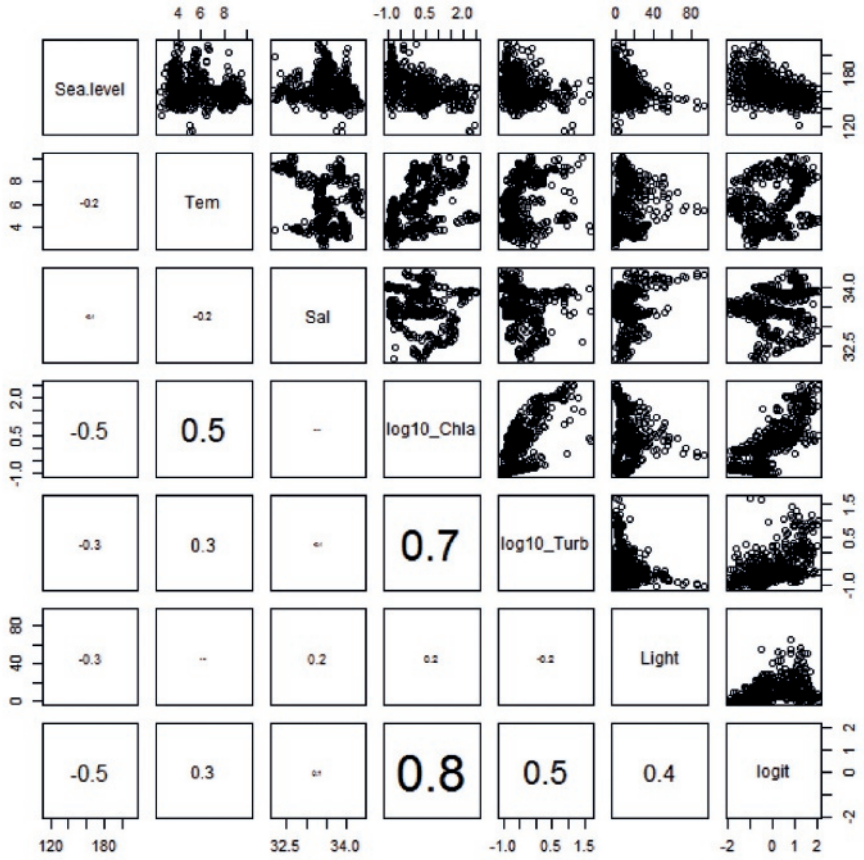

Fig. A7: Correlation plot between average gaping activity (as logit) and the environmental variables: sea level (cm) temperature (Tem, °C), salinity (Sal, PSU), [Chlorophill-a] (log10_µg L^{-1}), turbidity (log10_FTU), and light conditions (µmol m^{-2} s^{1}).

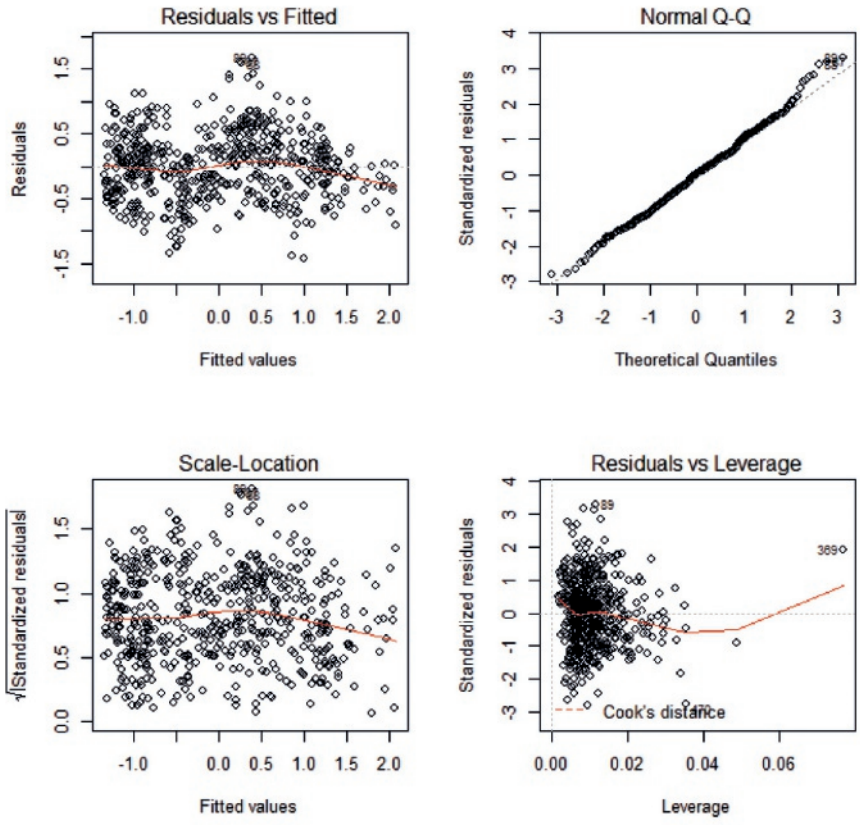

Fig. A8: Residuals plots model M1.

Table A1: Best regression model with one, two, three, four or five explanatory variables.

Model	Variables	R^2-adjusted	F-statistic
M1.1	logit(AvgGape) ~log_Chla	0.6566	1047
M1.2	logit(AvgGape) ~log_Chla + Light	0.7162	691.1
M1.3	logit(AvgGape) ~log_Chla + Light + Tem	0.7435	529.6
M1.4	logit(AvgGape) ~log_Chla + Light + Tem+ Sal	0.7461	402.8
M1	logit(AvgGape) ~log_Chla + Light + Tem+ Sal+Sea level	**0.7497**	**328**

Table A2: Regression table for model M2.

M2 logit(AvgGape) ~	Coeffcient	Std.Error	t-value	P-value
(Intercept)	-0.01497	0.02176	-0.688	0.4919
PC1	0.48232	0.01429	33.755	<2E-16
PC2	0.26014	0.01862	13.969	<2E-16
PC3	0.10709	0.02202	4.863	1.52E-16
PC4	0.06742	0.02758	2.445	0.0148
PC5	0.34796	0.02955	11.776	<2E-16
PC6	-0.62921	0.5412	-11.625	<2E-16
			R^2-adjusted=	**0.75**

Chapter 3

The effects of environment on *Arctica islandica* shell formation and architecture

Milano, Stefania; Nehrke, Gernot; Wanamaker Jr., Alan D.; Ballesta-Artero, Irene; Brey, Thomas; Schöne, Bernd R.

Published in Biogeosciences 14: 1577–1591 (2017)

Abstract

Mollusks record valuable information in their hard parts that reflect ambient environmental conditions. For this reason, shells can serve as excellent archives to reconstruct past climate and environmental variability. However, animal physiology and biomineralization, which are often poorly understood, can make the decoding of environmental signals a challenging task. Many of the routinely used shell-based proxies are sensitive to multiple different environmental and physiological variables. Therefore, the identification and interpretation of individual environmental signals (e.g. water temperature) often is particularly difficult. Additional proxies not influenced by multiple environmental variables or animal physiology would be a great asset in the field of paleoclimatology. The aim of this study is to investigate the potential use of structural properties of *Arctica islandica* shells as an environmental proxy. A total of eleven specimens were analyzed to study if changes of the microstructural organization of this marine bivalve are related to environmental conditions. In order to limit the interference of multiple parameters, the samples were cultured under controlled conditions. Three specimens presented here were grown at two different water temperatures (10 °C and 15 °C) for multiple weeks and exposed only to ambient food conditions. An additional eight specimens were reared under three different dietary regimes. Shell material was analyzed with two techniques: (1) Confocal Raman microscopy (CRM) was used to quantify changes of the orientation of microstructural units and pigment distribution and (2) Scanning electron microscopy (SEM) was used to detect changes in microstructural organization. Our results indicate that *A. islandica* microstructure is not sensitive to changes in the food source, and likely, shell pigment are not altered by diet. However, seawater temperature had a statistically significant effect on the orientation of the biomineral. Although additional work is required, the results presented here suggest that the crystallographic orientation of biomineral units of *A. islandica* may serve as an alternative and independent proxy for seawater temperature.

Keywords

Confocal Raman microscopy; scanning electron microscopy; shell microstructure; water temperature; diet; bivalve shell

INTRODUCTION

Biomineralization is a process through which living organisms produce a protective, mineralized hard tissue. The considerable diversity of biomineralizing species contributes to high variability in terms of shape, organization and mineralogy of the structures produced (Lowenstam and Weiner, 1989; Carter et al., 2012). Different architectures at the micrometer and nanometer scale and different biochemical compositions determine material properties that serve specific functions (Weiner and Addadi, 1997; Currey, 1999; Merkel et al., 2007). Besides these differences, all mineralized tissues are hybrid materials consisting in hierarchical arrangements of biomineral units surrounded by organic matrix, also known as "microstructures" (Bøggild, 1930; Carter and Clark, 1985; Rodriguez-Navarro et al., 2006) or "ultrastructures" (Blackwell et al., 1977; Olson et al., 2012) or overall "fabrics" (Schöne, 2013; Schöne et al., 2013). The carbonate and organic phases represent the fundamental level of the organization of biomaterials (Aizenberg et al., 2005; Meyers et al., 2006). The mechanisms of microstructure formation and shaping, especially in mollusks, has attracted increasing attention during recent decades. At present, it is commonly accepted that the organic compounds play an important role in the formation of the inorganic phases of biominerals (Weiner and Addadi, 1991; Berman et al., 1993; Dauphin et al., 2003; Nudelman et al., 2006). However, the identification of the exact mechanisms driving biomineralization is still an open research question. Previous studies conducted on mollusks show that environmental parameters can influence microstructure formation (Lutz, 1984; Tan Tiu and Prezant, 1987; Tan Tiu, 1988; Nishida et al., 2012). These results set the stage for a research interest toward the use of shell microstructures as proxies for reconstructing environmental conditions (Tan Tiu, 1988; Tan Tiu and Prezant, 1989; Olson et al., 2012; Milano et al., 2017a).

Mollusks are routinely used as climate and environmental proxy archives because they can record a large amount of environmental information in their shells (Richardson, 2001; Wanamaker et al., 2011a; Schöne and Gillikin, 2013). Whereas structures at nanometric level are still underexplored as potential environmental recorders, shell patterns at lower magnification, such as individual growth increments, are commonly used for this purpose (Jones, 1983; Schöne et al., 2005b; Marali and Schöne, 2015; Mette et al., 2016). Mollusks deposit skeletal material on a periodic basis and at different rates (Thompson et al., 1980a; Deith, 1985). During periods of

fast growth, growth increments are formed whereas during periods of slower growth, growth lines are formed (Schöne, 2008; Schöne and Gillikin, 2013). The periodicity of such structures ranges from tidal to annual (Gordon and Carriker, 1978; Schöne and Surge, 2012). By crossdating time-series with similar growth patterns it is possible to construct century and millennia-long master chronologies (Marchitto et al., 2000; Black et al. 2008; Black et al., 2016; Butler et al., 2013). This basic approach, in combination with geochemical methods, has great potential in reconstructing past climatic conditions (Wanamaker et al., 2011b). At present, the most frequently used and well-accepted geochemical proxy is oxygen isotopic composition of shell material ($\delta^{18}O_{shell}$) (Epstein, 1953; Grossman and Ku, 1986; Schöne et al., 2004; Wanamaker et al., 2007) which may serve as a paleothermometer and/or paleosalinometer (Mook, 1971; Andrus, 2011); however, $\delta^{18}O_{shell}$ value is influenced by both seawater temperature and the isotopic composition of seawater ($\delta^{18}O_{water}$; related to salinity). Thus, $\delta^{18}O_{shell}$-based temperature reconstructions are particularly challenging in habitats with fluctuating $\delta^{18}O_{water}$ conditions such as estuaries or restricted basins (Gillikin et al., 2005). Because of the multiple impacts on $\delta^{18}O_{shell}$ values, there have been substantial efforts to develop alternative techniques to reconstruct environmental variables from mollusk shells (Schöne et al., 2010; Milano et al., 2017b).

This study investigates the possibility using shell microstructure properties to serve as a new environmental proxy. For this purpose, the effects of seawater temperature (grown at 10 °C and 15 °C) and dietary regime on the microstructural units of *Arctica islandica* cultured under controlled conditions were analyzed and quantified. *A. islandica* was chosen as model species because of its great potential in paleoclimatology and paleoceanography (see Schöne, 2013; Wanamaker et al., 2016). Its extreme longevity of up to more than 500 years makes this species a highly suitable archive for long-term paleoclimate and environmental reconstructions (Schöne et al., 2005b; Wanamaker et al., 2008a; Wanamaker et al., 2012; Butler et al., 2013).

MATERIALS AND METHODS

The analyses were conducted on eleven *A. islandica* shells. Three juvenile *A. islandica* shells, sampled for the seawater temperature experiment, were collected alive on November 21, 2009

aboard the *F.V. Three of a Kind* off Jonesport, Maine USA (44° 26' 9.829''N, 67° 26' 18.045''W) in 82 m water depth. From 2009 to 2011, all animals were kept in a flowing seawater laboratory at the Darling Marine Center, Walpole, Maine, USA (see Beirne et al., 2012 for additional details). In 2011, clams were grown at two different temperature regimes for 16 weeks (Table 3.1). At the completion of the experiment, shells were estimated to be between 4 to 5 years old. Eight one-year old juveniles were collected in July 2014 from Kiel Bay, Baltic Sea (54° 32' N, 10° 42' E; Fig. 3. 1) and kept alive in tanks at 7 °C for six months at the Alfred Wegener Institute for Polar and Marine Research (AWI), Bremerhaven, Germany. During this time interval, the animals were fed with an algal mix of *Nannochloropsis* sp., *Isochrysis galbana* and *Pavlova lutheri.* Then, they were transferred to the Royal Netherlands Institute for Sea Research (NIOZ), Texel, The Netherlands, and cultured in tanks at three different dietary conditions for 11 weeks (Table 3.1).

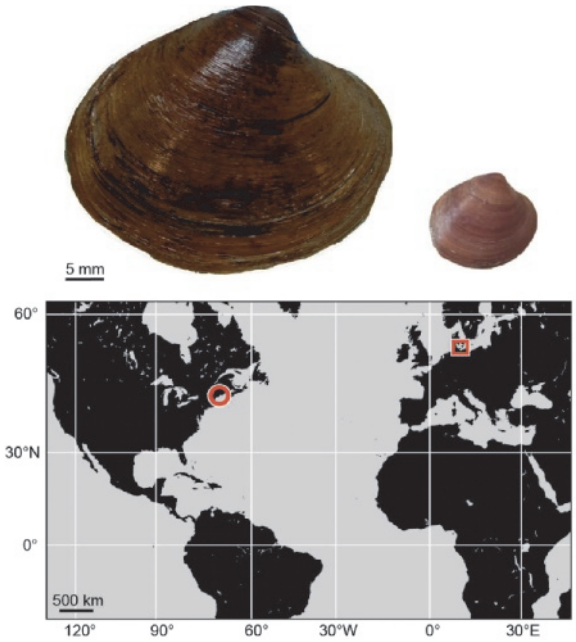

Fig. 3. 1: Shell of adult *Arctica islandica* used in the temperature experiment (left) and juvenile from the Baltic Sea used in the food experiment (right). The map indicates the localities where the two sets of shells were collected: Jonesport, Maine (circle) and Kiel Bay (square).

Table 3. 1: List of the studied specimens of *Arctica islandica* and experimental conditions.

Sample ID	Locality	Age	Experiment	Treatment
A2	Maine	5	Temperature	10 °C + 15 °C
A4	Maine	4	Temperature	10 °C + 15 °C
A5	Maine	4	Temperature	10 °C + 15 °C
S12	Kiel Bay	1	Diet	Food 1
S14	Kiel Bay	1	Diet	Food 1
S15	Kiel Bay	1	Diet	Food 1
G11	Kiel Bay	1	Diet	Food 2
G12	Kiel Bay	1	Diet	Food 2
G15	Kiel Bay	1	Diet	Food 2
N13	Kiel Bay	1	Diet	No additional food
N15	Kiel Bay	1	Diet	No additional food

Seawater temperature experiment

The seawater temperature experiment started on 27 March 2011 and ended on 21 July 2011. Prior to the start of the experiment the animals were marked with calcein. The staining leaves a clear fluorescent marker in the shells that can be used to identify which shell material has formed prior to and during the experiment. Initially, the animals were kept at 10.3 ± 0.2 °C for 48 days. Then, they were briefly removed from the tanks and marked again. Subsequently, the clams were cultured for 69 more days at 15.0 ± 0.3 °C. Ambient seawater was pumped from the adjacent Damariscotta River estuary and adjusted to desired temperature. The salinity was measured with a Hydrolab® MiniSonde. It ranged between 30.2 ± 0.7 and 30.7 ± 0.7, in the two experimental phases, respectively. During the entire culture period, all clams were exposed to ambient food conditions. At the end of the experiment the soft tissues were removed.

Food experiment

The food experiment was carried out from 9 February 2015 to 29 April 2015. The animals were placed in aquaria inside a climate room at 9 °C. Water temperature in the tanks ranged between

8 and 10 °C. Water salinity was measured by using an ENDECO 102 refractometer and ranged between 29.6 and 29.9 ± 0.1 in each aquarium. The 15-liter tanks were constantly supplied with aerated water from the Wadden Sea. The clams were acclimated for three weeks before the start of the experiment. Three dietary regimes were chosen. One treatment consisted of feeding the animals with Microalgae Mix (food type 1), a ready-made solution of four marine microalgae (25 % *Isochrysis,* 25 % *Tetraselmis,* 25 % *Thalassiosira,* 25 % *Nannochloropsis*) with a particle size range of 2 - 30 µm. A second treatment was based on PhytoMaxx (food type 2), a solution of living *Nannochloropsis* algae with 2 - 5 µm size range. A third treatment served as control, i.e., the animals were not fed with any additional food. In treatments with food type 1 and 2, microalgae were provided at the constant optimum concentration of 20×10^6 cells/liter (Winter, 1969). A dispenser equipped with a timer was used to distribute the food five times per day. At the end of the experiment the soft tissues were removed. A distinct dark line in the shells indicated the transposition to the NIOZ aquaria and the associated stress. This line marks the beginning of the tank experiment.

Sample preparation

The right valve of each specimen was cut into two 1.5 millimeter-thick sections along the axis of maximum growth. For this purpose, a low speed precision saw (Buehler Isomet 1000) was used. Given the small size and fragility of the juvenile shells used in the food experiment, the valves were fully embedded in a block of Struers EpoFix (epoxy) and air-dried overnight prior the sectioning. Sections of the clams used in the temperature experiment were embedded in epoxy after the cutting. All samples were ground using a Buehler Metaserv 2000 machine equipped with Buehler silicon carbide papers of different grit sizes (P320, P600, P1200, P2500). In addition, the samples were manually ground with Buehler P4000 grit paper and polished with a Buehler diamond polycrystalline suspension (3 µm). Sample surfaces were rinsed in demineralized water and air-dried. In the samples of the temperature experiment, the calcein marks were located under a fluorescence light microscope (Zeiss Axio Imager.A1m microscope equipped with a Zeiss HBO100 mercury lamp and filter set 38: excitation wavelength, ca. 450 - 500 nm; emission wavelength, ca. 500 - 550 nm).

***Arctica islandica* shell organization**

The shell of *A. islandica* consists of pure aragonite and it is divided in two major layers, an outer (OSL) and the inner shell layer (ISL). The OSL is further subdivided in outer (oOSL) and inner portion (iOSL) (Schöne, 2013). These layers are characterized by specific microstructures (Ropes et al., 1984; Fig. 3. 2). The oOSL largely consists of homogenous microstructure with granular aspect (Schöne et al., 2013). This type of architecture is characterized by approximately equidimensional units of about 5 µm in width. The unit shape tends to be irregular with a bulky aspect. The organization lacks of specific structural arrangement typical of other type of microstructures such as the crossed-lamellar and cross-acicular microstructures. The latter are the main component characterizing the iOSL and ISL (Dunca et al., 2009). Here, elongated units are arranged with two main dip directions, resulting in a relative oblique alignment. As shown in Fig. 3. 2, the elongation of the structures becomes more evident in the ISL.

The present study focuses on ventral margin of the shells. Analyses were carried out exclusively in the OSL.

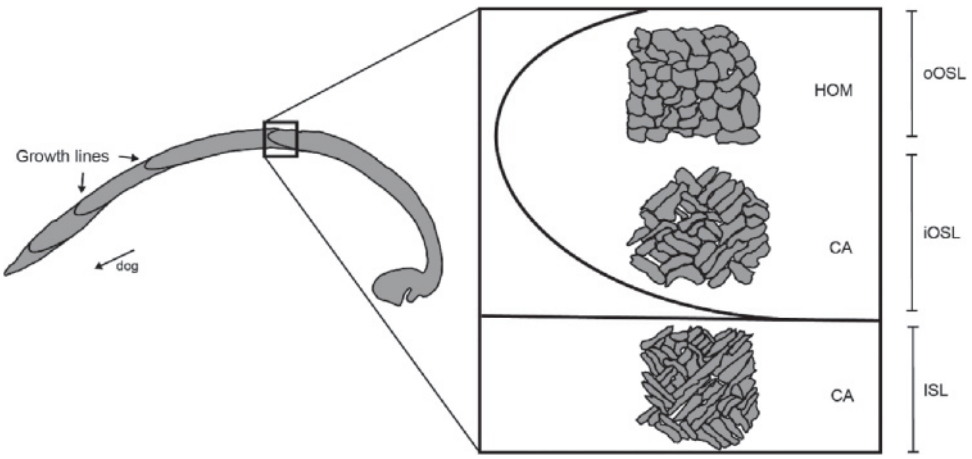

Fig. 3. 2: Sketch showing the microstructures characterizing the different shell layers of *Arctica islandica.* The oOSL is formed by homogenous microstructure (HOM), whereas the oOSL and ISL are composed of crossed acicular structure (CA). dog = direction of growth.

Similar to other mollusks, the shell of *A. islandica* contains pigment polyenes which are obviously visible when using CRM (Hedegaard et al., 2006). Polyenes are organic compounds containing single (C-C) and double (C=C) carbon-carbon bonds forming a polyenic chain. Their distribution across the shell is not homogenous. The pigments are abundant in the oOSL whereas they become scarce in the iOSL. Furthermore, an enrichment in polyenes has been observed in the growth lines, potentially indicating their involvement in the biomineralization process (Stemmer and Nehrke, 2014). However, the specific functions of these organic compounds have not been disclosed yet (Hedegaard et al., 2006; Karampelas et al., 2009). Given the high phenotypic variation in pigmentation among and within mollusk species, it has been proposed that coloration does not have a primary function as adaptive tool (i.e. camouflage, warning signaling) as in other animals (Seilacher, 1972; Evans et al., 2009). This, in turn, can indicate a certain degree of influence of the environment on the pigments, in particular by diet (Hedegaard et al., 2006; Soldatov et al., 2013). In the current study, the effect of different dietary regimes was tested in order to explore the potential of polyenes as environmental proxy.

Confocal Raman microscopy and image processing

Shells were mapped with a WITec alpha 300 R (WITec GmbH, Germany) confocal Raman microscope. Scans of 50 × 50 µm, 100 × 50 µm and 150 × 50 µm were performed using a piezoelectric scanner table. All Raman measurements were carried out using a 488 nm diode laser. A spectrometer (UHTS 300, WITec, Germany) was used with a 600 mm^{-1} grating, a 500 nm blaze and an integration time of 0.03 s. On each sample two to six scans were made, depending of the thickness of the shell. For instance, in juvenile shells (food experiment), two scans of each sample were made. On larger shells used in the temperature experiment, six maps were completed, i.e., two maps in the oOSL, two in the middle of the iOSL and two in the inner portion of the iOSL. Each scan contained between 40,000 and 120,000 data points, depending on the map size. The spatial resolution equaled 250 nm. Half of the maps were performed on the shell portion formed before the experiments. The other half were made on the shell portion formed under experimental conditions. In order to avoid areas affected by transplantation or marking stress, the scans were located far off the calcein and stress lines. Raman maps on food experiment shells

were performed 300 µm away from the stress line. In the shells from the temperature experiment, the scans were made 1 mm away from the calcein mark.

Polarized Raman microscopy is known to provide comprehensive information about the crystallographic properties of the materials (Hopkins and Farrow, 1985). The aragonite spectrum is characterized by two lattice modes (translation mode T_a, 152cm^{-1} and librational mode L_a, 206cm^{-1}) and the two internal modes (in-plane band v_4, 705cm^{-1} and symmetric stretch v_1, 1085cm^{-1}). The ratio ($R_{v1/Ta}$) between peak intensities belonging to v_1 and T_a is caused by different crystallographic orientations of the aragonitic units (Hopkins and Farrow, 1985; Nehrke and Nouet, 2011). Within each scan, $R_{v1/Ta}$ was calculated for each data point. New spectral images were generated using WITecProject software (version 4.1, WITec GmbH, Germany). These images were then binarized by replacing all values above 2.5 with 1 and the others with 0. The orientation was quantified by calculating the area formed by pixels of value 1 over the total scan area. The imaging software Gwyddion (http://gwyddion.net/last checked: June 2016) was used for this purpose. The results were expressed in percentage.

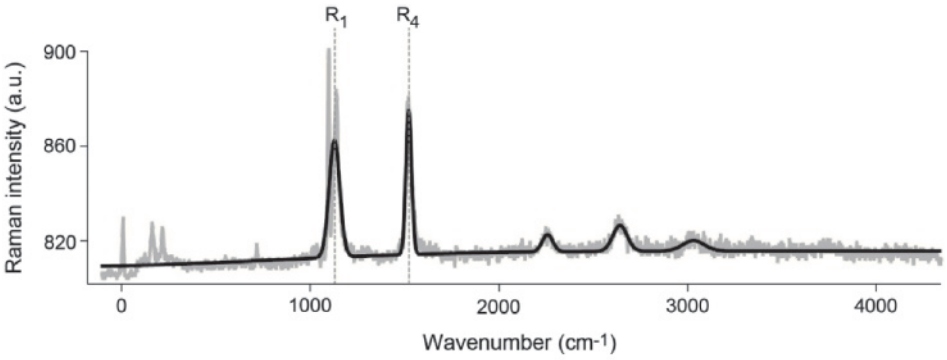

Fig. 3. 3: Raman spectrum of *Arctica islandica* showing the typical aragonite peaks (grey line). The exact position of the polyene peaks R_1 and R_4 was determined by using a peak fitting routine based on a Gaussian function (black line).

The Raman scans of the food experiment shells were analyzed to investigate the pigment composition. Polyene peaks have definite positions in the spectrum according to the number of the C-C and C=C bonds of the chain, which are specific for certain types of pigments. The two

major polyene peaks at ~ 1130 (R_1) and 1520 cm^{-1} (R_4) were identified by using the "multipeak fitting 2" routine of IGOR Pro (version 7.00, WaveMetrics, USA). Their exact position was determined adopting a Gaussian fitting function (Fig. 3. 3). The number of single (N_1) and double carbon bonds (N_4) was calculated by applying the equations by Schaffer et al. (1991):

(1) $N_1 = 476 (R_1 - 1{,}082)$

(2) $N_4 = 830 (R_4 - 1{,}438)$

Spectral images of the R_4 band were used to locate the polyenes in the shell and measure the thickness of the pigmented layer. The images were analyzed using the software Panopea (© Schöne and Peinl). The thickness of the pigmented layer was calculated as distance between the outer shell margin and the point where the concentration of polyenes suddenly declined. The measurements were taken perpendicular to the shell outer margin. This analysis was conducted only on the shells of the food experiment. Given the larger size of the shells used in the temperature experiment, the spectral maps were not sufficient for a correct localization of the pigmented layer boundaries and estimation of its thickness.

To quantify changes of the orientation of individual biomineral units of the juvenile shells (food experiment), the spectral maps were subdivided into two portions. The outermost shell portion (oOSL) was enriched in pigments whereas the iOSL showed a decrease in polyene content.

Scanning electron microscopy

After performing Raman measurements, the samples were prepared for SEM analysis. Each shell slab was ground with a Buehler Metaserv 2000 machine and Buehler silicon F2500 grit carbide paper. To reduce the impact of grinding on the sample surface of juvenile shells, extra grinding was done by hand. Then, the slabs were polished with a Buehler diamond polycrystalline suspension (3 µm). Afterward, shell surfaces were etched in 0.12 N HCl solution for 10 (food experiment samples) to 90 s (temperature experiment samples) and subsequently placed in 6 vol % NaClO solution for 30 min. After being rinsed in demineralized water, air-dried samples were sputter-coated with a 2 nm-thick platinum film by using a Low Vacuum Coater Leica EM ACE200.

A scanning electron microscope (LOT Quantum Design 2nd generation Phenom Pro desktop SEM) with backscattered electron detector and 10 kV accelerating voltage was used to analyze

the shells. Images were taken at the same distances from the calcein and stress lines as in the case of the Raman measurements to assure comparability of the data.

In addition, stitched SEM images of the ventral margins were used to accurately determine the shell growth advance during the culturing experiments. Growth increment widths were measured with the software Panopea. Given the difference in duration of the two phases of the temperature experiment, the measurements were expressed as total growth and instantaneous growth rate (Fig. 3. 4a + b). The latter was calculated using the following equation (Brey et al., 1990; Witbaard et al., 1997a):

(3) Instantaneous growth rate = (ln (y_t / y_0) / a)

where y_0 represents the initial shell height, y_t is the final shell height and a is the duration of the experiment. In the case of the food experiment, only the total growth was calculated (Fig. 3. 4c).

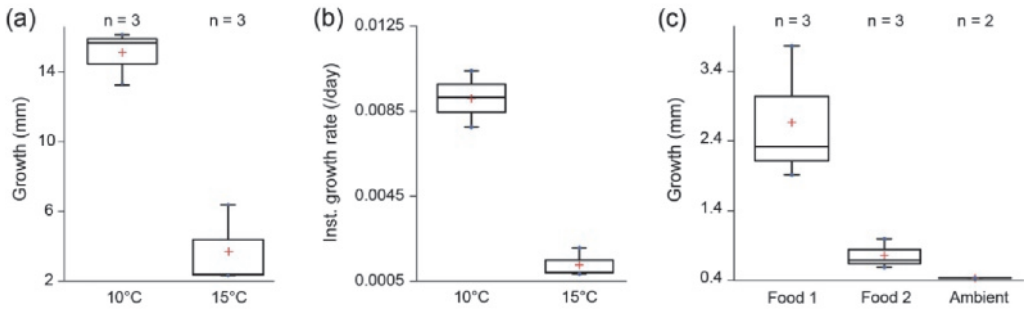

Fig. 3. 4: *Arctica islandica* shell growth under controlled conditions. (a) Total growth and (b) instantaneous growth rate during the temperature experiment. (c) Total growth during the food experiment.

RESULTS

Effect of seawater temperature and diet on *A. islandica* shell growth

When exposed to a water temperature of 10 °C, the shells grew between 11.67 and 14.17 mm during a period of 48 days. During a period of 69 days at 15 °C, the growth ranged between 2.32

and 5.77 mm (Fig. 3. 4a). Instantaneous growth rate showed a decrease between the two experimental phases. At 10 and 15 °C, the average instantaneous growth per day was 0.0091 and 0.0013, respectively (Fig. 3. 4b). The decrease in total growth and growth rate between the two temperatures was statistically significant (*t*-test, $p < 0.01$).

During the food experiment, shells grew between 0.37 and 3.71 mm with large differences due to the different food types. Growth of specimens exposed to food type 1 ranged between 1.87 to 3.71 mm, whereas those cultured with food type 2 grew between 0.55 to 0.96 mm. Both control specimens added 0.37 mm of shell during the experimental phase (Fig. 3. 4c). ANOVA and Tukey´s HSD post hoc tests showed significant differences between specimens cultured with food type 1 and 2 ($p < 0.05$) and between food type 1 and control shells ($p < 0.05$).

Effect of seawater temperature on *A. islandica* microstructure

At a water temperature of 10 °C, the area occupied by microstructural units oriented with $R_{v1/Ta}$ higher than 2.5 a.u. (= arbitrary units) ranged between 31.3 and 50.6 % in the oOSL and between 21.3 and 33.5 % in the iOSL. When exposed to 15 °C, values ranged between 25.6 and 48.7 % and between 45.7 and 55.9 % in the oOSL and iOSL, respectively (Fig. 3. 5). Whereas the slight difference of area with $R_{v1/Ta} > 2.5$ in the oOSL was not significant between the two water temperatures (*t*-test, $p = 0.62$), the area with $R_{v1/Ta} > 2.5$ in the iOSL significantly increased at 15 °C (*t*-test, $p = 0.02$). Under the SEM, no difference was visible between units formed at 10 °C and 15 °C (Fig. 3. 6).

Effect of food on *A. islandica* microstructure and pigments

In the shells cultured with food type 1, the area occupied by biomineral units oriented with $R_{v1/Ta}$ higher than 2.5 a.u. during the experiment ranged between 24.8 % (oOSL) and 43.0 % (iOSL). In the shell portion deposited during the acclimation phase, the ratio varied between 19.4 % (oOSL) and 36.2 % (iOSL). Although a trend was recognized, these variations were not statistically different (*t*-tests. OSL: $p = 0.43$; ISL: $p = 0.57$; Fig. 3. 7a). On the contrary, in the clams exposed to food type 2, the area occupied by units oriented with $R_{v1/Ta} > 2.5$ ranged between 11.7 % (oOSL) and 20.4 % (iOSL). Before the experiment, the proportions were higher, i.e., 18.1% (oOSL) and

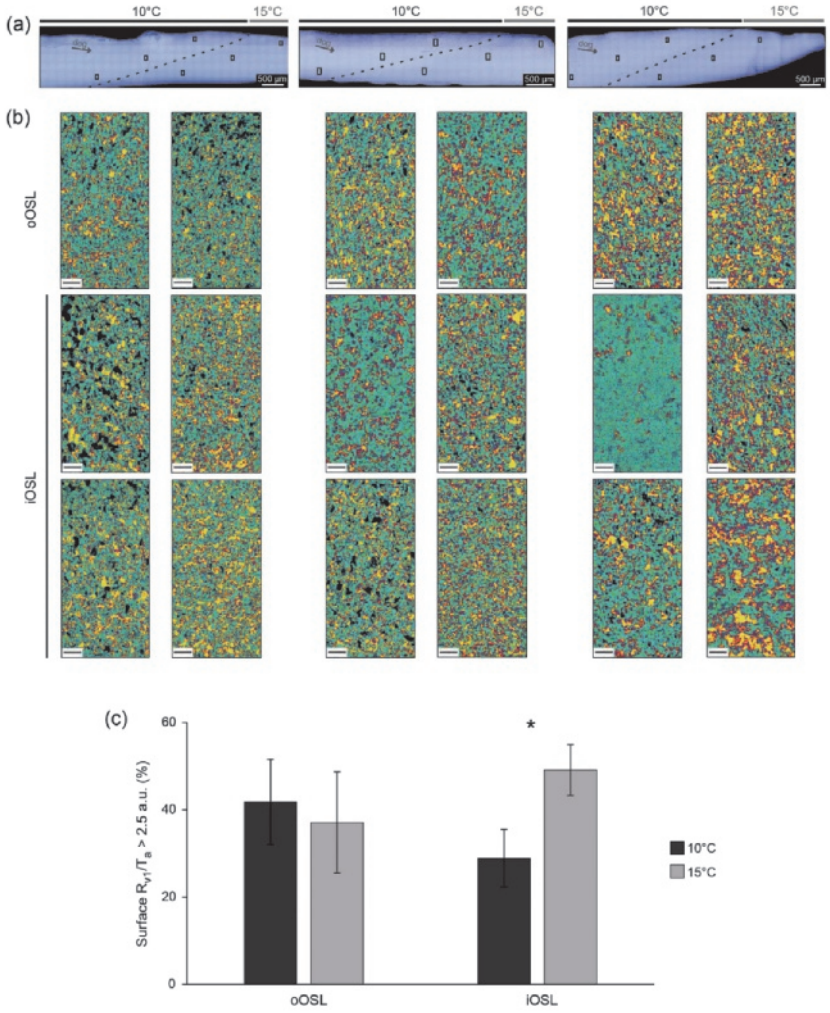

Fig. 3. 5: Effect of temperature increase on biomineral orientation. (a) Position of the Raman maps of the three specimens reared at 10 °C and 15 °C. Dotted lines indicate the location of the calcein marks. dog = direction of growth. (b) Raman spectral maps of $R_{v1/Ta}$. Left images of each column represents shell portion formed at 10 °C, right images represent shell portions formed at 15 °C. First row of pairs refers to oOSL, the other two represent the iOSL. Scale bars = 10 µm. (c) Proportions of biominerals with $R_{v1/Ta}$ > 2.5 a.u. with respect to the total map area. Asterisks indicate significant difference between the orientation of iOSL microstructures formed at 10 and 15°C ($p < 0.05$).

26.3% (iOSL) (Fig. 3. 7b). As for the other treatment, the difference was not significant (*t*-tests. oOSL: $p = 0.34$; iOSL: $p = 0.28$). In the control shells grown with no extra food supply, the area with $R_{v1/Ta} > 2.5$ ranged between 24.6 % (oOSL) and 44.8 % (iOSL) during the experiment and 21.2 % (oOSL) and 44.5 % (iOSL) before the experiment (Fig. 3. 7c). Hence, no trend was visible and the two portions did not show significant differences (*t*-tests. oOSL: $p = 0.59$; iOSL: $p = 0.99$). As for the temperature experiment, under the SEM, the microstructure of the shells from the food experiment did not show any change (Fig. 3. 9).

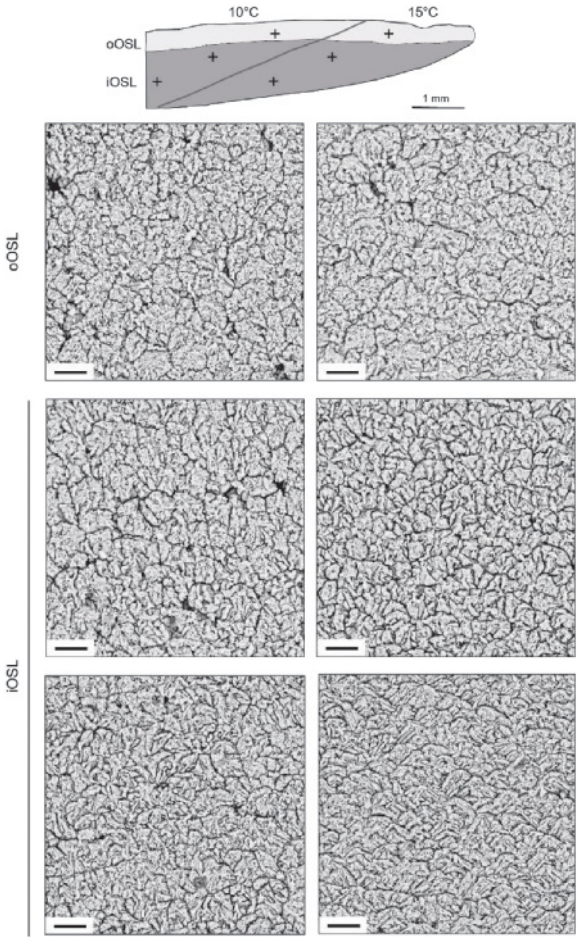

Fig. 3. 6: SEM images of *Arctica islandica* shell microstructures formed at 10 °C (left column) and at 15 °C (right column). The sketch indicates the position of the images 1 mm away from the calcein mark (grey line). The first row of images refers to the oOSL, the other two row refers to the iOSL. Scale bars if not otherwise indicated = 5 µm.

All treatments showed a slightly thicker pigmented layer formed during the experiment than during the acclimation phase (Fig. 3. 9a). During the experiment, clams cultured with food type 1 showed, on average, a thickening by 6.4 %. In the food type 2 specimens, the layer thickness increased by 9.9 %. Control shells showed an increase of 10.4 % (Fig. 3. 9b). However, none of these differences was statistically significant (*t*-test. Food type 1: $p = 0.43$; Food type 2: $p = 0.39$; Control: $p = 0.10$). According to the position of the polyene peaks, the number of single carbon bonds in the pigment chain did not change between the acclimation and experimental phase ($N_1 = 10.1 \pm 1.3$ and $N_1 = 10.0 \pm 0.9$, respectively). Likely, no significant variation was observed in the number of double carbon bonds ($N_4 = 10.5 \pm 0.2$ and $N_4 = 10.4 \pm 0.3$, respectively; Table 3.2).

Table 3. 2: Details of the pigment composition of the *Arctica islandica* shells used in the food experiment. The position of the major polyene peaks R_1 and R_4 in the Raman spectrum is indicated together with the number of single and double carbon bonds of the pigment molecular chain (N_1 and N_4). Each shell was analyzed in the portions formed before and during the experimental phase.

Sample ID	Shell portion	R_1 (cm^{-1})	R_4 (cm^{-1})	N_1	N_4
	Food 1	1121.4	1515.3	12.1	10.7
S14	Acclimation	1133.2	1519.4	9.3	10.2
	Food 1	1132.2	1518.6	9.5	10.3
S15	Acclimation	1129.5	1516.5	10.0	10.6
	Food 1	1132.1	1519.8	9.5	10.1
G11	Acclimation	1132.6	1518.4	9.4	10.3
	Food 2	1129.5	1517.0	10.0	10.5
G12	Acclimation	1131.7	1518.7	9.6	10.3
	Food 2	1132.1	1518.2	9.5	10.4
G15	Acclimation	1132.4	1519.5	9.4	10.2
	Food 2	1128.0	1520.9	10.3	10.0
N13	Acclimation	1130.2	1515.6	9.9	10.7
	Ambient food	1131.4	1514.1	9.6	10.9
N15	Acclimation	1117.9	1516.0	13.3	10.6
	Ambient food	1130.7	1517.0	9.8	10.5
Average	1129.7 ± 4.2	1517.5 ± 2.0	10.1 ± 1.1	10.4 ± 0.3	1129.7 ± 4.2

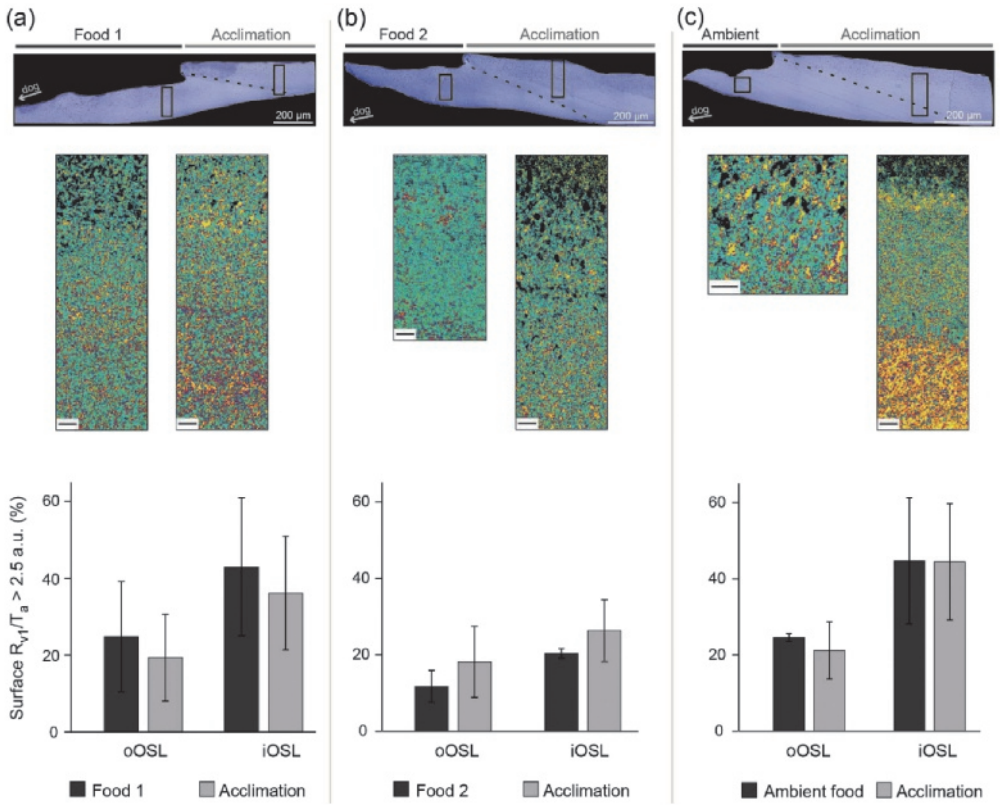

Fig. 3. 7: Effect of different diets based on (a) food type 1, (b) food type 2 and (c) ambient food on biomineral orientation. The optical microscope images indicate the position of the Raman scans. Dotted line marks the start of the experiment. The portion of shell prior the line was formed during the acclimation phase. dog = direction of growth. The Raman spectral maps indicate the ratio $R_{v1/Ta}$ for each data point of the scan. For each shell, maps on the left represent shell portions during the experiment, maps on the right represent shell portions formed during the acclimation phase. In the acclimation portion of the sample reared with ambient food, a significant change in the microstructure orientation is visible. The respective area of the Raman map was not considered in further calculations because it was influenced by the emersion and transportation stress at the start of the experiment. Scale bars = 10 µm. The graphs show the proportions of biominerals of oOSL and iOSL with $R_{v1/Ta}$ > 2.5 a.u. with respect to the total map area.

DISCUSSION

According to the results, variations of both food type and water temperature can influence the shell production rate of *A. islandica.* However, the shell microstructure and pigmentation react differently to these two environmental variables. Whereas changes of the dietary conditions do not affect the shell architecture and pigment composition, the crystallographic orientation of the biomineral units responds to seawater temperature fluctuations.

Environmental influence on shell microstructure

The environmental conditions experienced by mollusks during the process of biomineralization appear to influence shell organization (Carter, 1980). Among the different environmental variables, water temperature is the most studied driving force of structural changes of the shell. For instance, shell mineralogy can vary depending on water temperature (Carter, 1980). According to the thermal potentiation hypothesis, nucleation and growth of calcitic structural units is favored at low temperatures by kinetic factors (Carter et al., 1998). As a consequence, bivalve species living in cold water environments exhibit additional or thicker calcitic layers compared to the corresponding species from warm waters (Lowenstam, 1954; Taylor and Kennedy, 1969). Changes in the calcium carbonate polymorph also affect the type of microstructures (Milano et al., 2016a). However, architectural variations often occur without mineralogical impact (Carter, 1980).

The present results indicate that temperature induces a change in the crystallographic orientation of the biomineral units of *A. islandica*. Although water temperature was previously shown to have an impact on microstructure formation, the attention has been mainly addressed to the effects on the morphometric characteristics (e.g. size and shape) or on the type of microstructure. Milano et al. (2017b) demonstrated that size and elongation of prismatic structural units of *Cerastoderma edule* were positively correlated to seawater temperature variation throughout the growing season. Likely, low temperatures induced the formation of small nacre tablets in *Geukensia demissa* (Lutz, 1984). Seasonal changes of the microstructural type were reported in the freshwater bivalve *Corbicula fluminea* (Prezant and Tan Tiu, 1986; Tan

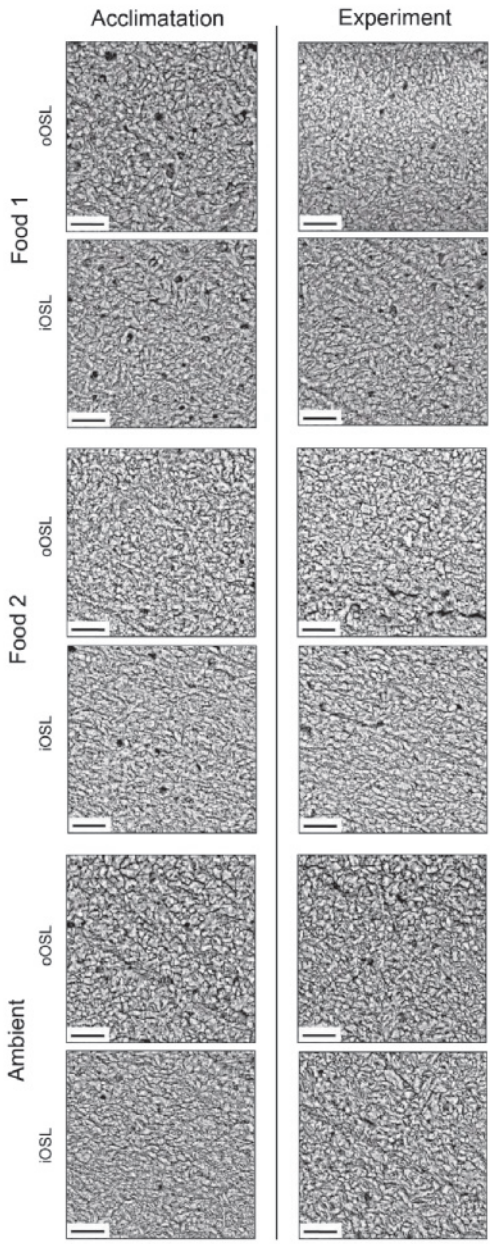

Fig. 3. 8: SEM images of *Arctica islandica* shell microstructures formed during the acclimation phase at AWI (left column) and during the food experiment (right column). Scale bars = 4 µm.

Tiu and Prezant, 1989). During the warm months, crossed acicular structure was produced, whereas simple crossed-lamellae were formed during the winter period. So far, variations of the crystallographic properties of bivalve biominerals have been exclusively investigated as a response to hypercapnic (acidified) conditions. *Mytilus galloprovincialis* and *Mytilus edulis* showed a significant change in the orientation of the prisms forming shell calcitic layer when subjected to hypercapnia (Hahn et al., 2012; Fitzer et al., 2014). Altered crystallographic organization may derive from the animal exposure to suboptimal conditions. These findings together with the present results suggest that thermal- and hypercapnic-induced stress are likely to affect the ability of the bivalves to preserve the orientation of their microstructural units (Fitzer et al., 2015).

Different food sources do not significantly influence the orientation of the biomineral units or the composition and distribution of pigments in shells of *A. islandica*. In previous studies, the relationship between microstructure and diet was virtually overlooked resulting in a lack of data in the literature. As suggested by Hedegaard et al. (2006), however, the type of polyenes is influenced by food. The ingestion of pigment-enriched microalgae potentially leads to an accumulation of pigments in mollusk tissues and the shell (Soldatov et al., 2013). On the other hand, it has been argued that polyenes do not generate from food sources like other pigments (i.e., carotenoids), but they are locally synthesized (Karampelas et al., 2009). In accordance to Stemmer and Nehrke (2014), the results presented here support the view that the specific diets on which the animals rely on do not influence shell pigment composition. The chemical characteristics of the polyenes are likely to be species-specific and independent from the habitats.

Confocal Raman microscopy as tool for microstructural analysis

From a methodological perspective, the present study represents an innovative approach in the investigation of shell microstructural organization. Electron backscatter diffraction (EBSD) has been previously used to determine the crystallographic orientation of gastropod (Fryda et al., 2009; Pérez-Huerta et al., 2011) and bivalve microstructural units (Checa et al., 2006; Frenzel et al., 2012; Karney et al., 2012). Whereas, CRM on mollusk shells is generally applied within studies on taphonomic mineralogical alteration and pigment identification (Stemmer and Nehrke, 2014;

Beierlein et al., 2015). Both techniques provide considerably high spatially resolved analysis up to 250 nm, allowing the identification of individual structural units at µm- and nm-scale (Cusack et al., 2008; Karney et al., 2012). CRM offers important advantages supporting a broader application of this methodology in the biomineralization research field. For instance, samples do not require any pre-treatment. Unlike EBSD, there is no need of preparing thin-sections (~ 150 µm thick) or etching the shell surface (Griesshaber et al., 2010; Hahn et al., 2012). Therefore, further structural and geochemical analyses can be easily performed on the same sections (Nehrke et al., 2012). In addition, the size of CRM scans can be remarkably large (~ 7-8 mm^2) without compromising the achievable resolution. By overlapping adjacent scans, it is possible to produce stitched scans allowing to further increase the region of interest on the shell surface. On the other side, EBSD provides a relevant advantage to take into consideration. It allows absolute measures of the crystallographic orientation of the carbonate structures. The CRM, instead, determines the relative change in the orientation between the single units without providing absolute values.

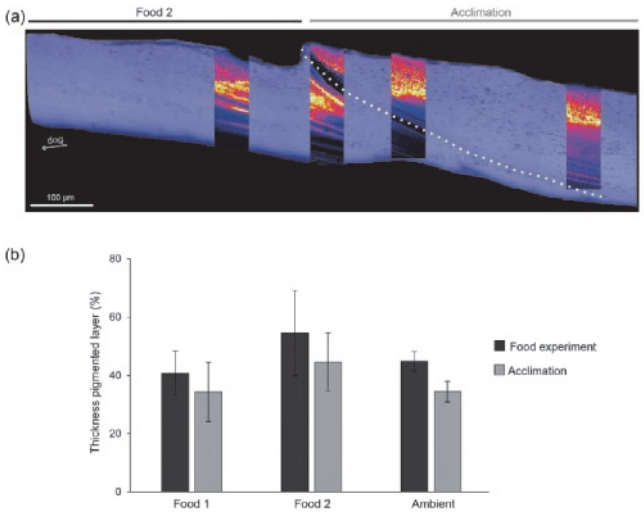

Fig. 3. 9: Effects of diet on shell pigment distribution. (a) Raman spectral maps of the 1524 cm^{-1} band representing the distribution of the polyenes in the shell cultured with food type 2. Dotted line marks the start of the experiment. dog = direction of growth. (b) The graph shows the thickness of the pigmented layer over the whole shell thickness before and during the food experiments.

SEM has previously been demonstrated to provide a convenient approach for the identification of individual structural units and the quantification of potential changes occurring within them (Milano et al., 2017b, 2016b). However, SEM exclusively provides information about the morphometric characteristics of the microstructural units. As highlighted by the present study, to achieve an exhaustive examination, it is suggested to combine SEM with techniques assessing crystallographic properties of the biomaterials. For instance, our results show that the effect of water temperature is detectable in crystallographic orientation but not in morphometric features of the biomineral units.

Environmental influence on shell growth

Numerous previous studies demonstrated that growth rate of *A. islandica* is linked to environmental variables (e.g., Witbaard et al., 1997a, 1999; Schöne et al., 2004; Butler et al., 2010; Mette et al., 2016). However, the relative importance of the main factors, temperature and food supply/quality driving shell formation are still not well understood. Positive correlations between shell growth and water temperature have been identified (i.e., Schöne et al., 2005b; Wanamaker et al., 2009; Marali et al., 2015), but the relationship between shell growth and environment is more complex (Marchitto et al., 2010; Stott et al., 2010; Schöne et al., 2013) and likely dependent on the synergic effect of food availability and water temperature (Butler et al., 2013; Lohmann and Schöne, 2013; Mette et al., 2016). Tank experiments were run in order to precisely identify the role of these two parameters of shell growth of *A. islandica* (Witbaard et al., 1997a; Hiebenthal et al., 2012). A tenfold increase in instantaneous growth rate was observed between 1 and 12 °C, with the greatest variation occurring below 6 °C (Witbaard et al., 1997a). On the contrary, a temperature increase between 4 and 16 °C was shown to produce a slowdown of shell production (Hiebenthal et al., 2012). Our results are in agreement with the latter study and show a decrease in the instantaneous growth rate between 10 and 15 °C. High temperatures are often associated with an increase of free radical production (Abele et al., 2002). A large amount of energy then has to be allocated to limit oxidative cellular damage (Abele and Puntarulo, 2004). This translates into a higher accumulation of lipofuscin and slower shell production rate (Hiebenthal et al., 2013). The contrasting results of previous studies may be

explained by individual differences in the tolerance toward temperature change (Marchitto et al., 2000).

Along with water temperature, food availability was also shown to influence *A. islandica* shell growth (Witbaard et al., 1997a). At high algal cell densities, the siphon activity increased. This, in turn, was positively correlated to shell growth. Previous experiments used different combinations of algae such as *Isochrysis galbana* and *Dunaliella marina* (Witbaard et al., 1997a), or *Nannochloropsis oculata, Phaeodactylum tricornutum* and *Chlorella* sp. (Hiebenthal et al., 2012) to grow the clams. However, there are still uncertainties about the composition of the primary food source for this species (Butler et al., 2010). Even though it is challenging to determine the preferred algal species, our results show that the use of a mixture of different algal species results in significantly faster shell growth than the used of just one algal species. In the natural environment, suspension feeders such as *A. islandica* preferentially ingest certain particle sizes (Rubenstein and Koehl, 1977; Jorgensen, 1996; Baker et al., 1998). The exposure to a limited algal size range, as in the case of food type 2, may affect shell growth. Furthermore, multispecific solutions contain a higher variability of biochemical components that better meet the nutritional requirements of the animal (Widdows, 1991). Our results are in good agreement with previous findings. For instance, it has been shown by Strömgren and Cary (1984) that *Mytilus edulis* shell growth increased as a result of a diet based on three different algal species. Furthermore, Epifanio (1979) tested the differences on the growth of *Crasssostrea virginica* and *Mercenaria mercenaria* of a mixed diet composed by *Isochrysis galbana* and *Thalassiosira pseudonana* and diets consisting of the single species. Faster growth was measured in the mixed diet treatment, indicating a synergic effect of the relative food composition (Epifanio, 1979). Likely, *Mytilus edulis* grew faster when reared with different types of mixed diets as opposed to monospecific diets (Galley et al., 2010).

CONCLUSIONS

Arctica islandica shell growth and biomineral orientation vary with changes in seawater temperature. However, exposure to different food sources affect shell deposition rate but do not

influence the organization of the biomineral units. Given the exclusive sensitivity to one environmental variable, the orientation of biomineral units may represent a promising new temperature proxy for paleoenvironmental reconstructions. However, additional studies are needed to further explore the subject. In particular, intra-individual variability influence on the results needs to be assessed. In the present study, a variation in the orientation between individuals was well visible and the risks associated have to be taken in account when considering further application of the possible proxy. Furthermore, the effect of other environmental variables such as salinity needs to be tested.

The innovative application of CRM for microstructural orientation and proxy development proved that the technique has large potential in this research direction. More studies are needed to validate its suitability in paleoclimatology experimental works.

Acknowledgements

The authors acknowledge the crew of the *F.V. Three of a Kind* for helping with the collection of the Maine animals and to Cyril Degletagne and Doris Abele for providing the Baltic specimens used in this study. Design and execution of the seawater temperature experiment were successfully realized thanks to the support of B. Beal, D. Gillikin, A. Lorrain and the Darling Marine Center scientific team. Funding for this study was kindly provided by the EU within the framework of the Marie Curie International Training Network ARAMACC (604802).


5
h
E
2
1
0

Chapter 4

Interactive effects of temperature and food availability on the growth of *Arctica islandica* (Bivalvia) juveniles

Ballesta-Artero, Irene; Janssen, Reneé; van der Meer, Jaap; Witbaard, Rob

Published in Marine Environmental Research 133:67-77 (2018)

Abstract

The interest in *Arctica islandica* growth biology has recently increased due to the widespread use of its shell as a bioarchive. Although temperature and food availability are considered key factors in its growth, their combined influence has not been studied so far under laboratory conditions. We tested the interactive effect of temperature and food availability on the shell and tissue growth of *A. islandica* juveniles (9-15 mm in height) in a multi-factorial experiment with four food levels (no food, low, medium, and high) and three different temperatures (3, 8, 13 °C). Shell and tissue growth were observed in all treatments, with significant differences occurring only among food levels (2-way ANOVA; P-value < 0.05). Siphon activity (% open siphons), however, was affected by temperature, food, and the interaction between them (2-way ANOVA; P-value < 0.05). Siphon observations, as indication of feeding activities, played a key role to better understand the growth variation between individuals.

Keywords

Bivalve, shell and tissue growth, temperature, phytoplankton concentration, siphon activity, sclerochronology

INTRODUCTION

In sclerochronology, shell growth increments are used for retrospective climate studies, in the same way as growth rings of trees are used in dendrochronology (Jones, 1980; Witbaard et al., 1994; Karney et al., 2011). Based on *Arctica islandica* annual growth increments, it is possible to distinguish periods of rapid and slow growth to create shell-growth chronologies (Schöne and Gillikin, 2013). These chronologies can be coupled with local environmental records, providing insight into past environmental and ocean climatic conditions (Schöne et al., 2003; Witbaard et al., 2003; Butler et al., 2013; Mette et al., 2016).

The long-living bivalve *A. islandica* can be found on both sides of the North Atlantic: from Cape Hatteras to the Canadian arctic, and from the North Sea to the Barents Sea, including Iceland (Jones, 1980; Dahlgren et al., 2000). This species has an optimal thermal range between 6-16 °C (Golikov and Scarlato, 1973; Cargnelli et al., 1999; Zettler et al., 2001; Begum et al., 2009), but tolerates temperatures between 0 and 20 °C (Kraus et al., 1992; Witbaard et al., 1997a; Hippler et al., 2013). With a lifespan of up to 507 years (Marchitto et al., 2000; Schöne et al., 2005b; Wanamaker et al., 2008a; Butler et al., 2013), its growth rate is characterized by a sharp decrease after the first 20 years of life (Thompson et al., 1980a; Kennish et al., 1994). Shell length can reach a maximum size of ~14cm (Ropes, 1985). However, size may not be a strong indicator of age since there is geographical variation in the growth of the species (Ropes, 1985; Witbaard et al., 1999).

There is a lack of consensus about the intra-annual timing of shell growth in *A. islandica*, the period during which the annual growth increment is formed, and the main environmental forces regulating its growth. The growing season has been defined from eight months (Weidman et al., 1994; Schöne et al., 2005a; Dunca et al., 2009; Ballesta-Artero et al., 2017) to twelve months (Jones, 1980; Wanamaker et al., 2008a; Mette et al., 2016). Further, the shell growth rate has been assumed both as being constant throughout the growing season (Weidman et al., 1994; Marchitto et al., 2000), or, alternately, exhibiting intra-annual variability (Witbaard et al., 2003; Witbaard and Hippler, 2009; Schöne et al., 2005a; Dunca et al., 2009; Wanamaker et al., 2008a; Mette et al., 2016). Lastly, the cessation of the main growing season has been proposed as occurring during autumn/winter (Jones, 1980; Murawski et al., 1982; Weidman et al., 1994;

Schöne et al., 2005a), early spring (Mette et al., 2016), or late summer (Witbaard et al., 2003; Dunca et al., 2009; Ballesta-Artero et al., 2017). Studies from different locations, e.g. from the New Jersey Coast (Jones, 1980), Middle Atlantic Bight (Murawski et al., 1982), Nantucket Shoals (Weidman et al., 1994), Fladen Ground (Witbaard et al., 1997b; Witbaard et al., 2003; Butler et al., 2009), North and Baltic Seas (Schöne et al., 2005a), Gulf of Maine (Wanamaker et al., 2008a), Swedish West Coast (Dunca et al., 2009), and Northern Norway (Mette et al., 2016; Ballesta-Artero et al., 2017), suggest that different environmental conditions play key roles in explaining the variability in the length or timing of the growing season. Therefore, the specific mechanistic link between shell growth and the environment has to be well understood, to not limit the utility of this species as a retrospective monitor of ocean conditions.

In situ observational studies on juvenile *A. islandica* in the Baltic Sea and the Gulf of Maine showed variable shell growth. In Maine, growth rates ranged between 0.50-76.67 µm d^{-1} (Lutz et al., 1983; Kraus et al., 1992; Kennish et al., 1994). In the Baltic Sea, Brey et al. (1990) found growth rates between 12.60-36.71 µm d^{-1}. Hippler et al. (2013) found a maximum growth rate of 157 µm d^{-1} with Baltic specimens cultivated in the NIOZ harbor (Texel Island, the Netherlands). All these authors hypothesized that the different growth rates were mainly the result of different environmental conditions, highlighting the importance of food availability and water temperature in the study areas.

Under laboratory conditions, Witbaard et al. (1997a) tested the effect of five different food levels at 9° C, and the effect of five different temperatures at optimal food conditions (>10x10^6 cells L^{-1}; Winter, 1969) on the growth of *A. islandica*. There was a tenfold increase in shell height between 1°C and 12 °C, with a maximum growth rate of 74 µm d^{-1} (Witbaard et al., 1997a; Hippler et al., 2013). Witbaard et al. (1997a) also reported an increase of siphon activity at higher food concentrations, corresponding with greater shell and tissue growth. Other laboratory studies tested the combined effects of temperature and salinity as well as temperature and acidification on specimens collected from the Baltic Sea (Hiebenthal et al., 2012; Hiebenthal et al., 2013). The average growth rate per treatment was between 2.86- 25.71 µm d^{-1} (Hiebenthal et al., 2012; Hiebenthal et al., 2013). These studies showed that acidification did not have an influence on *A. islandica* shell growth; however, high temperature (16 °C) and low salinity (15) resulted in

decreased growth rate. Milano et al. (2017b) tested the effect of temperature (10 and 15° C) and diet (three types) on the microstructural organization of *A. islandica* shells. In their food experiment (performed on shells from Baltic Sea), they found higher growth rates (41.22 µm d^{-1}) at the most biodiverse diet, i.e., the one composed of different phytoplankton species. In their temperature experiment (executed on shells from Maine), the specimens at 10 °C had the highest growth rate reported so far under experimental conditions i.e. 295.21 µm d^{-1} (Milano et al., 2017a).

The combined effects of temperature and food availability have not yet been studied in a single multi-factorial experiment. Most existing studies have focused on a single parameter and did not take into account the possible interaction between environmental factors (e.g., Witbaard et al., 1997a; Milano et al., 2017a). Therefore, to improve paleoclimatic reconstructions based on *A. islandica* shell chronologies, a better understanding of the relationship between food, temperature and growth is necessary. Thus, we analyzed the interactive effects of temperature and food availability on the shell and tissue growth of *A. islandica*. Furthermore, we studied siphon activity as an indication of feeding activity. We aim to clarify the diversity of results found on *A. islandica* growth rate relative to two key environmental factors: temperature and food availability.

METHODS

Experimental setup

Living juveniles of *Arctica islandica* (< 20mm; 1-3 years old) were collected in July 2014 from Kiel Bay, Baltic Sea (54° 32' N, 10° 42'E). They were transferred to the Alfred Wegener Institute (AWI, Bremerhaven) where they were kept at 7ºC and salinity 21 for 6 months. During this period, the individuals were fed with a microalgae mix of *Nannochloropsis* sp*., Isochrysis galbana*, and *Pavlova lutheri.* In January 2015, they were transported to NIOZ (Texel) under refrigerated conditions. They were placed in small aquaria with aerated seawater inside a controlled climate room (air temperature 9 ºC). Seawater temperature varied between 8 and 10 ºC and salinity between 29 and 30. *A. islandica* specimens were fed twice per week with a commercial mix of

marine microalgae: *Isochrysis sp., Tetraselmis sp., Paulova sp., Thalassiosira sp.* and Nannochloropsis spp (Mixalgae; www. acuinuga.com). They were kept under these conditions for a year.

In February 2016, 250 individuals (of ~400) were randomly selected for the growth experiment and subdivided among four 15-liters aquaria for acclimation to their target temperatures (about 1°C change per day). These animals were fed with Mixalgae twice per day during one month (February 22nd to March 22nd, 2016) to achieve similar body conditions. Optimal food concentration level (10 -11 x10^{6}cells L^{-1}; Winter, 1969) was maintained until the beginning of the experiment**.** Cell concentration of the water was measured using a BD Accuri C6 flow cytometer.

The starting shell height of the experimental animals ranged between 7.86 and 15.48 mm (± 0.01). Prior to the start of the experiment, the specimens were soaked in a calcein solution of 125mg L^{-1} for 24 hours (Linard et al., 2011; Ambrose et al., 2012). Calcein is a non-toxic fluorescent dye which becomes incorporated in the shell and that gives a shell time marker for growth studies (Linard et al., 2011; Ambrose et al., 2012). The experiment was done under dimmed light conditions, and took place during spring (March 22nd to June 23rd, 2016; 14 weeks) to avoid undesirable effects on growth due to autumn/winter physiological state of the specimens (Hiebenthal et al., 2013; Ballesta-Artero et al., 2017).

Experimental design

The experimental set-up had 12 treatments: all combinations of four food levels (no ; low: 0.5 x10^{6} phytoplankton cells L^{-1}; medium: 5 x10^{6} cells L^{-1}; and high:15x10^{6} cells L^{-1}) and three different temperatures (3°C, 8°C, and 13 °C; see Table 4. 1 for more details). There were 3 replicates per treatment (3 aquaria), which meant a total of 36 aquaria (4 food levels x 3 temperatures x 3 replicates). Five *A. islandica* juveniles were randomly assigned to each aquarium, amounting to a total 180 *A. islandica* specimens. Since individual specimens within one experimental unit (aquarium) are interdependent pseudo-replicates, single average values for mortality, siphon activity, shell and tissue growth were calculated for each aquarium separately. Thus, we present the average response of all individuals within each aquarium (replicate); in particular, the specific combination of food and temperature of that aquarium.

Each aquarium measured 30x40x17 cm (polypropylene; www.hulkenberg.nl) and contained 15 liters of aerated seawater. This volume was refreshed at a rate of 600 mL h^{-1} (~100 % d^{-1}) with fresh filtered seawater taken from the Marsdiep tidal inlet. Suspended material was filtered out over sandbed filters. Fresh water was cooled or heated before it arrived to the experimental set up so that the right temperature was constantly maintained in the experimental aquaria.

Table 4. 1: Summary of treatments.

	3°C	**8°C**	**13°C**
No food			
Target concentration (cells L^{-1} x 10^6)	0	0	0
Actual concentration (cells L^{-1} x 10^6)	0.04 ± 0.03	0.04 ± 0.00	0.03 ± 0.02
Mg dry weight ind^{-1} d^{-1}	-	-	-
Low food			
Target concentration (cells L^{-1} x 10^6)	0.50	0.50	0.50
Actual concentration (cells L^{-1} x 10^6)	0.85 ± 0.43	0.22 ± 0.02	0.53 ± 0.18
Mg dry weight ind^{-1} d^{-1}	0.62	0.62	0.62
Medium food			
Target concentration (cells L^{-1} x 10^6)	5	5	5
Actual concentration (cells L^{-1} x 10^6)	6.19 ± 0.64	2.34 ± 0.17	1.53 ± 0.05
Mg dry weight ind^{-1} d^{-1}	5	5	5
High food			
Target concentration (cells L^{-1} x 10^6)	15	15	15
Actual concentration (cells L^{-1} x 10^6)	24.56 ± 2.85	12.99 ± 0.82	6.45 ± 2.08
Mg dry weight ind^{-1} d^{-1}	14	14	14
Actual temperature (°C)	2.49 ± 0.02	7.94 ± 0.07	13.11 ± 0.05
Salinity	30.26 ± 0.10	30.38 ± 0.08	29.39 ± 0.24

To reach the desired micro-algal concentrations (Table 4. 1), the estimated filtration rate per individual (~350 mL h^{-1}; Winter, 1969) and the water flux (600 mL h^{-1}) were considered as loss factors, from which the amounts to be added to each treatment were determined. Due to the importance of a constant food supply on bivalve's growth (Langton and McKay, 1976; Winter and Langton, 1976), food was provided eight times per day, every three hours using a peristaltic pump and a timer. During the entire experiment, the amount of added food was kept constant at each food level (Table 4.1). Every second day, a new food batch was prepared. The amount of concentrated algal suspension needed (for the three replicates of each treatment) was diluted with seawater based on the flux of the peristaltic pump and the required concentration in each aquarium.

Mixalgae ($2x10^9$ cells mL^{-1}; 18% dry weight) were used for this experiment based on a previous *A. islandica* growth experiment, which showed highest shell growth rates (41.22 µm d^{-1}) at the most biodiverse diet (Milano et al., 2017a). This phytoplankton mix provided a particle size range from 3 to 16 µm and a balanced fatty acid composition (Lipids 16%: 16% EPA and 10% ARA), ensuring an optimal nutritional profile (Widdows, 1991; Milano et al., 2017a). Each shell was placed in a numbered plastic jar of 7-cm of diameter and 4-cm high. Each jar was filled with micro glass beads (www.kramerindrustriesonline.com) to avoid undesirable food input and provide a uniform sediment for all shells. The average size of the beads was 350 µm (Ballesta-Artero et al., 2017).

A BD Accuri C6 flow cytometer was used to evaluate the differences in the number of cells between treatments and replicates, and a portable multipara-meter (HI98192; www.hannainst.com) to check temperature and salinity values during the entire experimental period. Numbers of cells were counted once per week, while temperature and salinity were checked once daily.

Shell growth

Shell size (height, length, and width) was measured three times: at the beginning, mid-term, and at the end of the three-month experiment. Measurement error might be relatively large due to the small size of the animals, and we therefore triplicated each measurement and calculated the

average. The electric caliper error was ± 0.01 mm and the average measurement error (over all measurements and individuals) for height, length and width was: 0.07, 0.06, and 0.06 mm respectively (standard deviation). Shell growth per individual was determined based on the difference in the shell sizes between the representative periods of the experiment (beginning, midterm and end).

To verify the reliability of the externally-measured growth determined with the caliper, 73 shells were cross-sectioned to accurately identify the shell portion that grew during the experimental period on the basis of the calcein mark. The right valve of each specimen was cut into one 3-mm thick section along the axis of maximum growth (saw Buehler Isomet 1000). Given the small size and fragility of the juvenile shells, the valves were fully embedded in a block of Struers EpoFix (epoxy). All samples were ground at different grit sizes (P320, P600, P1200, P2500, and P4000) and then polished with a Buehler diamond polycrystalline suspension (3-µm). The calcein marks were located under a fluorescence light microscope (Zeiss Axio Imager.A1m microscope), to enable measuring the newly formed shell portion (for more details refer to: Milano et al., 2017a). Subsequently, a comparison was made between the externally- and internally-measured shell growth.

Body Mass Index (BMI)

To calculate the reference Ash Free Dry Weight ($AFDW = Dry\ Weight - Ash\ Weight$), twenty animals of the 250 preconditioned shells were sacrificed at the start of the experiment. Dry weight was determined after drying the soft tissue at 60 ºC for 3 days. Then, the dried flesh was incinerated at 540 ºC for 4 hours to obtain the ash weight. Based on these AFDW and the individual shell heights, we determined a height-weight relationship. This relationship was subsequently used to estimate the weights of the experimental animals at the beginning of the experiment. AFDW data was also used to calculate the Body Mass Index of the animals ($BMI = AFDW/H^3 * 1000$) as a fitness parameter.

After 45 days, 36 individuals were sacrificed, one per aquarium, for which the AFDW and BMI were determined. At the end of the experiment, which lasted 93 days, the AFDW and BMI of the

rest of individuals (89) was measured (Table 4. 2). The BMI was compared between the representative periods of the experiment.

Table 4. 2: Summary of individuals used.* Due to the small size of the individuals their shells were quite fragile.

Specimens	Number	Comments
Starting individuals	180	5 x 36 aquaria
Dead individuals	53	37 dated + 16 not dated
Sacrificed individuals at midterm	36	34 BMI (two specimen broken*)
Remaining individuals at midterm	127	126 used (one outlier removed)
Remaining individuals at the end	90	89 (one specimen broken*)

Siphon activity (%)

Siphon activity is an indication of feeding (Møhlenberg and Riisgård, 1979; Newell et al., 2001a; Riisgård and Larsen, 2015) and thus, it may be linked to growth (Witbaard et al., 1997a; Ballesta-Artero et al., 2017). Here siphon activity is expressed as the percentage of observations with open siphons relative to the total number of observations per specimen. The siphon activity of all individuals was checked at least twice per week at randomly- selected times. The data were recorded as 0 and 1, closed and open siphon, respectively. The average per aquarium (experimental unit) was calculated after the experimental period and used in the subsequent analyses.

Mortality (%)

At the end of the experiment, the percentage of dead specimens was calculated per aquarium (replicate). During the experiment, dead specimens were replaced by new ones to keep the density constant, and thus the loss of food by filtration. However, these new individuals were not considered in the statistical analyses of shell and tissue growth (Table 4. 2).

Data analysis

Response variables were transformed to obtain normality and homogeneity of variance. Percentages, that is siphon activity and mortality, were logit transformed (Warton and Hui, 2011); shell growth and BMI were log-transformed. Data were analyzed by a 2-factorial ANOVA with a significance level of α=0.05. Afterwards, a residual analysis was used to study the relationship between initial size and shell growth. Differences between treatment levels were calculated by Tukey's HSD post hoc test. Pearson correlation coefficients were used to study the strength of the relationship between the response variables. All analyses were performed using R version 3.2.2 (www.r-project.org).

RESULTS

Shell growth

Visual inspection of the experimental animals identified new shell growth during the experiment because the new deposited shell had a darker colored periostracum (Fig. 4. 1a). Five outliers were identified based on the relationship between external and internal shell growth, possibly due to external measurement error. Therefore, the outliers were corrected based on the linear relationship of the rest of individuals, $y = 1.0742x$ (R^2 = 0.94), where y and x were the external and internal shell height, respectively (Fig. 4. 1b).

At the end of the experiment, externally-measured shell growth varied between 0.21 and 2.29 mm (Fig. 4. 2) while internal shell growth varied between 0.04 and 1.88 mm (Table 4. 3). The difference in absolute values between external and internal growth indicated a small difference on the inclination of the measurements axis relative to the axis of maximum height. Nevertheless, the significant and high correlation (r= 0.90, P-value < 0.01; Table 4. 4) between internal and external growth verified the accuracy of the 'external' measurements taken with the caliper. To keep results comparable with findings from other studies, the rest of the analysis is based on the 'external' measurements.

At midterm (after 45d), the average external shell growth was < 1 mm in all treatments (Fig. 4. 2; Table 4. 3). At the end of the experiment, the maximum growth rate per day was 58.26 µm d^{-1} at 'high' food and a temperature of 13°C. The externally-measured growth in shell height showed

significant differences at different food levels at the end and midterm (2-way ANOVA, P-value < 0.05; Table 4.5). Residual plots showed no relationship (no pattern) between initial shell size and total shell growth. The effect of temperature on shell growth was almost significant at mid-term (P-value=0.06; Table 4.5) and it was associated with higher growth rates at the two highest food levels (medium & high; Fig. 4. 2; Table 4. 3). Such temperature effects could not be detected at the two lowest food levels (no food & low food; Fig. 4. 2; Table 4. 3). A one factorial Tukey HSD test showed that shell growth in the treatments 'no' food and 'low' significantly differed from 'medium' and 'high' (one-factorial TUKEY P-value < 0.01).

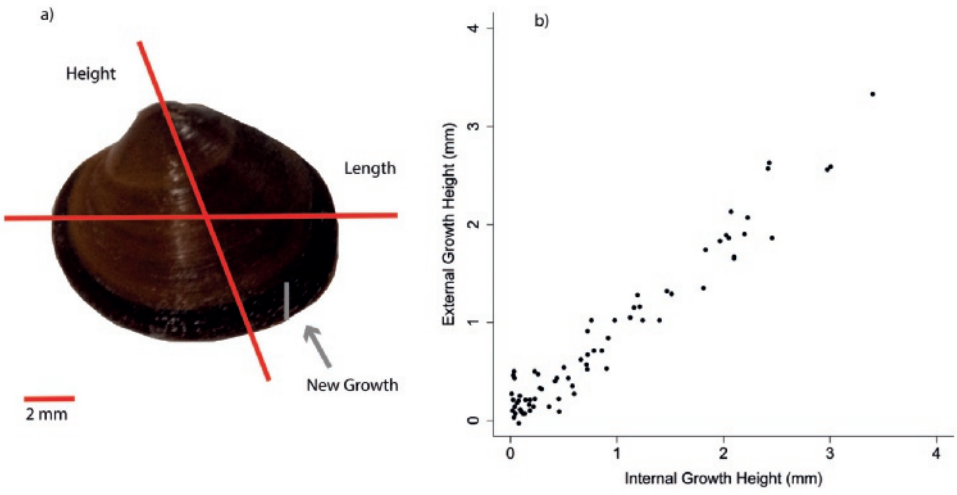

Fig. 4. 1: a) Visible shell growth in one specimen of *Arctica islandica* due to change of periostracum color b) Relationship between external and internal growth in height (GH in mm; n=73). Internal growth was determined on the basis of calcein mark.

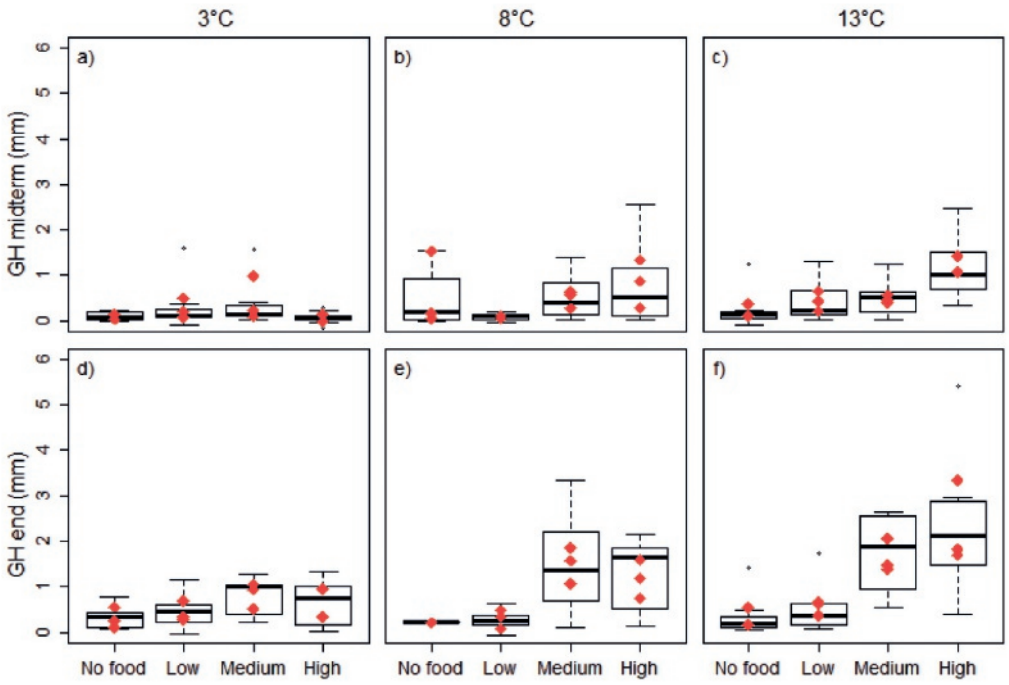

Fig. 4. 2: Shell growth in height (GH; mm) at midterm (45 days): a) 3°C, b) 8°C, c) 13°C, and at the end of the experiment (93 days) d) 3°C, e) 8°C, f) 13°C. Red diamonds indicate average per aquarium (data used for the statistical analysis) and boxplot showed the inter-specimen variation (n=126).

Table 4. 3: Summary of all response variable per treatment (mean ± SD). Note: GH means growth in height, BMI is body mass index, and AFDW is ash free dry weight.

	3°C	8°C	13°C
No food			
External GH midterm (mm)	0.11 ± 0.06	0.58 ± 0.82	0.19 ± 0.16
External GH end (mm)	0.30 ± 0.23	0.21 ± 0.00	0.28 ± 0.22
Internal GH (mm)	0.17 ± 0.12	0.18 ± 0.00	0.04 ± 0.03
BMI midterm (mg AFDW/mm3)	3.96 ± 0.29	5.48 ± 0.88	4.59 ± 1.76
BMI end (mg AFDW/mm3)	3.03 ± 0.90	3.34 ± 0.00	2.45 ± 0.10
% Siphon Activity	65.00 ± 21.51	27.97 ± 8.33	10.68 ± 3.08
% Mortality	44.67 ± 11.55	73.33 ± 11.55	26.67 ± 23.09
Low food			
External GH midterm (mm)	0.26 ± 0.22	0.08 ± 0.03	0.43 ± 0.22
External GH end (mm)	0.43 ± 0.22	0.30 ± 0.20	0.55 ± 0.16
Internal GH (mm)	0.39 ± 0.28	0.28 ± 0.22	0.39 ± 0.45
BMI midterm (mg AFDW/mm3)	5.30 ± 2.25	4.48 ± 0.27	4.64 ± 0.61
BMI end (mg AFDW/mm3)	3.67 ± 0.36	2.55 ± 0.53	2.79 ± 0.55
% Siphon Activity	71.12 ± 29.11	83.61 ± 8.13	39.90 ± 12.13
% Mortality	13.00 ± 11.55	33.00 ± 11.55	33.33 ± 23.09
Medium food			
External GH midterm (mm)	0.43 ± 0.48	0.50 ± 0.19	0.47 ± 0.09
External GH end (mm)	0.83 ± 0.28	1.50 ± 0.40	1.63 ± 0.37
Internal GH (mm)	0.91 ± 0.24	1.66 ± 0.35	1.82 ± 0.52
BMI midterm (mg AFDW/mm3)	4.64 ± 1.17	8.99 ± 1.90	9.54 ± 1.82
BMI end (mg AFDW/mm3)	6.12 ± 0.23	4.83 ± 0.67	5.28 ± 0.24
% Siphon Activity	77.07 ± 6.47	89.38 ± 7.63	71.65 ± 9.07
% Mortality	33.33 ± 23.09	6.67± 11.55	13.33 ± 11.55
High food			
External GH midterm (mm)	0.09 ± 0.09	0.84 ± 0.53	1.19 ± 0.21
External GH end (mm)	0.75 ± 0.36	1.17 ± 0.43	2.29 ± 0.92
Internal GH (mm)	0.72 ± 0.39	1.34 ± 0.40	1.48 ± 0.05
BMI midterm (mg AFDW/mm3)	5.26 ± 2.27	8.11 ± 2.90	9.33 ± 1.46
BMI end (mg AFDW/mm3)	6.24 ± 2.86	7.89 ± 2.43	7.77 ± 1.05
% Siphon Activity	68.49 ± 13.75	77.08 ± 9.11	63.70 ± 15.54
% Mortality	26.67 ± 23.09	20.00 ± 20.00	26.67 ± 11.55

Table 4. 4: Correlation among the different response variables and the factors food and temperature (Temp): Height growth in mm at midterm (GHmid; 45d) and the end of the experiment (GH; 93 d), internal growth in height (IntGH), siphon activity (S.Act.), body mass index at midterm (BMImid) and the end of the experiment (BMI), and mortality (Mort). The top right part shows the P-values of the corresponding correlations.

	Log(GH)	Log (GHmid)	Logit (S.Act)	Log (BMI)	Log(BMI mid)	Sqrt (intGH)	Logit (Mort)	Temp	Food
Log(GH)		0.000	0.024	0.000	0.000	0.000	0.111	0.155	0.000
Log(GHmid)	0.76		0.638	0.001	0.000	0.000	0.321	0.027	0.002
Logit(S.Act)	0.39	0.08		0.006	0.092	0.000	0.139	0.022	0.002
Log(BMI)	0.78	0.55	0.46		0.002	0.000	0.482	0.538	0.000
Log(BMImid)	0.68	0.59	0.29	0.52		0.000	0.775	0.044	0.004
Sqrt(IntGH)	0.90	0.62	0.57	0.83	0.66		0.148	0.446	0.000
Logit(Mort)	-0.33	-0.25	-0.22	-0.14	-0.15	-0.29		0.718	0.039
Temp	0.25	0.37	-0.38	-0.11	0.35	0.14	-0.02		1
Food	0.73	0.51	0.49	0.82	0.49	0.75	-0.35	0	

Fitness Condition

The weights (AFDW) of all the experimental animals at the beginning of the experiment (y) was calculated as $= 0.0008e^{0.1702x}$, where x was equal to the height of the individuals at the start of the experiment ($R^2 = 0.54$). Then, AFDW data was used to calculate the BMI of these animals which had a mean value of 4.89 mg mm^{-3}.

Food level significantly affected the BMI of *Arctica islandica* (2-way ANOVA, P-value < 0.05; Table 4.5) over the entire experiment. Temperature, was significant only at midterm (P-value = 0.02; Table 4.5). At most of the treatments, the mean BMI per treatment decreased from the mid-term to the end of the experiment (Fig. 4. 3; Table 4.3). Since the quantity of food added to each treatment did not change, this is an indication of asynchrony between shell and tissue growth. Individuals at higher temperatures had increased BMIs at food levels 'medium' and 'high', but there was almost no BMI change between temperatures at food levels 'no' and 'low' (Fig. 4. 3). In food-limited treatments ('no' and 'low' food), most of the individuals had a decrease in BMI between the midterm and the end of the experimental period (Fig. 4. 3).

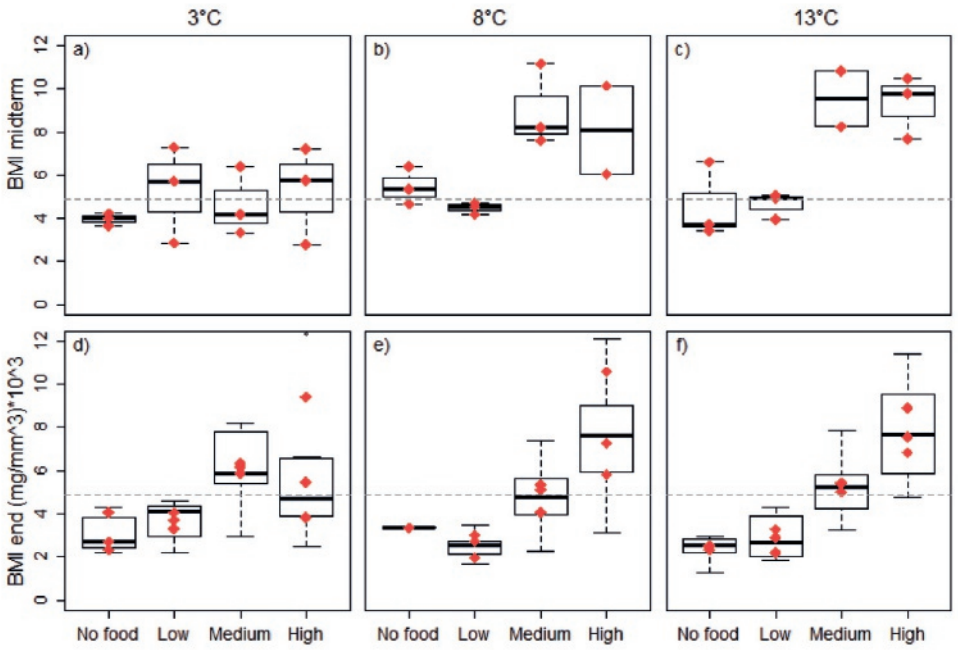

Fig. 4. 3: Body Mass Index (BMI) per treatment: at midterm (45 d; n=34): a) 3°C, b) 8°C, c) 13°C, and at the end of the experiment (93 d) d) 3°C, e) 8°C, f) 13°C. Horizontal line denotes average BMI at the start of the experiment (reference BMI). Red diamonds indicate average per aquarium (data used for the statistical analysis) and boxplot show the inter-specimens variation ($n_{midterm}$=34,n_{end}= 89).

At the end of the experiment, tissue growth, as well as shell growth, was only significantly affected by food level and not by temperature. 'No' and 'low' food treatments were significantly lower from those of 'medium' and 'high' food (one-factorial TUKEY P-value < 0.01).

Siphon activity

Siphon activity varied significantly with temperature, food level, and the interaction between them (2-way ANOVA, P-value < 0.05; Table 4.5). Mean siphon activity increased at higher food levels (except for the highest concentration): between 11 and 77% at temperature 13°C (64% at the highest concentration), between 28 and 89% at 8 °C (77% at the highest concentration); and between 65 and 78% at 3 °C (68% at the highest concentration; Fig. 4. 4a, b, c; Table 4. 3). The differences in siphon activity between food levels were far smaller at 3 °C than at the other temperatures (8 and 13 °C, Table 4.3; Fig. 4. 4a, b, c).

Moreover, the starving animals ('no' food) had a much lower average siphon activity (35%) than the rest of treatments (65-79%, one-factorial TUKEY P-value < 0.01; Fig. 4. 4a, b, c). Only at 3 °C, the starving animals had a relatively high siphon activity (65%; Table 4. 3).

Siphon activity was significantly correlated with shell growth (r=0.39, P-value < 0.05; Fig 4d; Table 4. 4) and marginally significant with tissue growth (r=0.46, P-value = 0.06; Fig. 4. 4e; Table 4. 4).

Table 4. 5: Two-way ANOVA Table 4.testing on the effects of temperature and food level on the different response variables. Significant factors per model are highlighted in italic (P-value < 0.05).

Variable response	Effect	df	Sum Sq	Mean Sq	F-value	Pr (> F)
log(GHmid)	*Food (F)*	3	1.9824	0.6608	4.835	0.0094
	Temperature (T)	2	0.8886	0.4443	3.251	0.0571
	Interaction F*T	6	1.2275	0.2046	1.497	0.2234
	Residuals	23	3.1417	0.1367		
log(BMImid)	*Food*	3	0.27517	0.091725	5.7569	0.0046
	Temperature	2	0.17364	0.086819	5.4490	0.0120
	Interaction F*T	6	0.16106	0.026844	1.6848	0.1719
	Residuals	22	0.35052	0.015933		
log(GH)	*Food*	3	3.198	1.0660	18.709	2.94E-06
	Temperature	2	0.357	0.1783	3.129	0.0637
	Interaction F*T	6	0.393	0.0655	1.149	0.3680
	Residuals	22	1.253	0.0570		
log(BMI)	*Food*	3	0.99031	0.33010	36.9768	9.09E-09
	Temperature	2	0.01138	0.00569	0.6373	0.5382
	Interaction F*T	6	0.09588	0.01598	1.7900	0.1477
	Residuals	22	0.19640	0.00893		
logit(Activity)	*Food*	3	26.489	8.8296	16.4803	4.99E-06
	Temperature	2	13.144	6.5718	12.2662	0.0002
	*Interaction F*T*	6	10.208	1.7014	3.1756	0.0194
	Residuals	24	12.858	0.5358		
logit(Mortality)	*Food*	3	13.70	4.567	2.955	0.053
	Temperature	2	0.41	0.204	0.132	0.877
	Interaction F*T	6	20.51	3.418	2.211	0.077
	Residuals	24	37.10	1.548		

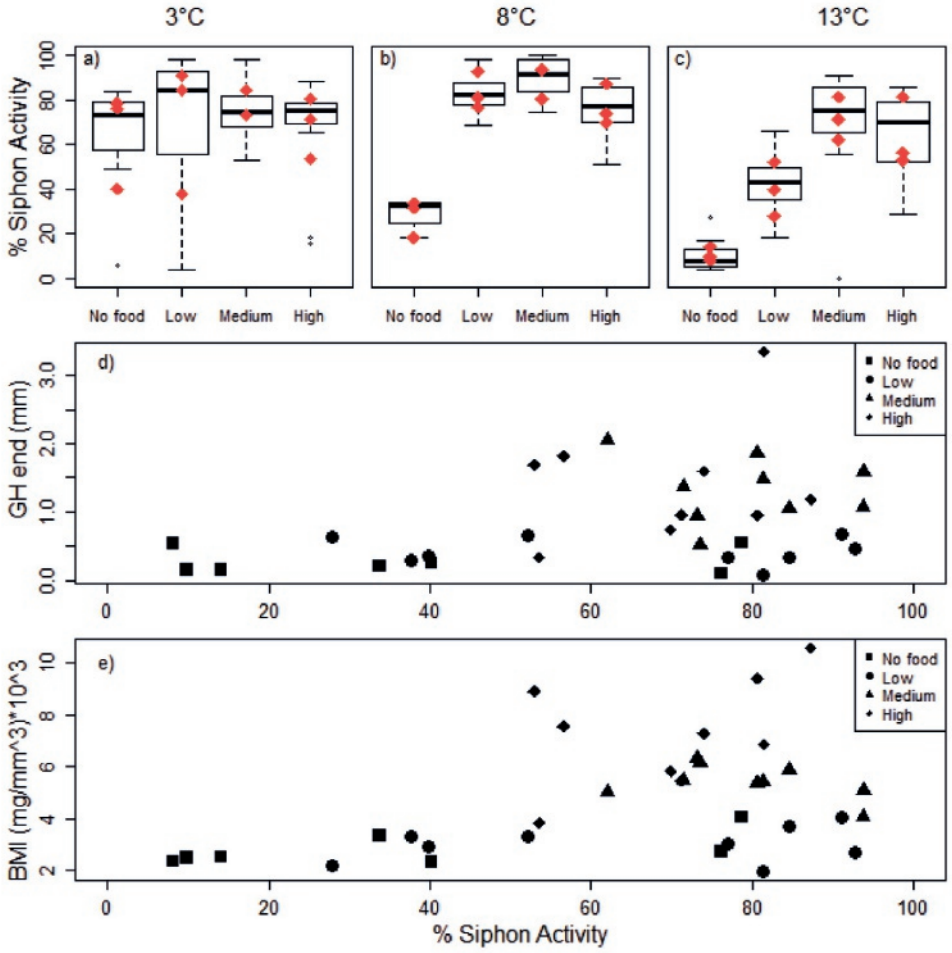

Fig. 4. 4: Percentage of average siphon activity at: a) 3°C, b) 8 °C and c) 13°C. Red diamonds indicate average per aquarium (data used for the statistical analysis) and boxplots show the inter-specimen variation (n=126). Relationship between average siphon activity and d) external growth in height (GH per aquarium; n=36) e) Body Mass Index (BMI) per aquarium (n=36).

Mortality (%)

There was a 29% mortality during the entire experimental period over all treatments and replicates. There were only significant differences in mortality among food levels (2-way ANOVA; P-value < 0.05; Table 4. 5 and Fig. 4. 5a, b, c). More individuals died at 'no' food (n=22) than at the other food treatments (low, n=12; medium, n=8; high, n=11; Fig. 5d). A few specimens were not included in Fig. 4. 5d because we could not precisely determine the date of death (Table 4. 2). The observed mortality was not significantly correlated to any of the other response variables (Table 4. 4).

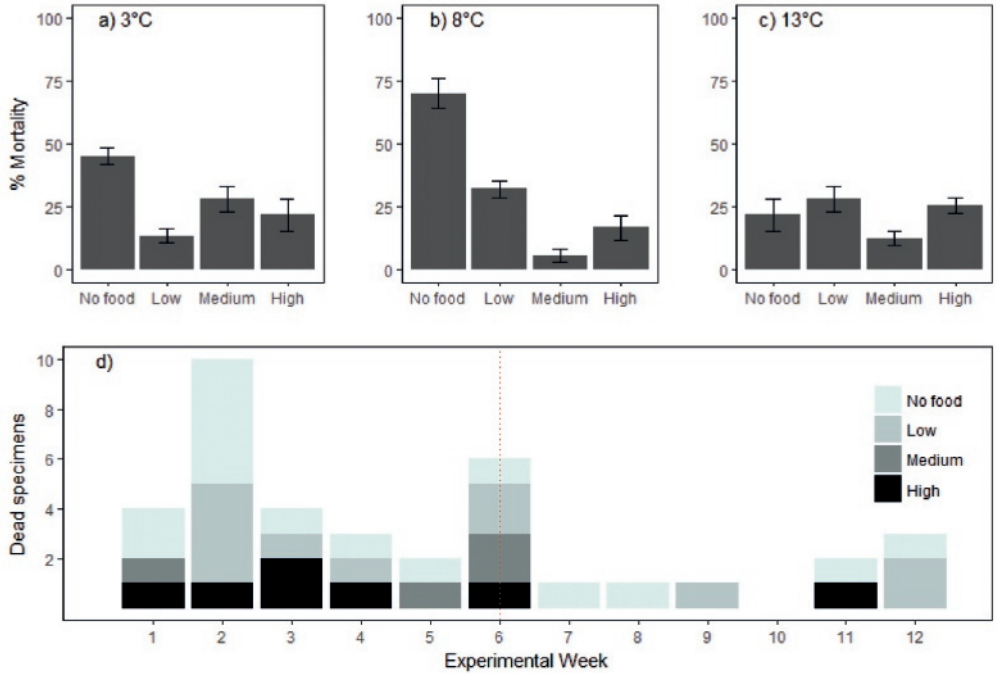

Fig. 4. 5: Percentage of average mortality at: a) 3 °C, b) 8 °C and c) 13°C. d) Number of dead specimens per food level and experimental week. Vertical line indicates the week that the midterm measurements were done. NOTE: No specimens died at week 10.

DISCUSSION

Within the temperature range tested (3-13°C), only food level significantly affected shell and tissue growth of *Arctica islandica* juveniles. Siphon activity, however, was affected by both factors as well as by the interaction between them. Siphon observations played a key role to better understand the growth differences among individuals (Fig. 4. 4).

Food availability and growth

We found increased shell and tissue growth at higher food concentrations (all temperatures; Fig. 4. 2 & 3). More growth at elevated food levels have been also reported in other bivalve species such as *Mytilis edulis, Tapes japonica* or *Pinctada margaritifera* (Winter and Langton, 1976; Langton et al., 1977; Linard et al., 2011; Thomsen et al., 2013; Joubert et al., 2014). Thus, our findings support that bivalve growth is strongly influenced by food supply. Our growth rate measurements (0.32 -58.26 μm d^{-1}) were in the range of growth rates found in other laboratory growth experiments (Witbaard et al., 1997a; Hiebenthal et al., 2012; Hiebenthal et al., 2013; Hippler et al., 2013; Stemmer et al., 2013), although lower than *A. islandica* growth rates reported *in situ* (Hippler et al., 2013; Milano et al., 2017a). The minimal shell growth found at all treatments without food (all replicates at all temperatures) has to be interpreted with caution. All specimens could have grown on the basis of the energy reserves that were accumulated during the acclimation time (average reference BMI=4.9; Fig. 4. 3). They were fed at optimal conditions and thus had reserves to survive some period of starvation.

Mean BMIs of most treatments decreased at the end of the experiment with respect to mid-term (Fig. 4. 3). Since the quantity of food added to each treatment did not change, this is an indication of asynchrony between shell and tissue growth. Figure 6 supports that finding because it shows how the concentration of phytoplankton cells per treatment decreased or remained almost equal through time. This indicated equal or higher food intakes at the second part of the experiment. Moreover lower levels of phytoplankton cells coincided with higher siphon activity at most of the treatments (Fig. 4. 6).

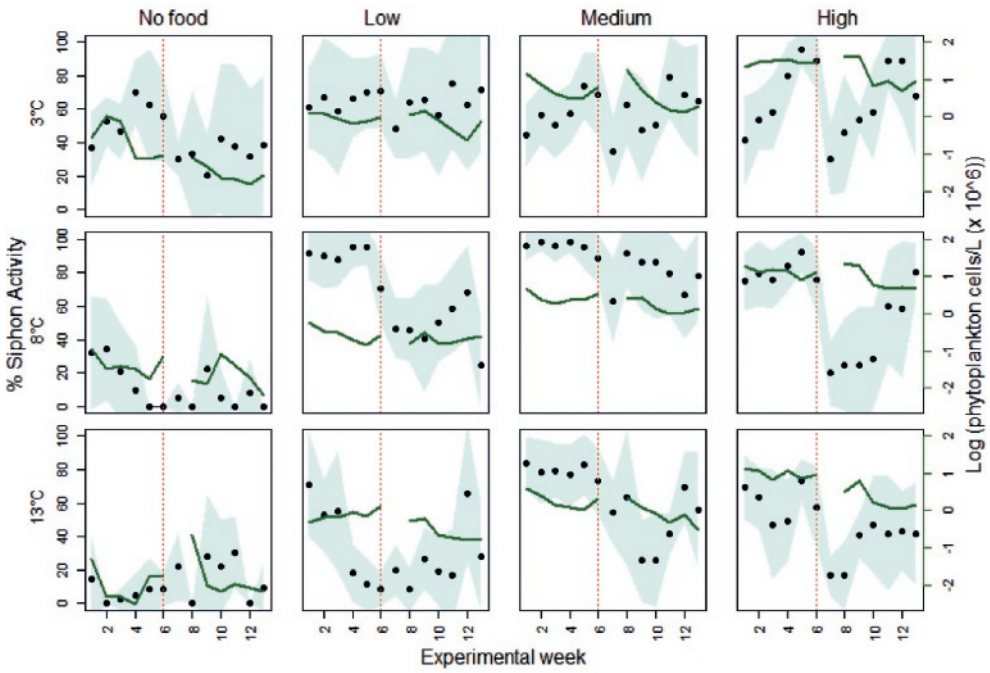

Fig. 4. 6: Percentage of siphon activity per treatment (dots) and mean phytoplankton cells concentrations (solid line) during the entire experimental period. Grey shadow represents siphon activity standard deviation (all specimens considered). Dashed vertical line marks midterm.

At the food-limited treatments, 42% of the animals died (11 of 26, Fig. 4. 5d) in the second week of the experimental period. At the 'medium' and 'high' food level, 27 % of the animals died (3 of 11) and mortality was more spread over the duration of the experiment (Fig. 4. 5d). Those results suggest that mortality is related to food level and the duration of starvation (P-value < 0.05). In the food-limited treatments, mortality decreased with time and the observations suggest that this might be due to a decrease in feeding activity as evidenced by a lower siphon activity (Fig. 4. 6). Lower siphon activity means lower energy cost and thus, energy conservation by which the specimens could survive starvation for longer periods of time. We furthermore, observed that after measuring the specimens at mid-term, for 1-2 weeks the specimens changed their 'normal' siphon activity registered until that moment (Fig. 4. 6) and were seen less with open siphons. Similar reduction in gape activity had been observed in *in-situ* valve gape measurements where

specimens also needed up to two weeks to return to their previous valve gape level after disturbance (Ballesta-Artero et al., 2017). These findings clearly illustrate the disturbing effect on the behavior of these clams caused by manipulation.

Temperature and growth

Our results are in agreement with Begum et al. (2010) who constructed a growth and energy budget model for six different North Atlantic populations of *Arctica islandica* (temperature range 4-10 °C). Since the Q_{10} for *A. islandica* respiration is about 2.5, they predicted that temperature should have an effect on shell and tissue growth (measured as tissue and shell AFDW). Nevertheless, they could not find such a temperature effect, and they postulated that site-specific effects (for example differences in salinity) could have obscured the temperature effect on their results (Begum et al., 2010). Likewise, food availability could be the reason for this. In previous laboratory experiments conducted in the range of 1 and 12 °C, faster shell and tissue growth at higher temperatures was reported (Witbaard et al., 1997a). Other studies conducted between 10 and 16°C found, that shell and tissue growth decreased at increasing temperatures (Hiebenthal et al., 2012; Milano et al., 2017a). Field studies also showed conflicting results regarding the effect of temperature on the growth of *A. islandica* (Witbaard et al., 1996; Marchitto et al., 2000; Epplé et al., 2006; Wanamaker et al., 2008a; Stott et al., 2010; Marali and Schöne, 2015). Different authors reported occasions where *A. islandica* growth rate was lower than expected on the basis of temperature alone, and suggested that food availability determined growth rate within the optimal temperature range of the species (Witbaard et al., 1996; Witbaard et al., 1997b; Witbaard et al., 1999; Schöne et al., 2003; Witbaard et al., 2003; Strahl, 2011; Ballesta-Artero et al., 2017). We only used specimens from one population, Kiel Bay, and we cultivated them at constant controlled environmental conditions (Table 4. 1). The results suggest that the temperature between 3 and 13 ° C had a limited effect on shell and tissue growth when compared to the role of food availability. On basis of our results, however, we cannot exclude the role of temperature. Exclusion of outliers in the statistical analyses turned temperature into a significant factor. Future experiments at higher temperatures and/or broader temperature range (0–20° C) could better elucidate its effect on *A. islandica* growth.

We observed that at the same food level the algal concentrations tended to be lower at higher temperatures, suggesting that filtration rate increases with temperature. The typical filtration rate curve in bivalves shows how filtration rate increases up to the optimal species-specific temperature. Above that optimal temperature, filtration rate collapses (Winter, 1978). Moreover, larger body size of the specimens as well implicate higher filtration rate (Walne, 1972; Winter, 1978). Consequently, only at the coldest temperature, the mean of phytoplankton concentration measured in the aquaria was higher than the desired target level for each of the treatments (Table 4. 1). Based on the phytoplankton concentration measurements at the different temperatures (Table 4 .1), we did not find an indication of an abrupt reduction in their filtration rate. The absence of that abrupt change suggests that the highest experimental temperature remained still equal or below the optimum for filtration. Therefore, our study together with results obtained in other laboratory growth experiments suggest that between 1 and 13 °C, the growth rate of *A. islandica* increases (Witbaard et al., 1997a), but that temperatures above 14-15 °C could be suboptimal (Hiebenthal et al., 2012; Milano et al., 2017a), leading to a decrease in filtration and growth. These findings are in agreement with earlier studies which found that *A. islandica* distribution limit follows the 16 °C isocline (Mann, 1982; Cargnelli et al., 1999; Weinberg et al., 2002).

Siphon activity and growth

We noticed that siphon activity at the 'high' food levels was lower, than at the 'medium' food levels (Fig. 4. 4; Table 4. 3). This may indicate that the food concentration of the highest food level was close to gut capacity, making the specimens to regulate their filtration rate in such a way that the amount of food ingested is kept constant (Winter, 1978). If this is true, our findings would support the idea that *Arctica islandica,* similar to *Mercenaria mercenaria* and *Cardium edule,* controls ingestion primarily by reducing filtration rate instead of producing copious pseudofaeces such as *Mytilus edulis* and *Crassostrea virginica* (Bricelj and Malouf, 1984). The reduction of filtration rate above a critical algal concentration prevents overloading of the feeding system and is a way to optimize the ingestion rate and growth (Møhlenberg and Riisgård, 1979; Riisgård, 1991). These critical thresholds, however, may vary depending on the diet or pre-experimental

conditions of the individuals (Maire et al., 2007) and may be different for the species in other situations.

Ballesta-Artero et al. (2017) reported that *A. islandica* in a natural setting had the highest valve gape coinciding temporally with the highest ambient levels of chlorophyll-*a* (Chl-*a*). This result agreed with earlier studies arguing that the main driver for opening valves in bivalve species as *Mytilus edulis*, *Austrovenus stutchburyi*, and *Crassostrea virginica*, was the occurrence of Chl-*a* (Higgings, 1980; Williams and Pilditch, 1997; Riisgård et al., 2006). Open valves are needed for siphon extension in filter-feeding bivalves. Therefore, open siphons (and open valves) can be used as an indicator of feeding activity. Our laboratory results not only confirm above field experiment (Ballesta-Artero et al., 2017) but also confirm the findings of a previous *A. islandica* growth experiment (Witbaard et al., 1997a), where siphon activity ranged from 12% in the individuals that did not receive any food to 76% with the highest food concentration (from 11 to 89% in our study). A low activity in the absence of food (% open siphons and gaping activity) can be interpreted as a physiological mechanism that allows *A. islandica* to save energy and survive starvation periods in nature (Taylor, 1976; Witbaard et al., 1997a; Riisgård et al., 2006; Tang and Riisgård, 2016; Ballesta-Artero et al., 2017). In the experiment reported here, we observed that specimens at 8 and 13 °C showed a marked change in their siphon activity between the no-food and food treatments. However, this change did not occur at 3°C (Fig. 4. 4), suggesting that the metabolic energy cost for the species is lower at 3°C (Abele et al., 2002; Abele and Puntarulo, 2004; Hiebenthal et al., 2013; Milano et al., 2017a), and could allow for higher siphon activity at all tested concentrations.

Finally, we found, similarly to Witbaard et al. (1997a), a strong correlation between shell and tissue growth, and siphon activity (Fig. 4. 4d, 4e; Table 4. 4). Therefore, the inter-specimen variation in growth of *A. islandica* can partly be explained by differences in their siphon activity, i.e., in their individual feeding activities. Food density seems to be driving the siphon/gaping activity of this species, and with that, shell and tissue growth (this study; Witbaard et al., 1997a; Ballesta-Artero et al., 2017). The present study supports this link between valve gape, open siphons, and shell growth in the bivalve *A. islandica* (Witbaard et al., 1997a; Ballesta-Artero et al., 2017).

Application to paleoclimate studies

Paleoclimate studies based on *Arctica islandica* chronologies usually use old and large specimens to reconstruct past environmental conditions. Such large specimens have extremely low growth rates (Thompson et al., 1980a; Murawski et al., 1982; Kennish et al., 1994) which hampers experimental growth studies with them. It is virtually impossible to reliably measure size differences over short (experimental) time spans. That is much easier when juvenile specimens are used, but they might respond differently to variations in food and temperature when compared to adults. The *A. islandica* valve gape study done with adults (up to 9-cm height; Ballesta-Artero et al., 2017) showed, however, a similar link between shell growth and valve gape (siphon activity) as we report here. This supports the idea that adults and juveniles have the same behavioral response to variations in food and temperature. On basis of this similarity, we think that our experimental results will help with the interpretation of growth line records in adults, being of great utility for the sclerochronology community.

CONCLUSIONS

Our study helps to understand the role of food and temperature on the growth rate of *A. islandica*. Within the temperate range tested (3-13°C), the interaction between feeding conditions and temperature did not have a significant effect on the growth of the species. The concentration of algal food was the main factor driving siphon activity and with that shell and tissue growth. Very low and very high algal concentrations led to shell closure and reduction (or cessation) of filtration in *A. islandica*. Therefore, paleoclimatic reconstructions based on *A. islandica* shell chronologies should not only consider temperature but also food supply of the area under study.

Compliance with Ethical Standards

The authors declare that they have no conflict of interest. All applicable international, national, and/or institutional guidelines for the care and use of animals were followed.

Data DOI: 10.4121/uuid:1a96a8c1-8230-496a-a67a-9919133dbccd

Acknowledgments

Thanks to Cyril Degletagne and Doris Abele for providing the specimens for this study. Thanks to Evaline van Weerlee and Evelien Witte for their assistance with the laboratory tasks. Special thanks to Andrés Parra González for his unconditional help and support throughout all the experiment.

This work was funded by the EU within the framework (FP7) of the Marie Curie International Training Network ARAMACC (604802).

Chapter 5

Environmental and biological factors influencing trace elemental and microstructural properties of *Arctica islandica* shells

Ballesta-Artero, Irene; Zhao, Liqiang; Milano, Stefania; Mertz-Kraus, Regina; Schöne, Bernd R.; van der Meer, Jaap; Witbaard, Rob

Published in Science of the Total Environment 645: 913–923 (2018)

Abstract

Long-term and high-resolution environmental proxy data are crucial to contextualize current climate change. The extremely long-lived bivalve, *Arctica islandica*, is one of the most widely used paleoclimate archives of the northern Atlantic because of its fine temporal resolution. However, the interpretation of environmental histories from microstructures and elemental impurities of *A. islandica* shells is still a challenge. Vital effects (metabolic rate, ontogenetic age, and growth rate) can modify the way in which physiochemical changes of the ambient environment are recorded by the shells. To quantify the degree to which microstructural properties and element incorporation into *A. islandica* shells is vitally or/and environmentally affected, specimens of *A. islandica* were reared for three months under different water temperatures (3, 8 and 13 °C) and food concentrations (low, medium and high). Concentrations of Mg, Sr, Na, and Ba were measured in the newly formed shell portions by laser ablation-inductively coupled plasma-mass spectrometry (LA-ICP-MS). The microstructures of the shells were analyzed by Scanning Electron Microscopy (SEM). Shell growth and condition index (CI (g) = dry soft tissue mass /dry shell mass) of each specimen were calculated at the end of the experimental period.

Findings indicate that no significant variation in the morphometric characteristics of the microstructures were formed at different water temperatures or different food concentrations. Shell carbonate that formed at lowest food concentration usually incorporated the highest amounts of Mg, Sr and Ba relative to Ca^{+2} (except for Na) and was consistent with the slowest shell growth and lowest condition index at the end of the experiment. These results seem to indicate that, under food limitation, the ability of *A. islandica* to discriminate element impurities during shell formation decreases. Moreover, all trace element-to-calcium ratios were significantly affected by shell growth rate. Therefore, physiological processes seem to dominate the control on element incorporation into *A. islandica* shells.

Keywords:

Bivalve, environmental proxy, vital effects, temperature, phytoplankton concentration, sclerochronology

INTRODUCTION

Proxy records are crucial to study climate change in areas where instrumental records are absent (Freitas et al., 2006). In the last two decades, bivalve shells have become an important bioarchive tool and the number of respective studies has greatly increased (Gillikin et al., 2005; Freitas et al., 2006; Wanamaker et al., 2008c; Schöne et al., 2011; Milano et al., 2017a). Microstructural properties and trace element-to-calcium ratios can reflect the environment in which the bivalves lived (Schöne et al., 2013; Milano et al., 2017a). The long-living species *Arctica islandica* (up to 507 years old; Wanamaker et al., 2008c, Butler et al., 2013), also known as ocean quahog, has been widely used for multicentennial paleoclimatic reconstructions(Butler et al., 2013), but the study of its microstructural and geochemical shell properties as an environmental proxy is still under development. Therefore, knowledge of the interacting effects of extrinsic (environmental) and intrinsic (physiological) factors on *A. islandica* shells are essential to interpret this long-living bioarchive (Abele et al., 2009).

Levels of strontium (Sr) and magnesium (Mg) in bivalve shells have been proposed as proxies for water temperature (Klein et al., 1996; Schöne et al., 2013). However, Sr/Ca and Mg/Ca ratios are still difficult to interpret because the incorporation of trace and minor impurities in the shell carbonate is partly physiologically controlled (e.g., Urey et al., 1951; Purton et al., 1999; Lorrain et al., 2005; Freitas et al., 2005, 2006; Schöne et al., 2010, 2013; Marali et al., 2017a; Geeza et al., 2018). Published results on the relationship between the Sr/Ca and Mg/Ca ratios of bivalve shells and temperature are highly ambiguous; previous studies have reported a positive relationship (Stecher et al., 1996; Hart and Blusztajn, 1998; Toland et al., 2000), negative relationship (Dodd, 1965; Stecher et al., 1996; Surge and Walker, 2006; Schöne et al., 2011), and no relationship (Gillikin et al., 2005; Strasser et al., 2008; Izumida et al., 2011; Wanamaker and Gillikin, 2018). The variation on the type of relationship (positive, negative, or neutral) have been identified as species-specific and can even change depending on the season of the year (e.g., Gillikin et al., 2005; Freitas et al., 2006). In addition, Sr/Ca and Mg/Ca ratios can also differ among specimens of the same population, but the causes are not yet clear (Vander Putten et al., 2000; Lorrain et al., 2005; Freitas et al., 2006; Foster et al., 2008, 2009).

The potential use of other element-to-calcium ratios of bivalve shells as environmental proxies

has also been explored. For example, Na/Ca is strongly correlated to salinity (Rucker and Valentine, 1961; O'Neil and Gillikin, 2014) and water pH (Zhao et al., 2017a). Furthermore, it has been suggested that Ba/Ca and Na/Ca ratios are linked to primary production (e.g., Stecher et al., 1996; Gillikin et al., 2006; Poulain et al., 2015; Klünder et al., 2008). Ba/Ca profiles are typically characterized by a relatively flat background interrupted by episodic sharp peaks (e.g., Stecher et al., 1996; Vander Putten et al., 2000; Gillikin et al., 2006, 2008; Thébault et al., 2009; Elliot et al., 2009; Hatch et al., 2013), which are usually highly reproducible among specimens (e.g., Gillikin et al., 2008; Elliot et al., 2009; Marali et al., 2017a, b). Although the factors controlling the formation of Ba/Ca peaks are still controversially debated, the Ba/Ca ratio of bivalve shells is potentially strongly influenced by an environmental forcing (Gillikin et al., 2006, 2008; Poulain et al., 2015).

Previous studies of mollusks show that environmental parameters can also influence the microstructure of the shell (Lutz, 1984; Tan Tiu and Prezant, 1987; Tan Tiu, 1988; Nishida et al., 2012) and therefore, can serve as potential proxy for environmental conditions (Tan Tiu, 1988; Tan Tiu and Prezant, 1989; Schöne et al., 2010; Milano et al., 2017b). For example, the size and elongation of individual biominerals in *Cerastoderma edule* (Milano et al., 2017b) and the cyclical changes in thickness of the outer layer of *Scapharca broughtonii* (Nishida et al., 2012) shells are related to temperature changes. Moreover, the relationship between food conditions and microstructure have lately been explored; some studies reported an accumulation of pigments in mollusk shells due to the ingestion of pigment-enriched microalgae (polyenes; Hedegaard et al. 2006; Soldatov et al., 2013), while others argued that diets do not influence shell pigment composition, and that polyenes are likely species-specific and habitat independent (Nehrke and Nouet, 2011; Stemmer and Nehrke, 2014; Milano et al., 2017a). The study of shell microstructure can therefore help to develop alternative techniques to reconstruct environmental variables from bivalve shells (Milano et al., 2017a).

The objective of the present study is to clarify the effect of external (environmental) and internal (physiological) factors on microstructural properties and element incorporation into *A. islandica* shells. Under laboratory conditions, *A. islandica* individuals from the same population were reared at different temperatures and food concentrations. Several studies have used controlled laboratory experiments to determine the relationship between the elemental

composition of bivalve shells and variable environmental parameters (Lorens and Bender, 1980; Strasser et al., 2008; Wanamaker et al., 2008c; Poulain et al., 2015; Wanamaker and Gillikin, 2018). However, fewer studies have tested the effect of the environment on the shell microstructure. Furthermore, most previous studies only focused on single parameter validation and did not take into account the possible interaction among multiple parameters (e.g., Lorens and Bender, 1980; Poulain et al., 2015). Here, we present for the first time a controlled laboratory experiment that aims to provide a better understanding of the interplay between environmental (food and temperature) and physiological influence (shell growth and condition index) on the geochemical properties and shell microstructure of *A. islandica* shells.

MATERIALS AND METHODS

Sample collection

In July 2014, live juvenile specimens of *A. islandica* were collected from the Kiel Bay, Baltic Sea (54° 32′ N, 10° 42′ E) and used in a laboratory growth experiment conducted at Royal Netherlands Institute for Sea Research (NIOZ) between 22 March and 23 June 2016 (14 weeks; Ballesta-Artero et al., 2018). The specimens were divided among 12 different treatments, i.e., combinations of four food concentrations (no, low, medium, and high food) and three different temperatures (3 °C, 8 °C, and 13 °C; Table 5. 1). There were 3 replicates per treatment (3 aquaria), which meant a total of 36 aquaria (4 food levels x 3 temperatures x 3 replicates). Five *A. islandica* juveniles were randomly assigned to each aquarium, amounting to a total 180 *A. islandica* specimens. Specimens reared without food were not analyzed in this study because there was insufficient (or none) newly formed shell material for chemical analyses (Ballesta-Artero et al., 2018). Therefore, we only analyzed 9 treatments (27 trials) and a total of 73 specimens for the present study. Bivalves were fed 8 times per day with a commercial mix of marine microalgae containing *Isochrysis* sp., *Tetraselmis* sp., *Pavlova* sp., *Thalassiosira* sp. and *Nannochloropsis* spp (Mixalgae; Acuinuga, Spain). Numbers of cells in each aquarium were checked once per week with a flow cytometer (BD Accuri C6), while temperature and salinity were monitored on a daily basis with a table multiparameter probe (HI98192; Hanna instruments, USA).

Table 5. 1: Summary of treatments (mean ± SD). Results are given in µm/mol for Ba/Ca and mmol/mol for the other elements. Shell growth was measured in height (mm). DW= Dry weight and ind= individual.

	3 °C	**8°C**	**13 °C**
Low			
Na/Ca	23.94 ± 0.70	23.27 ± 0.75	23.58 ± 1.39
Mg/Ca	0.44 ± 0.05	0.40 ± 0.02	0.47 ± 0.08
Sr/Ca	1.58 ± 0.17	1.49 ± 0.06	1.68 ± 0.17
Ba/Ca	8.48 ± 2.78	8.27 ± 1.26	8.32 ± 3.75
Condition Index	5.27 ± 0.21	3.72 ± 0.57	4.33 ± 0.37
Shell growth	0.40 ± 0.28	0.28 ± 0.22	0.39 ± 0.44
[cells/ L] x 10^6	0.85 ± 0.43	0.22 ± 0.02	0.53 ± 0.18
mg DW /ind· /d	0.62 ± 0.01	0.62 ± 0.01	0.62 ± 0.01
Medium			
Na/Ca	25.42 ± 1.54	24.99 ± 0.40	24.25 ± 1.45
Mg/Ca	0.38 ± 0.14	0.32 ± 0.06	0.36 ± 0.02
Sr/Ca	1.55 ± 0.21	1.43 ± 0.06	1.50 ± 0.04
Ba/Ca	9.56 ± 7.18	11.84 ± 6.84	5.26 ± 1.69
Condition Index	7.83 ± 0.22	5.59 ± 0.57	6.92 ± 0.96
Shell growth	0.90 ± 0.24	1.65 ± 0.35	1.82 ± 0.52
[cells/ L] x 10^6	6.19 ± 0.64	2.34 ± 0.17	1.53 ± 0.05
mg DW /ind· /d	5.33 ± 0.21	5.33 ± 0.21	5.33 ± 0.21
High			
Na/Ca	25.98 ± 2.08	24.79 ± 0.23	23.95 ± 0.76
Mg/Ca	0.43 ± 0.17	0.31 ± 0.04	0.35 ± 0.11
Sr/Ca	1.41 ± 0.17	1.42 ± 0.09	1.75 ± 0.10
Ba/Ca	6.29 ± 3.56	7.17 ± 0.48	5.86 ± 1.91
Condition Index	7.62 ± 2.64	9.01 ± 2.13	9.24 ± 1.02
Shell growth	0.72 ± 0.39	1.34 ± 0.40	1.48 ± 0.05
[cells/ L] x 10^6	24.56 ± 2.85	12.99 ± 0.82	6.45 ± 2.08
mg DW /ind· /d	13.69 ± 0.03	13.69 ± 0.03	13.69 ± 0.03
T real (°C)	2.49 ± 0.02	7.94 ± 0.07	13.11 ± 0.05
Salinity(PPT)	30.26 ± 0.10	30.38 ± 0.08	29.39 ± 0.24

The starting shell height of the experimental animals ranged between 8.31 and 14.34 mm (± 0.01 mm). Prior to the start of the experiment, the specimens were soaked in a calcein solution of 125mg/l for 24 hours (Linard et al., 2011; Ambrose et al., 2012). This solution allowed us to accurately identify the newly formed shell portion that grew under experimental conditions.

Shell preparation

The right valve of each specimen was glued to a plexiglass cube, covered with a layer of JB KWIK epoxy resin and dried overnight. A low speed saw (Buehler IsoMet 1000; 250 rpm) was used to cut 3-mm-thick section from each specimen along the axis of maximum growth. Subsequently, the slabs were embedded in Struers EpoFix resin and air-dried overnight. The blocks were then ground using Buehler silicon carbide papers of different grit sizes (P320, P600, P1200, P2500) mounted on a Buehler Metaserv 2000 grinder-polisher machine. After each grinding step the blocks were rinsed in an ultrasonic bath for ca. 2 min. The samples were polished with a Buehler diamond polycrystalline suspension (3 μm) and rinsed once more. Prior to the analyses, shell sections were examined under a fluorescence light stereomicroscope (Zeiss AxioImager A1m fluorescent microscope equipped with a Zeiss HBO 100 mercury lamp for UV light, and Zeiss filter set 18 with an excitation wavelength of ~450-500 nm and an emission wavelength of ~500-550 nm), which clearly highlighted the calcein marks, indicating the newly formed shell portion. Photographs were taken using a Canon EOS 600D digital camera connected to the microscope. Newly formed increment widths (total growth over 14 weeks) were measured using the free image processing software, ImageJ (National Institutes of Health, USA).

Laser Ablation-Inductively Coupled Plasma-Mass Spectrometry (LA-ICP-MS)

Element concentrations of sodium (measured as ^{23}Na), magnesium (^{25}Mg), strontium (^{86}Sr) and barium (^{137}Ba) were determined in 73 *A. islandica* shells (9 ± 2 specimens per treatment) at the Institute of Geosciences, University of Mainz. We used an Agilent 7500ce inductively coupled plasma-mass spectrometer (ICP-MS) coupled to an ESI NWR193 ArF excimer laser ablation (LA) system which was equipped with a TwoVol^2 ablation cell.

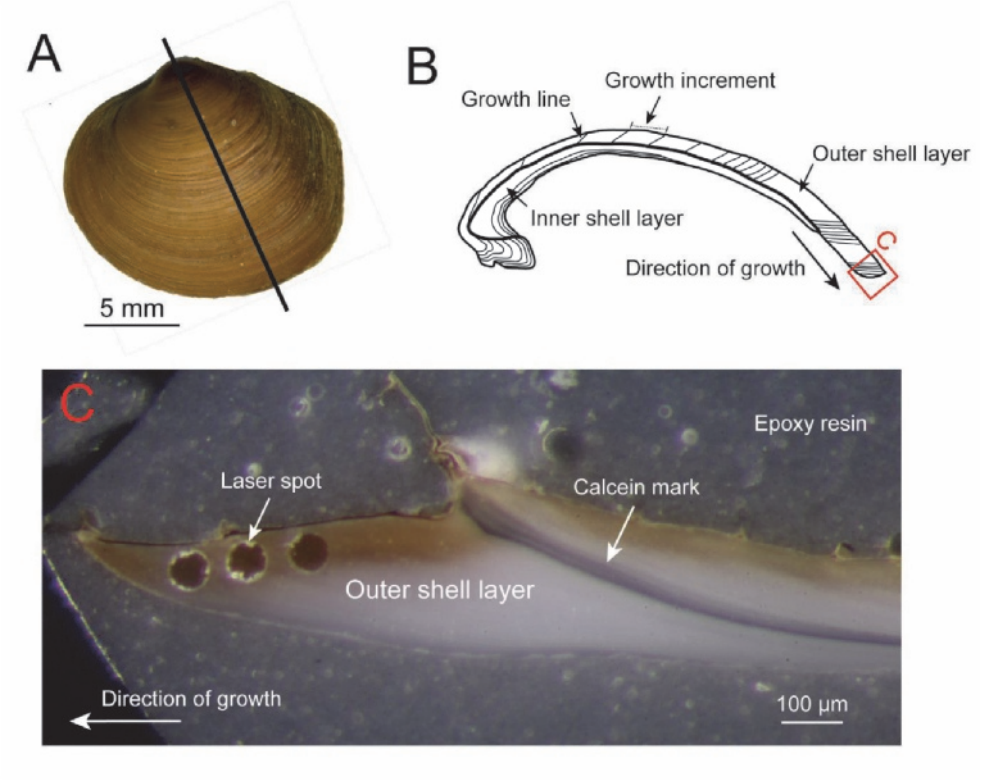

Fig. 5. 1: Shell of juvenile *Arctica islandica* A) outer shell surface with line of maximum growth (black line) B) cross-sectioned shell with major structures C) magnification of the outer shell margin revealing calcein mark and laser spots.

The ArF LA system was operated at a pulse repetition rate of 10 Hz, an energy density of ~3 J/cm², and an ablation spot diameter of 55µm. Background measurement were performed for 20 s, followed by ablation times of 40 s, and wash out times of 20 s. Ablation was carried out under a He atmosphere and the sample gas was mixed with Ar before entering the plasma. For each shell, measurements were performed at three equidistant spots in the middle of the aragonite layer of the newly formed shell portion (Fig. 5. 1). The multi-element synthetic glass NIST SRM 610 was used as calibration material, applying as the “true” concentrations the preferred values reported in the GeoReM database (http://georem.mpch-mainz.gwdg.de/; Jochum et al., 2005, 2011). For

all materials, ^{43}Ca was used as internal standard. For the reference materials, we applied the Ca concentrations reported in the GeoReM database, and for the samples 56.03 wt.%, the stoichiometric CaO content of $CaCO_3$. During each analytical session, we analyzed homogeneous basaltic USGS BCR-2G and synthetic carbonate USGS MACS-3 as quality control materials (QCMs). Reproducibility, which was expressed as the relative standard deviation based on repeated measurements of the QCM, was always better than 1.6 % for USGS BCR-2G (n = 9) and 7.5 % for MACS-3 (n = 9). The measured Na, Mg, Sr, and Ba concentrations of USGS BCR-2G agree within 1.4 %, 12.5 %, 2.1 %, and 0.5 % with the preferred values of the GeoReM database and within 1.1 %, 5.0 %, 0.6 %, and 0.7 % with the preliminary reference values for USGS MACS-3 (personal communication S. Wilson, USGS; Jochum et al., 2012). In the following, the average of the element concentrations (of the three spots measurements) are reported relative to Ca in mmol/mol for Sr, Mg and Na, and µmol/mol for Ba.

Shell microstructure

A. islandica produces a shell composed of a single calcium carbonate polymorph (aragonite) organized in layers characterized by different microstructures (Milano et al., 2017a). The outer portion of the outer shell layer (oOSL) consists of homogenous microstructure, whereas the inner portion of the outer shell layer (iOSL) and the inner shell layer (ISL) are dominated by crossed-acicular microstructures (Dunca et al., 2009; Schöne et al., 2013; Milano et al., 2017a). The homogenous microstructure is characterized by granular biomineral units distributed without a specific structural arrangement (Carter et al., 2012). The crossed-acicular microstructure contains elongated biomineral units obliquely aligned. The present study focuses on the ventral margin of the shells outside the pallial line. In this area, the ISL is missing. SEM analyses were carried out in the iOSL which has been previously identified as being potentially sensitive to environmental changes in *Cerastoderma edule* (Milano et al., 2017a).

The microstructure of 32 *A. islandica* shells was analyzed using a Scanning Electron Microscope (SEM). On average, four specimens were investigated per treatment (4 ± 2). The selection of specimens was based on the amount of aragonite deposited during the experimental phase.

Shells with limited or no growth were omitted from the analysis. To study the microstructures, samples were etched in 1 vol% HCl for 10 s and bleached in 6 vol% NaClO for 30 min. After being dried from air, the samples were coated with a 2 nm-thick platinum layer by using a sputter coater (Leica EM ACE200). The microstructures were qualitatively analyzed with a scanning electron microscope (LOT Quantum Design 2nd generation Phenom Pro desktop SEM) with backscattered electron detector and 10kV accelerating voltage. SEM images were taken over 100 µm away from the calcein line to avoid bias associated with the marking stress. In each specimen, the SEM images represent an area of ca. 2 mm^2 located in the middle of the shell portion formed during the experiment. In specimens with a large amount of aragonite deposited during the experiment, a second area was selected for SEM analysis ca. 300 µm away from the first area.

Shell growth

Shell growth was measured as the width between the ventral (outer) edge and the calcein mark that had formed at the start of the experimental period (mm; 93 days). In this study, shell growth is analogous to growth rate as all shells were grown over the same length of period.

Condition Index

Condition index (CI = dry soft tissue mass/ dry shell mass) of each specimen was calculated at the end of the experimental period as a measure of their physiological state at the end of the experiment. Dry weight was determined after drying the soft tissue at 60 °C for 3 days.

Statistical analysis

Experimental data were analyzed with R version 3.2.2 (www.r-project.org). Since individual specimens within one experimental unit (aquarium) were interdependent pseudo-replicates, we calculated single average values for trace elements, condition index, and shell growth for each aquarium. Then, data were checked for normality (Shapiro–Wilk's test; $p < 0.05$) and homogeneity of variance (Levene's *F*–test ; $p < 0.05$) before applying a two-way analysis of variance (ANOVA).

ANOVA was used to test for significant effects among the different food-temperature treatments. Ba/Ca and Mg/Ca ratios were log-transformed to follow ANOVA assumptions.

Univariate relationships between the average Na/Ca, Mg/Ca, Sr/Ca and Ba/Ca ratios of *A. islandica* shells per aquarium, environmental parameters (temperature and food), shell growth, and condition index were estimated by means of Pearson correlation analysis. Statistically significant differences were set at a $p < 0.05$.

Finally, a multi-regression analysis was performed with all the individual data to identify which factor/s (temperature, food, shell growth, and electric conductivity: EC) were mathematically linked to the trace element content of the shells using the following equation:

$$y_i = \beta_0 + \beta_1 \times Temperature_i + \beta_2 \times Food_i + \beta_3 \times Shell\ growth_i + \beta_4 \times EC_i + \varepsilon_i$$

Where y_i was the trace element-to-calcium ratio of specimen i (i range 1–73), β_0 was the intercept, β_{1-4} were the estimated coefficients of the different explanatory variables (temperature, food concentration, shell growth, and EC, respectively), and ε_i was the model error for each specimen ($\varepsilon_i \sim N(0,1)$. To avoid collinearity, explanatory variables were included in the analyses only when they had a (Pearson) correlation coefficient ≤±0.5 (Graham 2003; Duncan 2011; Ieno and Zuur 2015).

RESULTS

Experimental conditions

During the experiment, the water temperature and salinity were constant in the different treatments of the experiment (Table 5. 1). The concentration of phytoplankton cells, however, decreased with temperature (at the same food level). For instance, despite equal supply to the different temperature treatments, the average phytoplankton cells concentration at medium food level, varied from 6.19 (cells/L x 10^6) at 3 °C to 1.53 at 13 °C (Table 5. 1).

Table 5. 2: Two-way ANOVA test on the effects of temperature and food level over the different response variables (n=27, 27 trials). Significant factors per model are highlighted in italic. CI = condition index, GH = shell growth in height.

Variable response	Effect	df	Sum Sq	Mean Sq	F-value	Pr (> F)
Na/Ca	Food (F)	2	8.6698	4.3344	3.0953	0.0699
	Temperature (T)	2	7.3328	3.6664	2.6182	0.1004
	Interaction F*T	4	2.2196	0.5549	0.3963	0.8087
	Residuals	18	25.2060	1.4003		
log(Mg/Ca)	Food	2	0.0558	0.0279	2.9061	0.0806
	Temperature	2	0.0242	0.0121	1.2607	0.3073
	Interaction F*T	4	0.0115	0.0029	0.2996	0.8743
	Residuals	18	0.1728	0.0096		
Sr/Ca	Food	2	0.0367	0.0183	1.0657	0.3652
	Temperature	2	0.1862	0.0931	5.4131	0.0144
	Interaction F*T	4	0.1174	0.0294	1.7066	0.1924
	Residuals	18	0.3096	0.0172		
log(Ba/Ca)	Food	2	0.0656	0.03281	0.9155	0.4182
	Temperature	2	0.1060	0.05298	1.4781	0.2545
	Interaction F*T	4	0.0769	0.01923	0.5366	0.7107
	Residuals	18	0.6451	0.03584		
CI	*Food*	2	79.0870	39.5430	24.8314	6.67E-06
	Temperature	2	3.5250	1.7630	1.1069	0.3521
	Interaction F*T	4	12.3600	3.0900	1.9403	0.1473
	Residuals	18	28.6650	1.5920		
GH	*Food*	2	5.4311	2.7155	22.0637	2.52E-05
	Temperature	2	1.4654	0.7327	5.9530	0.0117
	Interaction F*T	4	0.8693	0.2173	1.7658	0.1851
	Residuals	16	1.9692	0.1231		

The average shell growth increased with increasing food supply, from 0.28 to 1.82 mm in 14 weeks (3µm/day - 19µm/day; Table 5. 1, Fig. 5. 2A). At the lowest food level, shell growth was not affected by temperature, but temperature had a positive effect on growth at medium and high food levels (Fig. 5. 2A; Table 5. 2). The condition index was not affected by temperature, but showed an increase with increasing food level (Fig. 5. 2B; Table 5. 2).

Sodium

In the different treatments, the average Na/Ca ranged between 23.27 and 25.98 mmol/mol (Table 5. 1; Fig. 5. 3A, B, C). The correlation matrix in Table 5. 3 suggests that the average Na/Ca in the newly deposited carbonate is inversely related to temperature (r= -0.38) and positively related to food level (r =0.42). Shell growth at 3 and 8 °C showed higher Na/Ca values ($p = 0.07$; Table 5. 2; Fig. 5. 3A, B, C) with higher amounts of supplied food. Only at 13° C, the trend was not clear (Fig. 5. 3C). When the Pearson coefficients were analyzed both food level and temperature showed a significant correlation with Na/Ca values (r =0.42 and r= -0.38 respectively, $p < 0.05$; Table 5. 3). At increasing food levels, *A. islandica* shells showed higher Na/Ca values ($p = 0.07$; Table 5. 2; Fig. 5. 3A, B, C). Only at 13° C, the trend was not clear (Fig. 5. 3C).

We calculated a linear multiple regression model (n = 73 observations) for Na/Ca ratios as a function of the supplied food, temperature, electrical conductivity (EC), and shell growth to identify whether external and internal factor(s) are linked to the incorporation of sodium into the shell carbonate. Na/Ca values are best explained by a combination of shell growth rate and temperature (Table 5. 4, $p < 0.05$; Fig. 5. 4A, B, C, D). A 32% of the variability in the Na/Ca (adjusted-R^2= 0.316) was explained by these two factors (correlation between these factors was 0.3). Although a univariate regression model suggested that Na and Condition Index (CI) were significantly correlated (r = 0.41; Table 5. 3), CI was not included in the multiple regression model because this variable is directly related to shell growth.

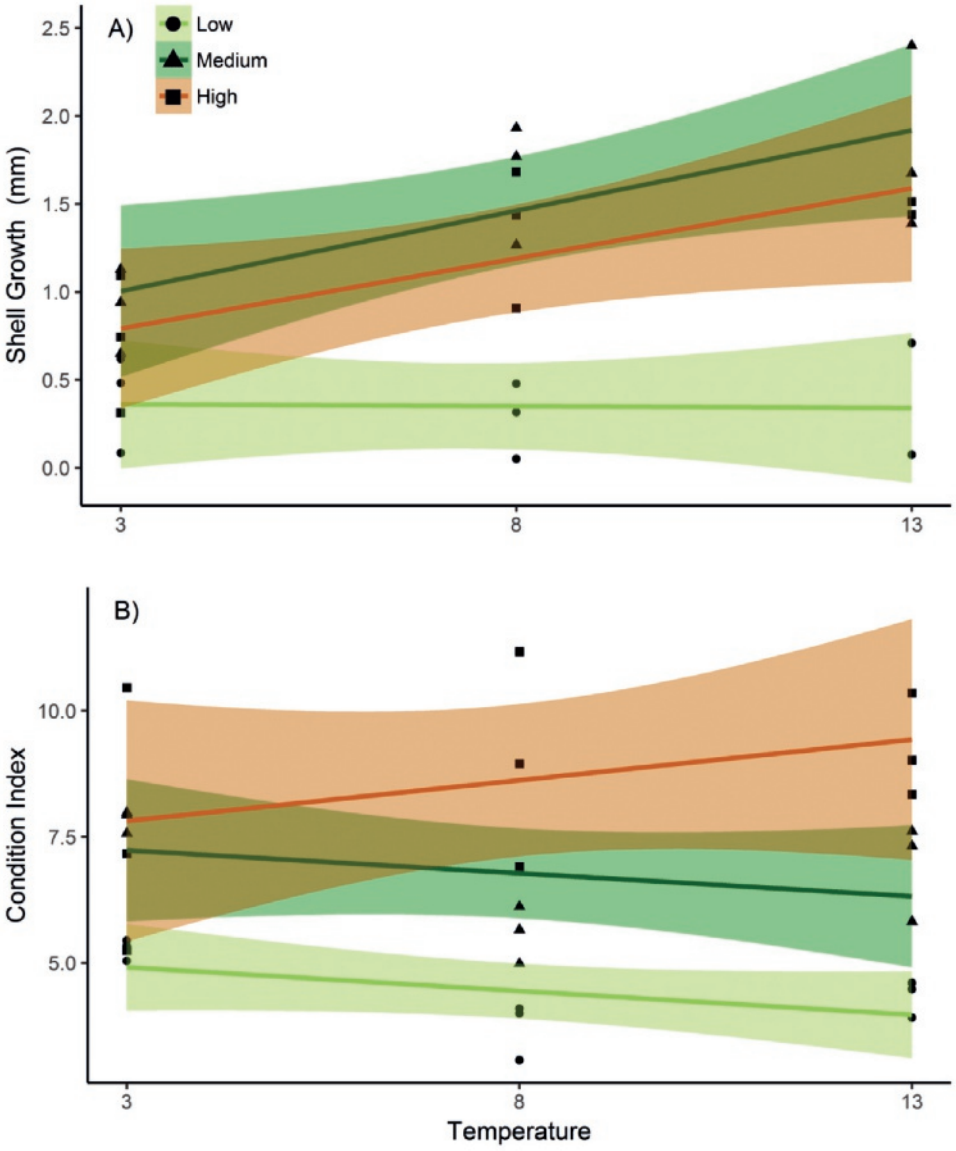

Fig. 5. 2: Linear regression of the A) average shell growth and B) average condition index of *Arctica islandica* by treatment (3 temperature x 3 food level x 3 replicates = 27 observations). Shadow colors show confident intervals. Circle = low food, triangle = medium food, square = high food.

Table 5.3: Correlation per treatment (27 observations) among the average element-to-Ca ratios in the shell and food, temperature (Temp), and physiological factors (shell growth in height (GH) and condition index (CI) at the end of the experiment). The top right part shows the P-values of the corresponding correlations.

	Temp	Food	Na/Ca	log(Mg/Ca)	Sr/Ca	log(Ba/Ca)	GH	CI
Temp		1	0.0487	0.6237	0.0727	0.3799	0.0392	0.9392
Food	0.00		0.0289	0.0384	0.4662	0.1989	0.0100	0.0000
Na/Ca	-0.38	0.42		0.0079	0.0013	0.0017	0.0982	0.0343
log(Mg/Ca)	-0.10	-0.40	-0.50		0.0043	0.0099	0.0011	0.0138
Sr/Ca	0.35	-0.15	-0.59	0.53		0.0694	0.1701	0.9619
log(Ba/Ca)	-0.18	-0.26	-0.58	0.49	0.35		0.1469	0.2598
GH	0.41	0.51	0.34	-0.62	-0.28	-0.30		0.0105
CI	-0.02	0.8	0.41	-0.47	-0.01	-0.22	0.50	

Magnesium

The average Mg/Ca of *A. islandica* varied between 0.31 and 0.47 mmol/mol (Table 5.1; Fig. 5. 3D, E, F). The Mg/Ca correlated inverse but significantly with food level ($r = -0.40$ $p < 0.05$) and CI ($r = -0.47$, $p < 0.05$; Table 5. 3). In a two way ANOVA neither the temperature, food level nor the interaction between these two factors showed statistically significant effects on the average Mg/Ca (Two-way ANOVA, $p > 0.05$; Table 5. 2). The linear multiple regression model however identified shell growth rate as the most likely factor to explain the variation in Mg/Ca ratios between shells (adjusted-R^2= 0.234 , Table 5. 4; Fig. 5. 4E, F, G, H).

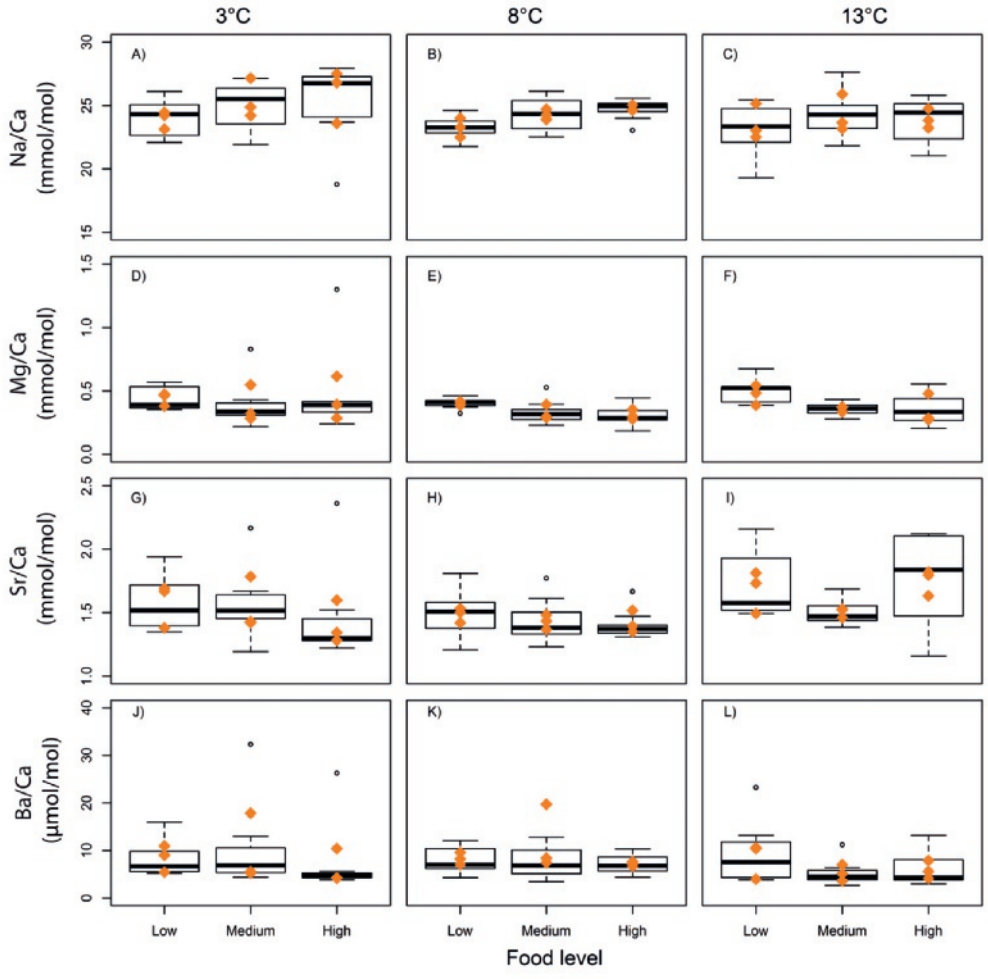

Fig. 5. 3: Overview of the shell trace-element values per treatment (temperature and food). Orange diamonds indicate average per aquarium (data used for ANOVA analysis) and the boxplots show the inter-specimens variation (n=73).

Strontium

Sr/Ca varied between 1.41 and 1.75 mmol/mol in the freshly grown shell material among the different treatments (Table 5. 1; Fig. 5. 3G, H, I). The Sr/Ca ratio only showed a weak correlation with temperature and had a Pearson correlation coefficient of r = 0.35 (p = 0.07; Table 5.3). The correlation with other factors (food level, condition index and shell growth) were insignificant. In the two way ANOVA (to test the effect of temperature, food and their interaction) only temperature showed a statistically significant effect on Sr/Ca (two-way ANOVA, $p \leq 0.05$; Table 5.2). The Sr-trend was negative between 3 and 8 °C but positive if we considered the entire temperature range (between 3-13° C), i.e., levels of Sr were lowest in shells grown at 8 °C.

When the role of external and internal factors were considered in a multiple regression model, the stepwise variable selection procedure included the variables growth rate and temperature (adjusted-R^2=15%, Table 5. 4; Fig. 5. 4I, J, K, L). Therefore, not only temperature, but also shell growth rate was statistically linked to Sr/Ca.

Barium

Ba/Ca ratios varied greatly among specimens of the same and different treatments. Mean values ranged from 5.26 to 11.84 µmol/mol (Table 5. 1; Fig. 5. 3 J, K, L). However, some specimens had peaks higher than 20 µmol/mol (Fig. 5. 3J, K, L). Temperature, food level and the interaction between these factors did not have a statistically significant effect on Ba/Ca (Two-way ANOVA*, p* > 0.05; Table 5.2). When external and internal factors were considered in a multiple regression model, only shell growth rate was significantly linked to Ba/Ca (adjusted-R^2= 0.229, Table 5. 4; Fig. 5. 4M, N, O, P).

In summary, shell carbonates that had been formed at lowest food concentration, leading to the lowest shell growth rates, usually incorporated the highest amounts of Mg, Sr and Ba in the shell. Only for Na the opposite was found (Fig. 5. 3, Table 5. 1). All trace element-to-calcium ratios were statistically significantly linked to shell growth rate (Fig. 5. 4; Table 5. 4). Moreover, the Na levels in the shell were also linked to food level and temperature, but Mg only to food, and Sr to temperature. None of the external factors studied (temperature, food, or EC) showed a significant

influence on the incorporation of Ba into *A. islandica* shell shell material grown during this experiment.

Table 5. 4: Regression models for each trace element ratio with the significant effect variable highlighted in italic ($p < 0.05$). Stepwise selection (both directions) selected the model highlighted in bold for each element (n=73, 73 specimens). EC =electric conductivity (µS/cm) and GH = shell growth in height.

Model	Variables	R^2-adjusted	F-statistic
M_Na	Na ~ *Temperature* + Food + *GH* + EC	0.303	7.85
	Na ~ *Temperature* + *GH*	**0.316**	15.57
	Na ~ *GH*	0.173	14.19
	Na ~ *Temperature*	0.035	3.58
M_Mg	Log(Mg) ~ Temperature +Food + *GH* + EC	0.217	5.36
	Log(Mg) ~ Temperature + *GH*	0.235	10.71
	Log(Mg) ~ *GH*	**0.228**	19.70
	Log(Mg) ~ Temperature	0.000	0.46
M_Sr	Sr ~ Temperature + Food + *GH* + EC	0.125	3.25
	Sr ~ Temperature + *GH*	**0.149**	6.52
	Sr ~ *GH*	0.116	9.24
	Sr ~ Temperature	0.026	2.88
M_Ba	Log(Ba) ~Temperature + Food + *GH* + EC	0.144	3.64
	Log(Ba) ~Temperature + *GH*	0.236	10.71
	Log(Ba) ~ *GH*	**0.229**	19.70
	Log(Ba) ~Temperature	0.000	0.46

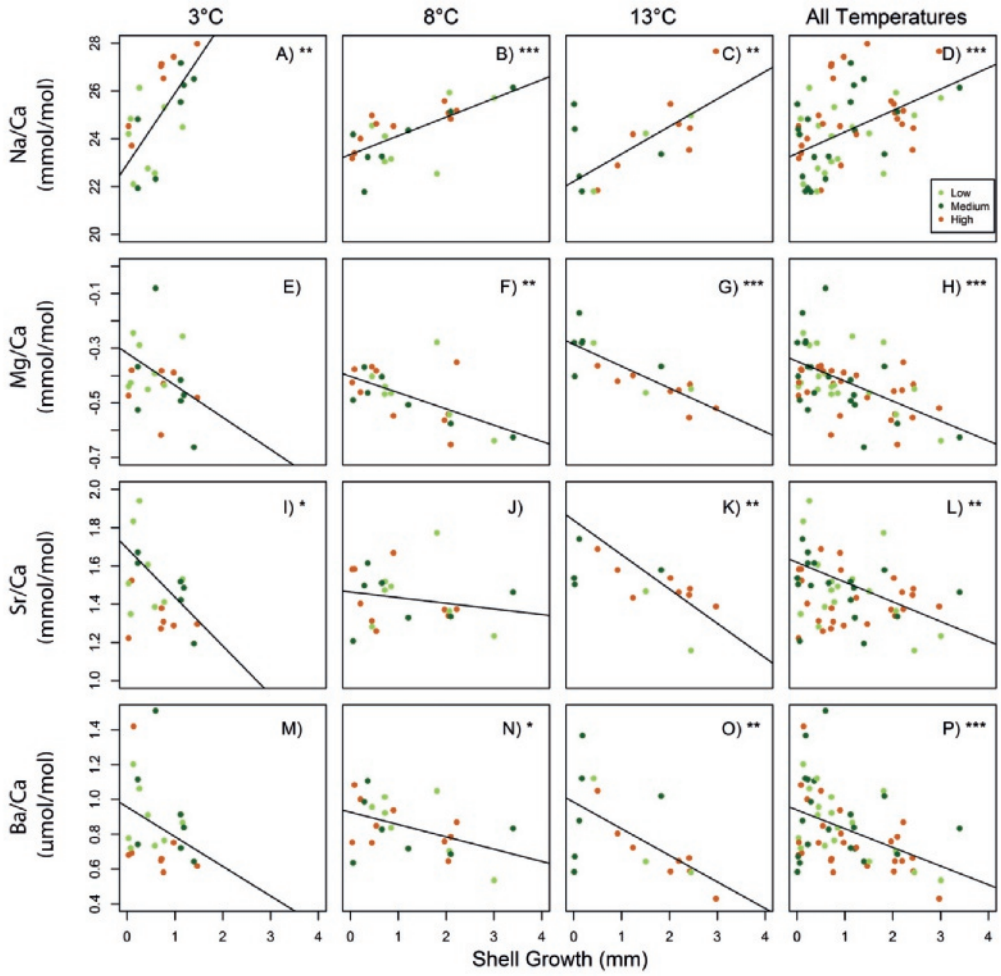

Fig. 5. 4: Linear relationships between trace element ratios and shell growth in height (73 observations). Dot colors indicate the different food levels: low (light green), medium (dark green) or high (orange). Statistically significant relationship are expresses as: '***' ($p < 0.001$) '**'($p < 0.01$) '*' ($p < 0.05$).

Microstructure

The morphology of the shell microstructures did not significantly vary in relation to the different temperatures and food levels (Fig. 5. 5). In the shells grown at 3 °C, the structural units were characterized by a bulky appearance with no considerable difference between specimens grown at food levels "low" and "medium" (Fig. 5. 5B). Shell material grown at the highest food level showed a slight increase in the size of individual biomineral units (Fig. 5. 5B). A similar increase in biomineral unit size was observed in shells reared at 13 °C and medium food level. A minor shift toward more elongated microstructural units was visible in shells exposed to a water temperature of 8 °C and medium food level (Fig. 5. 5B). The most significant morphological difference in shell microstructure was detected in shells grown at 13 °C and low food and in shells reared at 8 °C and high food (Fig. 5. 5B). In these cases, the microstructures resembled a well-pronounced crossed-acicular appearance commonly found in the ISL. However, this microstructural variation was not shared by all shells grown at the same treatment. Therefore, on basis of SEM we could not detect a significant variation of *A. islandica* shell microstructures reared at different temperatures and food levels.

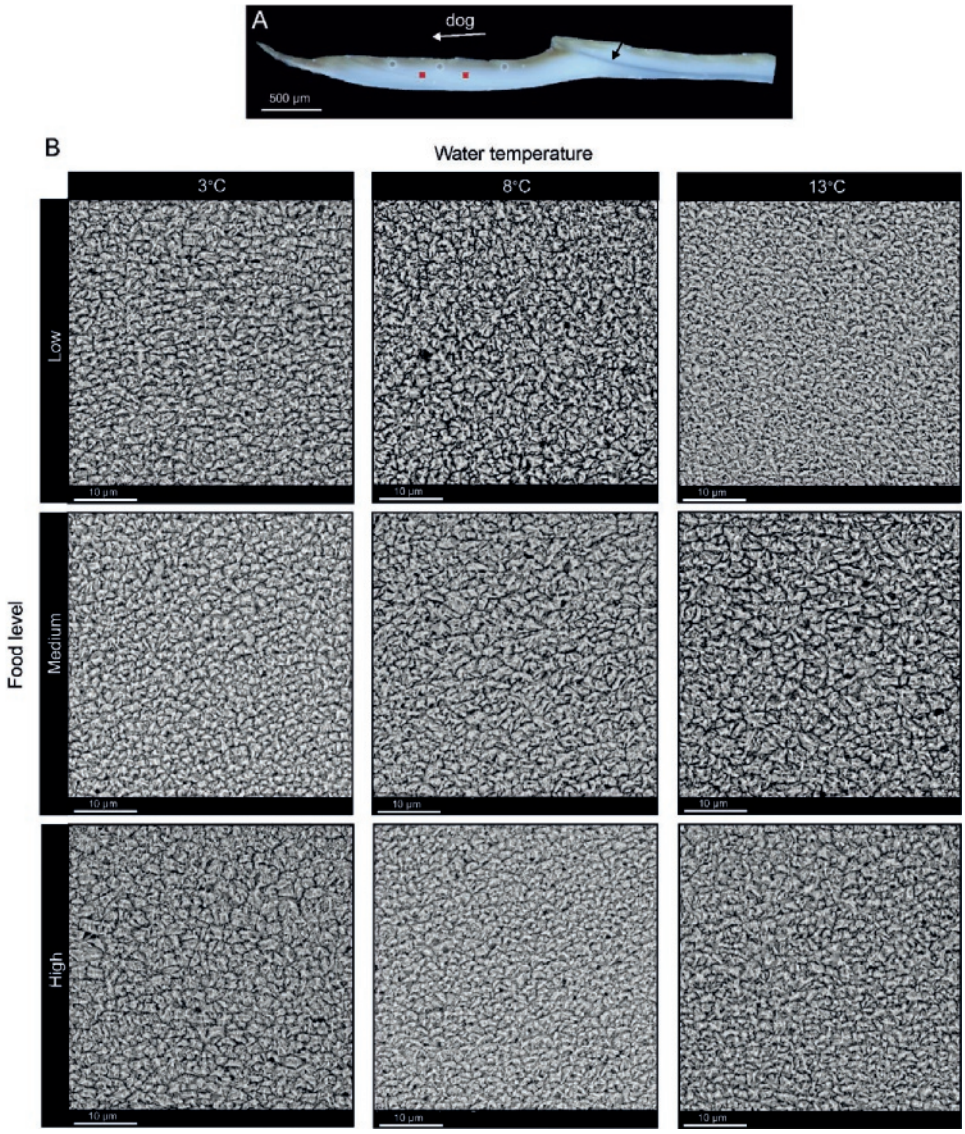

Fig. 5. 5: Microstructural organization of *A. islandica* reared in different environmental conditions. (A) Shell slab with well visible calcein line marking the start of the experiment (black arrow). The red squares indicate the approximate location of the SEM images. The three circular spots on the shell surface are the marks left behind by the LA-ICP-MS measurements. dog = direction of growth (B) Microstructures formed during the exposure at different water temperatures (3 °C, 8 °C, 13 °C) and food levels (low, medium, and high).

DISCUSSION

This study demonstrates that shell growth rate exerts a large control on incorporation of Sr, Mg, Ba and Na into shells (Table 5.4). The effect of temperature and food on shell chemistry seems overarched by shell growth and varied among the studied elements. Na seems to be affected by a combination of food and temperature, Mg by food, Sr by temperature, and for Ba, we could not demonstrate any effect of food or temperature (Table 5.3). Therefore, the findings of our study suggest that trace element incorporation into the shell of *A. islandica* is controlled by a complex interplay between environmental and physiological processes. Moreover, the comparison of the microstructural properties of shell growth by SEM could not find external or internal factors affecting *A. islandica* shell microstructural properties.

Controls on trace elemental incorporation into *Arctica islandica* shells

In many organisms, Sr/Ca and Mg/Ca ratios serve as useful paleo-temperature proxies (e.g., foraminifera, Nürnberg et al., 1996; corals, Goodkin et al., 2007; sclerosponges, Rosenheim et al., 2004; bivalves, Zhao et al., 2017b). As shown by several studies, in the bivalve *A. islandica* vital effects have an important effect on the incorporation of these two trace elements into the shell (Toland et al., 2000; Foster et al., 2008, 2009; Schöne et al., 2011, 2013; Marali et al., 2017a; Wanamaker and Gillikin, 2018). Most of these studies, which are based on small samples sizes (3-8 specimens vs. 73 this study), concluded that it is unclear whether these metal-to-calcium ratios in the shells of *A. islandica* can be used as temperature proxies. After mathematically eliminating effects of ontogenetic age and growth rate, Schöne et al. (2011) found a significant negative correlation between temperature and Sr/Ca and Mg/Ca ratios (explaining 41 and 27 % of the variability, respectively). In our controlled laboratory study, the amount of Sr incorporated into *A. islandica* was, however, positively and significantly ($r = 0.35$; $p < 0.05$; Table 5. 3) correlated to seawater temperature (Table 5. 2, 3). The difference between both studies could be due to the fact that we used juveniles and not adults, that the specimens came from different populations (Baltic Sea vs. Iceland), or to the small sample size analyzed by Schöne et al. (2011). Hart and Bluzstajn (1998) found, as in this study, a positive relationship between Sr/Ca ratios and temperature in *A. islandica.* Similar observations were previously reported for other bivalve

species by Lorrain et al. (2005), Gillikin et al. (2005), and Izumida et al. (2011). Because thermodynamics predict a negative correlation between Sr/Ca and temperature in aragonite, our results corroborate the idea that biological processes play a dominant role in the incorporation of Sr in *A. islandica* shells (Gillikin et al., 2005; Izumida et al., 2011), which is supported by the strong negative relation between shell growth and Sr concentration (Fig. 5. 4).

In contrast to Sr/Ca, and despite the broad range of temperatures tested in the present study (3 to 13 °C), Mg/Ca was significantly correlated to food level (r=-0.40), shell growth (r=-0.62) and CI (r=-0.67) rather than temperature (Table 5.3; Fig. 5. 4E, F, G, H). Moreover, multiple regression analysis showed that shell growth rate explained 23 % of the Mg/Ca variability, and identified the effect of temperature as being negligible in our data set (Table 5.4). Thus, it appears that the Sr/Ca and Mg /Ca ratios of *A. islandica* shells to a large proportion reflect physiological processes and do not exclusively reflect water temperature (Gillikin et al., 2005; Freitas et al., 2006; Elliot et al., 2009; Foster et al., 2008, 2009; Wanamaker et al., 2008c; Geeza et al., 2018; Wanamaker and Gillikin, 2018).

Although Ba/Ca ratios in some marine bivalves are used as proxy for paleo-productivity (e.g., Stecher et al., 1996; Vander Putten et al., 2000; Gillikin et al., 2008; Thébault et al., 2009; Hatch et al., 2013), we could not find a clear relationship between Ba/Ca ratios of our experimental *A. islandica* shells and food availability. The results however again suggest that Ba levels were related to shell growth rate, which could explain 23% of the variability in the shell Ba concentration, comparable to what has been found for the freshwater pearl mussel *Hyriopsis* sp. (Izumida et al., 2011). The large Ba peaks detected in some of our specimens did not show any pattern in relationship to the food concentration where those bivalves grew, instead we observed strong Ba/Ca peaks even at the lowest food level (Fig. 5. 3J, K, L). Moreover, not all specimens from the same aquarium (or same treatment) showed large Ba peaks, as it was previously reported about wild populations of *A. islandica* (Gillikin et al., 2008; Marali et al., 2017a, b). Although we kept the food concentration constant (per treatment) over the entire experimental period, and the food used was chemically homogenous, slight variations in the food supply could be the reason for the asynchrony of Ba peaks between individuals. Additionally, the time lag between feeding and incorporation of Ba into the shell, i.e., the moment that the animals really

deposited their shell, can differ between specimens and these differences can be more evident in studies of short-period of time such as ours (experimental period =14 weeks). Moreover, since different specimens had different shell growth rates the laser spots made to sublimate the carbonate might have reflected different periods or period lengths and thus have led to different sampled time frames or time frames with different time resolution (this could apply to all trace-elements analyzed). To get better insight about the timing of Ba peaks, constant series of laser spots should have been done over all the newly formed shell. Therefore, even though we did not find synchrony in the Ba peaks among specimens, we cannot exclude it either.

Interestingly, Na/Ca of *A. islandica* exhibited a significant correlation with food (r = 0.42) and temperature (r = -0.38; Table 5. 3). When several different external and internal factors were simultaneously considered in a multiple regression model, shell growth and temperature explained about 1/3 of the variability of Na/Ca (adjusted-R^2 = 32 %, Table 5. 4). Since salinity was kept stable during the course of the experiment (indicating that variation of Na/Ca ratio in the water was small), water chemistry interference on Na/Ca variations are unlikely (Table 5.2, 4). A possible explanation for the observed correlation between food and Na/Ca or temperature and Na/Ca (Table 5.3) could be that Na/Ca reflects the metabolic rate of *A. islandica*, with the latter being strongly affected by temperature and food supply (Winter 1978). Support for such an interpretation comes from the finding that the condition index was also significantly correlated with Na/Ca (r= 0.41; p <0.05). Zhao et al., (2017a) demonstrated that Na/Ca is related to the acid-base and ionic regulation in the calcifying fluid of *Mytilus edulis* shells, a process strongly linked to biomineralisation and highly dependent on the metabolic activity. Hence, when the change of Na/Ca_{water} is small, physiological influences may exert a major control on the incorporation of Na into bivalve shells.

Our findings seem to indicate that, under food limitation, *A. islandica* is less efficient in discriminating against trace and minor element impurities of the carbonate matrix and that physiological processes play an important role in the control on elemental incorporation into *A. islandica* shells.

Controls on microstructural characteristics of *A. islandica* shells

According to the results of the present study, the shell microstructure of *Arctica islandica* was not significantly affected by water temperature or dietary regimes. Although some slight differences were visible among the treatments (i.e., biomineral size increase and shape variation), the lack of consistency of these specific alterations suggest that the observed differences may not be related to the two studied environmental variables. The small morphological variability may be explained by differences among specimens. Our observations are in good agreement with Milano et al. (2017a) which results also indicated that the morphology of biomineral units in *A. islandica* shells is not influenced by water temperature or diet. Note that in their study, the role of these two environmental factors on crystal morphology were investigated in separate experiments whereas we went further in the current research by studying the effect of both environmental variables in one experiment. We did not find, however, an interaction effect on crystal morphology, size, or orientation at the temperature and food conditions considered.

Previously, microstructures of other mollusk species were shown to be influenced by the environment (Hedegaard et al., 2006; Nehrke and Nouet, 2011; Soldatov et al., 2013; Stemmer and Nehrke, 2014; Milano et al., 2017a). For instance, water temperature was identified as the major factor controlling size and shape of individual biomineral units in the non-denticular composite prismatic microstructure of *Cerastoderma edule* (Milano et al., 2017b). Similarly, the relative thickness of the composite prismatic layer of *Scapharca broughtonii* was shown to be negatively correlated with water temperature in naturally and laboratory-based grown specimens (Nishida et al., 2012, 2015). In these species, the sensitivity of the shell microstructure to environmental fluctuations, especially temperature, offers the potential to use microstructural properties as environmental proxies. However, the possibility of using shell architecture for paleoenvironmental reconstructions largely depends on the type of microstructure considered, the species under study, and the methodology applied (Nishida et al., 2012; Milano et al., 2017b; Purroy et al., 2018). Among the different mollusk species, microstructures are highly diversified, coming with different morphometric and mineralogical properties (Nishida et al., 2012; Milano et al., 2017b). In the case of homogenous microstructures as in *A. islandica*, the lack of a specific alignment among the biomineral units together with their irregular shape, challenges the

identification of potential structural changes. Unlike prismatic and crossed-lamellar structures, where variations in morphometric and alignment parameters can be easily detected using SEM, *A. islandica* microstructures may require assessments on the crystallophic properties, more than from the morphometric ones (Milano et al., 2017a).

CONCLUSIONS

Factors influencing the incorporation of trace elements into biogenetic carbonates are complex (Stecher et al., 1996) and species-specific (Gillikin et al., 2005; Freitas et al., 2006; Zhao et al., 2017b). Although element-to-calcium ratios in *A. islandica* shells contain environmental information, this information cannot be easily distinguished from physiological controls (mainly shell growth rate). Specifically, the pathways of elements from the water and food into the shell needs further study. Our study, however, supports the conclusion of Wanamaker and Gillikin (2018) that at present, there is not yet enough and consistent information that would allow to use trace element-to-calcium ratios of *A. islandica* shells as reliable environmental proxies.

With the SEM technique used in this study, we could not find a significant variation in the morphometric characteristics of *A. islandica* microstructures relating on the studied environmental variables (i.e. temperature and food). We think, however, that subsequent studies with different and more advanced methods (for instance: Confocal Raman Microscopy and Electron Backscatter Diffraction; Milano et al., 2017a) can identify physical properties of microstructures as proxies for paleoenvironmental reconstructions.

Acknowledgments

We thanks the Alfred-Wegener-Institute (AWI) for its collaboration and especially to Cyril Degletagne and Doris Abele for providing the specimens used in this study. This work was funded by the EU within the framework (FP7) of the Marie Curie International Training Network ARAMACC (604802).

The study data is available at doi:10.4121/uuid:bd1c80a5-1bd2-426a-a9d7-97ce67446886.

Appendix B

Fig. B1: Graphical abstract

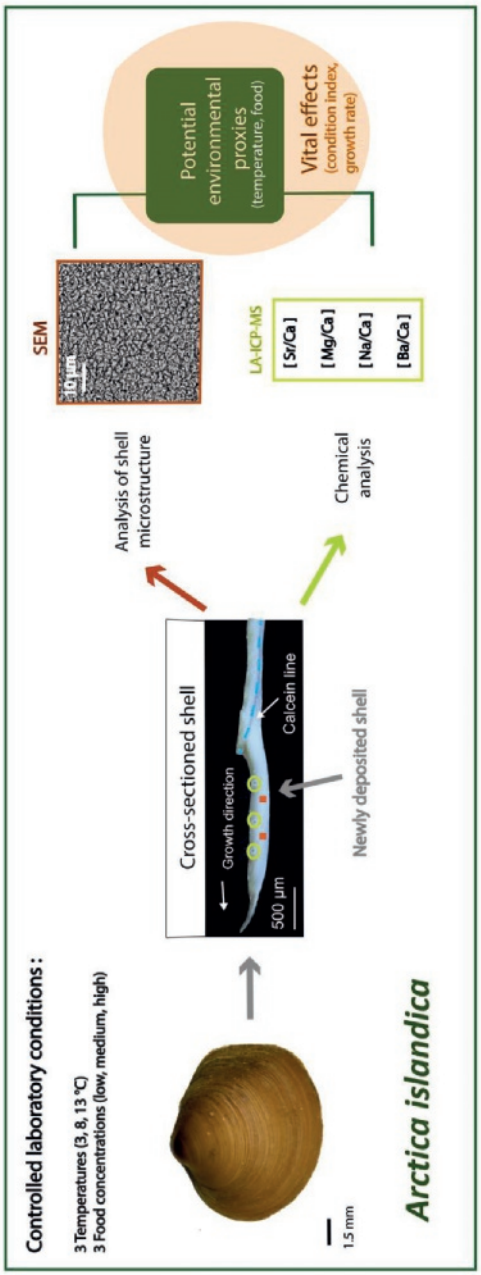

Chapter 6

Energetics of the extremely long-living bivalve *Arctica islandica* based on a Dynamic Energy Budget model

Ballesta-Artero, Irene; Augustine, Starrlight; Witbaard, Rob; Carroll, Michael L. ; Mette J., Madelyn; Wanamaker Jr., Alan D. ; van der Meer, Jaap

Submitted and under review manuscript (Journal of Sea Research)

Abstract

The ocean quahog *Arctica islandica* is the longest–living mollusk on Earth with a lifespan of at least 500 years. The slow senescence of this bivalve has promoted a great interest in its metabolic strategy. A dynamic energy budget (DEB) model was applied to describe how this species allocates its energy to maintenance, growth, maturation, and reproduction in a variable environment. We studied the relationship between *A. islandica* growth, lifespan, and food availability at eight different locations in the North Atlantic Ocean. Our results indicate that *A. islandica's* extreme longevity arises from its low somatic maintenance cost $[\dot{p}_M]$ and low ageing acceleration $\ddot{h}_a$, but there was not a direct relationship between food availability and lifespan in these *A. islandica* populations. The Monkey Bank (North Sea), Iceland, and Ingøya (northern Norway) populations had the highest food availability estimates of all the localities but did not have the lowest longevities, in contrast to the theory of caloric restriction.

Keywords

Ocean quahog, growth, metabolism, ageing, food conditions, temperature, Dynamic Energy Budget (DEB) Theory

INTRODUCTION

The slow-growing bivalve *Arctica islandica* is one of the longest-living organisms on Earth, with a life span of up to five centuries (Wanamaker et al., 2008a; Butler et al., 2013). This species has a decrease in growth after the first ~20 years of its life (Ropes, 1985; Kilada et al., 2007; Begum et al., 2009), exhibiting, as adults, one of the slowest growth rates reported among bivalves (values even < 0.05 mm per year; Thompson et al., 1980a; Murawski et al., 1982; Kennish et al., 1994; Wanamaker et al., 2008a; Mette et al., 2016). *A. islandica* is widely distributed on both sides of the North Atlantic, where its populations exhibit geographical differences in shell shape, color, and growth rate (Ropes, 1985; Witbaard and Duineveld, 1990; Witbaard et al., 1999; Dahlgren et al., 2000). Moreover, *A. islandica* populations vary greatly in their maximum lifespan, from ~40 years in Kiel Bight (Germany) to 507 in Iceland (Philipp and Abele, 2010; Begum et al., 2010; Butler et al., 2013). Most genetic and physiological studies indicate that such variations in growth and life span reflect a response to local environmental conditions rather than being a result of genetic differences (Witbaard et al., 1996; Dahlgren et al., 2000; Schöne et al., 2003; Witbaard et al., 2003; Holmes et al., 2003; Begum, 2009; Strahl and Abele, 2010). Previous studies on *A. islandica* showed that gaping activity, shell growth, and tissue growth were closely correlated with food availability and, to a lesser degree, with temperature (Ballesta-Artero et al. 2017, 2018). Limited food availability in winter (seasonal caloric restriction) and associated deep-burrowing and metabolic depression (Philipp and Abele, 2010; Ballesta-Artero et al., 2017) may be the keys to understanding this organism's long lifespan.

Here, we use the Dynamic Energy Budget (DEB) theory to investigate whether variations in *A. islandica* growth and energy allocation can be explained in terms of environmental factors (i.e., food and temperature) and if there is an evident relationship between local food conditions and lifespan (theory of caloric restriction, e.g., Sinclair 2005). We compare growth data from eight *A. islandica* populations on the North East Atlantic coast: Ingøya (northern Norway), Iceland, Faroe, Fladen Ground (northern North Sea), Fisher Bank (northern North Sea), Monkey Bank (central North Sea), Silver Pit (southern North Sea), and Kiel Bay (Baltic Sea; Fig. 6. 1).

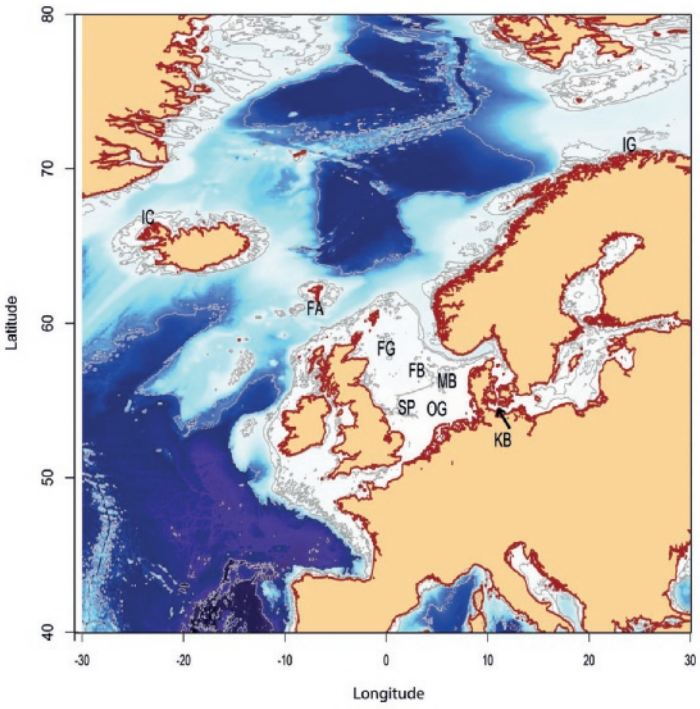

Fig. 6. 1: Geographic locations of *Arctica islandica* populations used in this study: Ingøya (IG), Iceland (IC), Faroe (FA), Fladen Ground (FG), Fisher Bank (FB), Monkey Bank(MB), Silver Pit (SP), and Kiel Bay (KB; laboratory specimens). Map colors represent water depth: white, shallower than 250 m and, from clear blue to black, water depths range from 250 to ≥ 5000 m (steps of 250 m).

A standard DEB model describes how an organism uses food to live in a changing environment (Kooijman, 2010). Using a DEB model, processes such as maintenance, growth, and reproduction are quantified as energy and mass fluxes (Fig. 6. 2; for more details see supplementary material Box 6A, Van der Meer, 2006 and Kooijman, 2010). So far, DEB models have been successfully used to describe the energy allocation of 895 species (Amp 2017). The strength of the DEB theory is that differences between species are reflected in the differences between parameters values (Van der Veer et al., 2001; Sousa et al., 2008; Freitas et al., 2009; Kooijman, 2010).

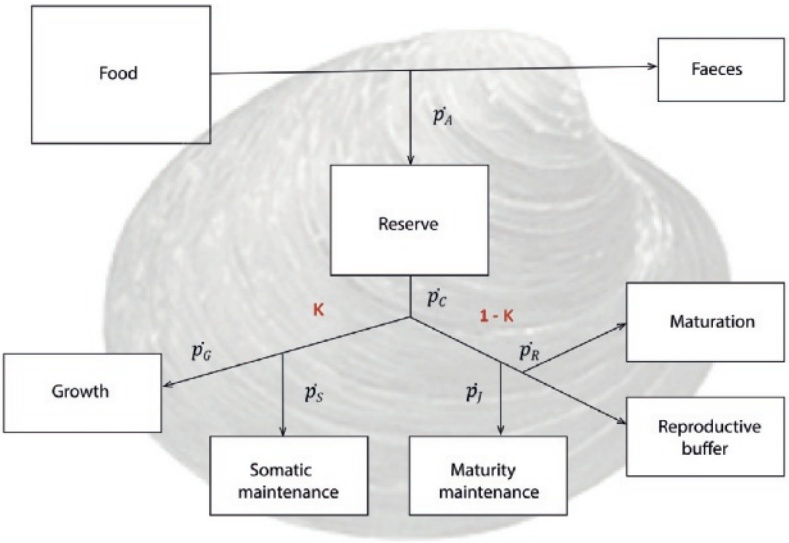

Fig. 6.2: Representation of the main metabolic processes in DEB theory (Kooijman 2010). There are six energy fluxes: assimilation ($\dot{p}_A$), mobilization ($\dot{p}_C$), somatic maintenance ($\dot{p}_S$), growth ($\dot{p}_G$), maturity maintenance ($\dot{p}_J$), and maturation + reproduction ($\dot{p}_R$). NOTE: The parameter κ (red kappa) is the fraction of the mobilized energy allocated to growth and somatic maintenance. The remaining portion 1-κ is the fraction allocated to maturity maintenance and to maturation (for juveniles) or reproduction (for adults). See supplementary material for equations.

In this study, we use DEB modeling to (1) describe the energetics of the long-living bivalve *A. islandica*, (2) predict the food conditions that explain the observed growth patterns in eight North Atlantic locations and to see whether these predictions correlate with local primary productivity estimates, and (3) investigate characteristics regarding its unique ageing. We compare the estimates of all DEB parameters for *A. islandica* with those of almost 1000 other species (Amp 2017) and explore which parameters related to ageing. Additionally, we examine whether differences in longevity among *A. islandica* populations coincide with local food conditions (theory of caloric restriction).

Box 6A: Main equations of the DEB model

The 'abj'- model which is here applied to *A. islandica* is similar to the standard DEB model ('std'), with the exception that metabolic acceleration occurs between birth and metamorphosis. Before and after acceleration, growth is isomorphic. Metamorphosis occurs at maturity level E_H^j (J), which might or might not correspond with changes in morphology. This model is a one-parameter extension of model 'std'. The dynamics of the state variables of the abj-DEB model are specified by the following equations:

$$\frac{d}{dt}E = \dot{p}_A - \dot{p}_C$$

$$\frac{d}{dt}V = \frac{\dot{p}_G}{[E_G]}$$

$$\frac{d}{dt}E_H = \begin{cases} \dot{p}_R \text{ if } E_H < E_H^p \\ 0 \text{ otherwise} \end{cases}$$

$$\frac{d}{dt}E_R = \begin{cases} 0 \; if \; E_H < E_H^p \\ \dot{p}_R \text{ otherwise} \end{cases}$$

Where $V = L^3$, is the structural volume. The energy fluxes in J/d are given by:

$$\dot{p}_A = \begin{cases} 0 \text{ if } E_H < E_H^b \\ f\,\{\dot{p}_{Am}\}\,\mathcal{M}(V)\,V^{2/3} \text{ otherwise} \end{cases} \qquad f = \frac{\mathrm{X}}{\mathrm{X}+X_K}$$

To account for the effects of food availability, the DEB model uses a scaled version of the Holling's type II functional response, f, where X is the amount of available resources as density (by volume), $X_K$represents the half saturation coefficient (density at which feeding rate is half of its maximum value).

$$\dot{p}_C = E\left(\frac{[E_G]\,\dot{v}\,\mathcal{M}(V)\,V^{2/3} + \dot{p}_S}{\kappa\,E + [E_G]\,V}\right)$$

$$\dot{p}_S = [\dot{p}_M]\,V$$

$$\dot{p}_G = \kappa\,\dot{p}_C - \dot{p}_S$$

$$\dot{p}_J = \dot{k}_J E_H$$

$$\dot{p}_R = (1-\kappa)\dot{p}_C - \dot{p}_J$$

$\mathcal{M}(L)$, is the shape correction function by which both $\dot{v}$ and $\{\dot{p}_{Am}\}$ need to be multiplied. During metabolic acceleration the organism changes in shape: surface area grows proportional to volume:

$$\mathcal{M}(V) = 1 \quad \text{if} \quad E_H < E_H^b \quad \text{(embryo)}$$
$$\mathcal{M}(V) = \left(\frac{V}{V_b}\right)^{1/3} \quad \text{if} \quad E_H^b \le E_H < E_H^j \quad \text{(early juvenile)}$$
$$\mathcal{M}(V) = \left(\frac{V_j}{V_b}\right)^{1/3} \quad \text{if} \quad E_H \ge E_H^j \quad \text{(late juvenile)}$$

Where V_b(cm) and V_j(cm) is the structural volume at birth and metamorphosis respectively. $L = V^{\frac{1}{3}}$ is the structural length which is taken proportional to shell length (see methods section).

All of the model parameters can be found in Table 6. 1. The acceleration factor, $s_{\mathcal{M}} = \frac{L_j}{L_b}$ is a food dependant quantity and is equal to 2.35 at f=1.

METHODS

DEB model

DEB theory describes an organism with the state variables structural volume V (cm^3), reserves E (J), maturity E_H (J), and reproduction buffer E_R (J) (see equations in supplementary material Box 6A). It also distinguishes three different life stages: embryo (no food is ingested), juvenile (eats but does not reproduce), and adult (eats and reproduces). At each life stage transition, which occurs when a specific level of maturity is reached, a metabolic switch takes place. For instance, puberty is the moment when energy allocation to maturation is redirected to reproduction (Kooijman, 2010). The ages at which switches are triggered depend on past food intake and may differ among individuals (Kooijman, 2010). The state variables are related to direct measurements such as length and body weight. In our case, shell length is proportional to structural length (through the shape factor δ_M), while reserve, structure, and reproductive buffer contribute to body mass (for more details, see Van der Meer, 2006; Kooijman, 2010; Lika et al., 2011).

The dynamics of the state variables are determined by six energy fluxes: assimilation ($\dot{p}_A$), mobilization ($\dot{p}_C$), somatic maintenance ($\dot{p}_S$), growth ($\dot{p}_G$), maturity maintenance ($\dot{p}_J$), and maturation + reproduction ($\dot{p}_R$; Fig. 6. 2, see equations in supplementary material Box 6A). First, ingested food is assimilated by the organism (assuming a fixed efficiency) and subsequently incorporated into a reserve pool from which energy is mobilized and allocated on the basis of the κ-rule. The κ-rule states that a fixed fraction (κ) of the energy is allocated to growth and somatic maintenance, and the remaining portion (1-κ) is used for maturity maintenance and maturation (for juveniles) or reproduction (for adults; Fig. 6. 2). All metabolic rates are also dependent on temperature through the Arrhenius rule (supplementary material Box 6B).

Mass invested in reproduction accumulates inside a reproduction buffer which is emptied at spawning events. However, not much is known about when spawning occurs for *A. islandica* nor what actually triggers it (Thompson et al., 1980b; Thorarinsdottir and Steingrimsson, 2000; Ballesta-Artero et al. in preparation (a)). Due to the lack of detailed reproduction information of the species, we did not account for the reproduction buffer when modelling weight as function of length. Species-specific reproduction buffer handling rules would be needed in order to specify these issues within a DEB modelling framework (see e.g. Gourault et al 2018).

DEB theory considers that some taxa, such as bivalves, exhibit an acceleration of metabolism during their life cycle that results in higher metabolic rates than the 'normal' expected trajectory for the standard species (Kooijman, 2014). Bivalve larval stages have a very different morphology compared to the subsequent juvenile and adult stages. These planktonic larval stages develop slower than the benthic juvenile and adult stages (Kooijman, 2014). Metabolism accelerates after the first feeding and/or settlement. This type of acceleration is represented by a one-parameter extension of the standard DEB model (Kooijman, 2010, 2014). The differential equations that describe the dynamics of the state variables are provided in the supplementary material Box 6A; the associated DEB parameters are given in Table 6. 1.

Box 6B: Temperature dependence of rates

The temperature dependence of rate (and age) constants can be accounted for by multiplying (or dividing) them with a temperature correction factor c_T that can be derived from the Arrhenius relation. The temperature correction is given by:

$$c_T = \left(\frac{T_A}{T_{ref}} - \frac{T_A}{T} \right)$$

All temperatures are given in Kelvin. In this equations, T_{ref} is a reference temperature of 293.15K (20 °C), T is the temperature at which the data was recorded, and T_A is the Arrhenius temperature, which can be estimated if sufficient data is available. In this study we assumed a typical value of 8000 K, as the data were not sufficient to allow estimation.

Data

We estimated *A. islandica* DEB parameters primarily using our own field and laboratory datasets. We included information from the literature only for the so-called zero-variate data (Table 6. 2). This is a minimum set of relatively simple species-specific biological scalars, such as age at birth or ultimate shell length, which are temperature dependent. The *A. islandica* univariate data, which are "a set of pairs of values for an independent and associated dependent variable (DEB wiki)" are length-weight and age-length-time data. They originate from:

- A laboratory growth experiment with juveniles of *A. islandica* reared at 3 different temperatures (3, 8, 13 °C) at high food conditions (~15 x 10^6 cells/L; Ballesta-Artero et al., 2018)
- A sample taken from a wild population from Ingøya (northern Norway). Mette et al. (2016) provided age-length data, and length-weight data were obtained from our own dissections (Ballesta-Artero et al. in prep).
- Seven different North Atlantic populations: Iceland, Faroe, Fladen Ground , Fisher Bank, Monkey Bank, Silver Pit, and Kiel Bay (Witbaard et al., 1999; Fig. 6. 2, Table 6. 3). Samples taken by Witbaard et al. (1999) provided age-length data. For the Iceland population, growth measurements were also obtained from Schöne et al. (2005b). This data included a very old specimen, whereas Witbaard et al. (1999) only covered a limited set of age classes (< 50 years old).

Food availability

A. islandica is a filter-feeding bivalve that feeds on the available phytoplankton at the sea bottom. According to DEB theory, the ingestion rate of an organism is proportional to the scaled functional response *'f',* which is related to the food density (X) by a Holling type II curve. That is:

$$f = \frac{\mathrm{X}}{\mathrm{X} + X_K}$$

where $X_K$is the half-saturation parameter. f varies between 0 and 1, i.e., from starvation to *ad libitum* feeding conditions. In our study, exact food conditions of the fieldwork locations were unknown thus f of each population was assumed constant (X_t, where t is time), and estimated from the data. We also estimated the f for the laboratory experiment.

Primary productivity (or phytoplankton production) is highly variable in time and space due to factors such temperature, light, and nutrient supply (Skogen et al., 2007). Different models and *in situ* records have been used to calculate primary productivity in the North Atlantic (Joint and Pomroy, 1993; Skogen and Moll, 2000; Skogen et al., 2007; Capuzzo et al., 2017). Primary productivity estimates considerably vary among studies (Table 6. 3). We used an average value of the various available estimates (Joint and Pomroy, 1993; Skogen and Moll, 2000; Skogen et al.,

2007; Steingrund and Gaard, 2005; Astthorsson et al., 2007; and Capuzzo et al., 2017) and compared it to our estimated scaled functional response (Table 6. 3).

Parameter estimation

We used an improved version of the co-variation method for parameter estimation (Lika et al., 2011), presented in detail in the online Amp manual (DEB Wiki; Marques et al., 2018a, b). Code, data, and results can be downloaded from the add-my-pet collection (AmP 2017). Estimated parameters are listed in Table 6. 1, and are stored in AmP as version 2017/11/12: https://www.bio.vu.nl/thb/deb/deblab/add_my_pet/entries_web/Arctica_islandica/Arctica_islandica_res.html

Table 6. 1: DEB parameter values for *Arctica islandica* at reference temperature 20 °C. AmP, version 2017/11/12,https://www.bio.vu.nl/thb/deb/deblab/add_my_pet/

symbol	value	unit	definition
$\{\dot{p}_{Am}\}$	15.06*	J cm^{-2} d^{-1}	Maximum surface area-specific assimilation rate
$[\dot{p}_M]$	3.532	J cm^{-3} d^{-1}	Volume-specific maintenance costs
$\dot{v}$	0.0433*	cm d^{-1}	Energy conductance
$[E_G]$	2365	J cm^{-3}	Volume-specific costs of growth
κ	0.57	-	Allocation fraction to soma
E_H^b	0.011	J	Maturity threshold at birth
E_H^j	0.1381	J	Maturity threshold at metamorphosis
E_H^p	22010	J	Maturity threshold at puberty
δ_M	0.370	-	Shape factor laboratory
δ_{Mb}	0.502	-	Shape factor field
z	2.419	-	Zoom factor
$\ddot{h}_a$	2.231^{-12}	d^{-2}	Weibull ageing acceleration
T_A	8000	K	Arrhenius temperature
s_M	2.327	-	Acceleration factor
$\dot{k}_j$	0.00046	d^{-1}	Maturity maintenance rate coefficient
f	see Table 6. 3	-	scaled functional response

NOTE: * values before acceleration, see supplementary material Box 6A for explanation

The overall goodness of fit was measured with the mean relative error (MRE), which can vary between 0 and ∞, the symmetric mean squared error (SMSE), varying between 0 and 1, for the

univariate data, and with the relative error (RE) for all zero-variate data (see Marques et al. 2018a for equations). The relative error is a ratio of the absolute error of a measurement to the measurement being taken.

RESULTS AND DISCUSSION

DEB parameters and predicted values

We estimated DEB model parameters and scaled functional responses from all data simultaneously using the technique of fitting multiple models to multiple data as described in Marques et al., (2018b). The overall goodness of fit of the model was good: the MRE is 0.242 and the SMSE is 0.202. The relative error for all zero variate data was less or equal to 20% except for the length at metamorphosis, which has a RE of 2.5 (Table 6. 2). Overall, the predicted lengths did not fit as well as the predicted rates, times, and weights. This result is not unexpected due the variability in morphology among populations and individuals. The maximum length (11 cm) was underestimated when compared to the 14-cm shell length given by Ropes (1985), although it still falls well within the range of published values (9-14 cm, Sager and Sammler, 1983; Begum et al., 2010).

The site-specific empirically reconstructed growth curves were generally well captured by the DEB model assuming a constant food level (Fig. 6. 3). The mean relative error between the data and model was between 0.07 and 0.30. The largest discrepancy between the model and data was found for the Ingøya population, and the underlying cause is not yet clear. The Ingøya population showed a sudden transition from rapid to slow growth, which seems to coincide with the juvenile-adult transition. Holmes et al. (2003) suggests that the reason growth slows during ontogeny is that the allocation to growth and somatic maintenance it is suddenly reduced after sexual maturation. According to the DEB theory, growth and maturation are parallel processes that do not directly compete with each other for resources (the kappa rule).

The duration of the egg and larval stages were well captured by the model (Table 6. 2). *A. islandica* needs 4 days to birth (from embryo to larvae), and 27 days to metamorphosis (from planktonic larvae to benthonic juvenile or spat). According to the constructed DEB model, the

species reaches maturity at an age of ~5.5 years old (1978 days) when shell length is ~4cm (Table 6. 2). Better knowledge concerning the weight at metamorphosis would help determine how accurate the DEB model is since morphology at metamorphosis might be more variable than in the later juvenile and adult stages. Meanwhile, the predicted dry weight at metamorphosis at *ad libitum* food is 8 µg. An advantage of a modelling framework like DEB is that unknown quantities can be predicted and then subsequently tested. The duration and timing of key events like first feeding, metamorphosis, and reproduction are well captured by the model.

Unexpectedly, we needed to use two shape factors (δ_M) to get a good fit for the growth of the laboratory specimens and the field populations at the same time (Table 6. 1). We think this was due to the fact that the specimens from the laboratory were juveniles (not adults as in the field locations), and furthermore, come from a location (Kiel Bay, Germany) where uniquely stressful local environmental conditions (low salinity and high temperature, Zettler at al., 2001) contribute to particular shape features.

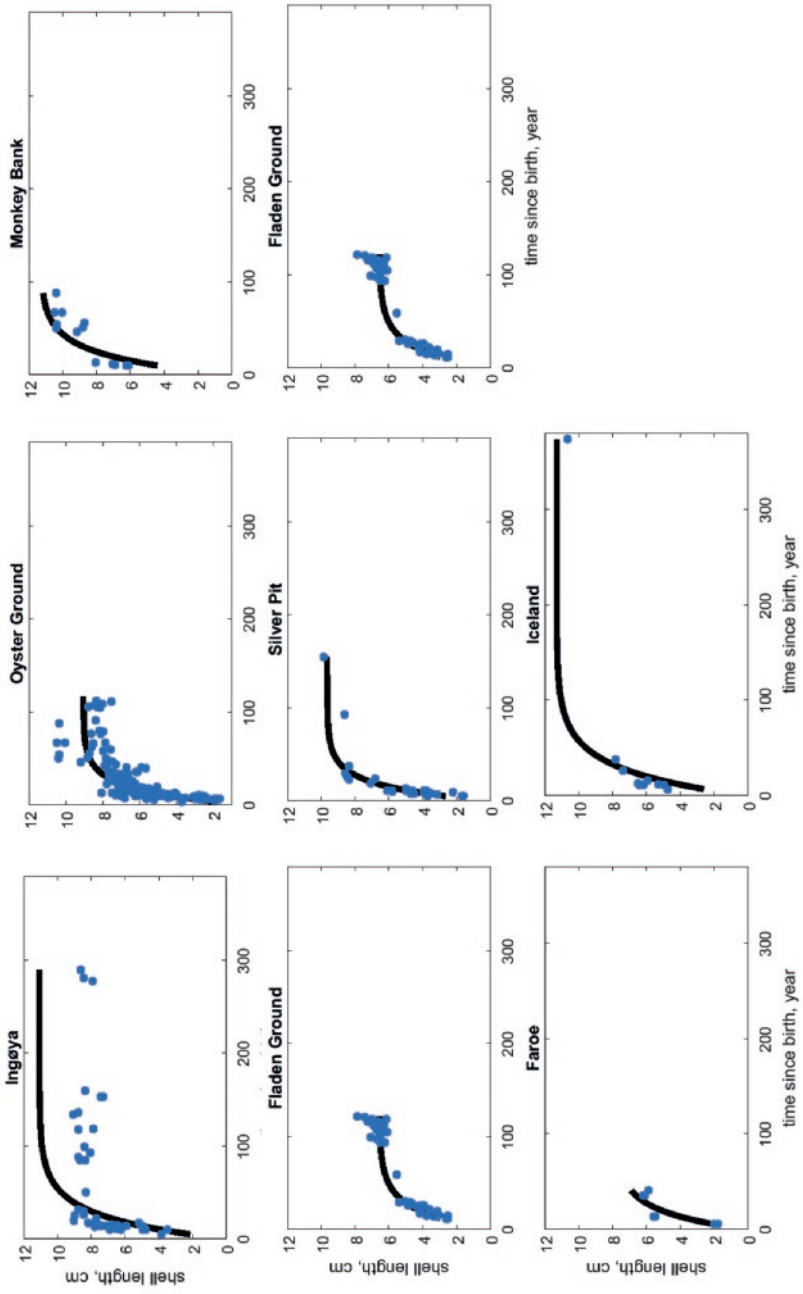

Fig. 6. 3: Growth curves at different North Atlantic populations. Points indicate observed data and lines indicate model predictions.

Table 6. 2: Comparison of observed and model predicted zero-variate data (temperature dependent data): maximum reproductive rate, age, length, and weight at different life stages. RE: Relative error.

Data	Observed	Predicted	RE	Unit	Description	Referencia
a_b	4	4.262	0.066	d	Age at birth	Lutz et al., 1982
t_j	34	27.23	0.199	d	Time since birth at metamorphosis	Lutz et al., 1982
t_p	2190	1978	0.097	d	Time since birth at puberty	Thompson et al., 1980b
a_m	1.85E+05	1.85E+05	0.000	d	Life span	Butler et al., 2013
L_J	0.024	0.085	2.521	cm	Shell length at metamorphosis	Lutz et al., 1982
L_P	4	4.234	0.059	cm	Shell length at puberty	Thompson et al., 1980b
L_i	14	11.34	0.190	cm	Ultimate shell length	Ropes, 1985
W_w^0	0.01375	0.013	0.070	mg	Wet weight of an egg.	Oertzen, 1972
W_w^p	0.98	1.007	0.028	g	Dry weight at puberty	Ballesta-Artero in prep.
R_L	1096	1124	0.026	egg/d	Reproduction rate at 5-cm	Oertzen, 1972

When compared to the rest of species from the DEB collection, *A. islandica* seems to have a low allocation fraction to soma (κ = 0.57; Fig. 6. 4a), a low volume specific somatic maintenance ($[\dot{p}_M]$ =3.53; Fig. 6. 4b), and an average energy conductance ($\dot{v}$ =0.101, values post-metamorphosis; Fig. 6. 4c).

The allocation fraction to soma (κ = 0.57) is lower than the median value of the 895 species in AmP at 2017/12 /14 (0.89, Fig. 6. 4a). The distribution of kappa values follows a beta distribution with surprising accuracy, both for bivalves and for all species together (see Lika et al. 2018). The estimated κ of 0.57 is close to the value that maximizes reproductive output of an organism, estimated to be around 0.45 (Lika and Kooijman, 2003). This suggests that *A. islandica*'s metabolism prioritizes reproductive output. A 5-cm *A. islandica* specimen produces ~400,000 eggs per year (Oertzen, 1972), equating to a reproduction rate of 1096 eggs (predicted 1124 eggs) per day for an individual of that size at a temperature of 10 °C (see comparison of *A. islandica* reproduction rate with other mollusks species in supplementary material Box 6C). Using the parameters obtained here (Table 6. 1), the expected reproduction rate for an individual of maximum size is 44,000 per day, with a cumulative reproductive output (number of eggs) of 75 x10^7 eggs (~864 g) over its entire life time (at high food and typical temperature of 6 °C). These findings assume that *A. islandica* reproduces during its entire adult life without signs of

reproductive senescence, in accordance with observational studies (Thompson et al., 1980b; Thorarinsdottir and Steingrimsson, 2000).

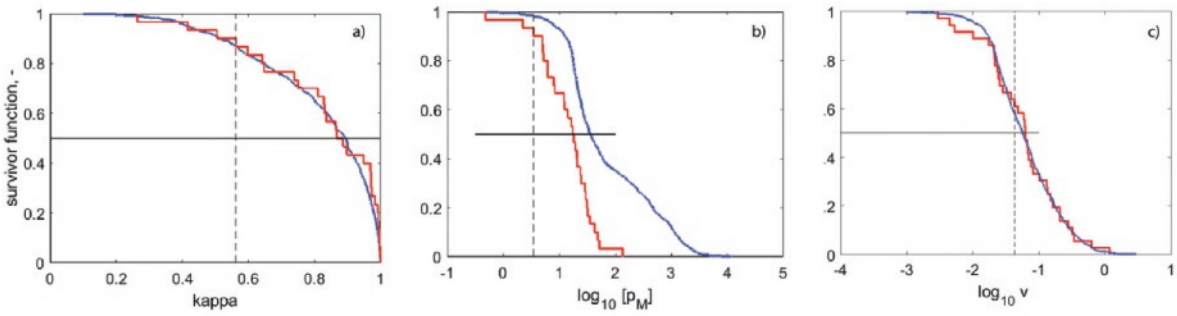

Fig. 6. 4: Survival functions (fraction of species that has a value larger than the x-axis) for all species in the DEB collection (blue curve), and all bivalves (red curve). Horizontal solid line shows the median. The estimated value for *A. islandica* is indicated by the dashed vertical line. a) Allocation fraction to soma κ; b) volume-specific maintenance cost $[\dot{p}_M]$; c) energy conductance $\dot{v}$ (post-metamorphosis).

The specific reserve capacity $[E_m] = \frac{\{\dot{p}_{Am}\}}{\dot{v}}$ (J/cm^3) quantifies the capacity of organisms to adapt to fluctuations in food availability. *A. islandica* resides in strongly seasonal environments and survives long periods of starvation (Taylor, 1976; Ballesta-Artero et al., 2017, 2018). We hypothesized, therefore, that the species might have an exceptionally high reserve capacity. In Fig. 6. 5a, the maximum reserve density as function of structural size is presented for all bivalves. The estimated reserve capacity value for *A. islandica* is not exceptionally high. On the contrary, it is on the lower end of the range of values for that size class. The energy conductance $\dot{v}$ is close to the median value for all DEB collection species (Fig. 6. 4c, Fig. 6. 5b). This suggests that low volume-specific somatic maintenance $[\dot{p}_M]$ rather than a low value of $\dot{v}$ may be the reason for *A. islandica*'s prolonged survival during starvation (Fig. 6. 4b). Our finding of a low maintenance costs for *A. islandica* is in agreement with earlier studies of the species (Begum et al., 2009, 2010).

The DEB modelling framework developed in this study not only allows estimating DEB parameters from data, but also provides a framework to assess how these parameters relate to

those of bivalves in general, providing first steps in the direction of understanding selection pressure of adapting to particular environments.

Box 6C: *A. islandica* reproductive output

Comparing *A. islandica* reproductive output with other mollusk species from the DEB collection revealed average to high values compare to the rest of species. See plots below:

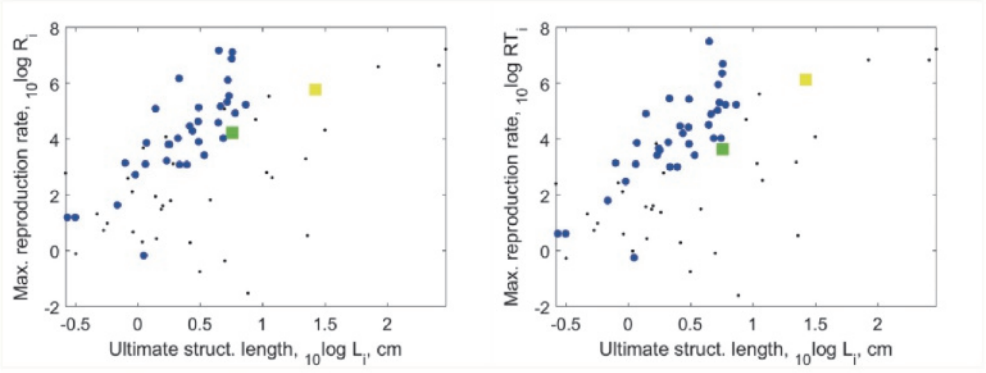

Plots of maximum reproduction rate as function of size. Left: values are plotted at reference temperature (20 C); right: values are provided at a typical temperature for each species. Small (black) dots: all Mollusca; large (blue) dots: only Bivalvia; green square: *A. islandica*; and yellow square: *T. gigas*

DEB parameters and ageing

To explore which DEB parameters could be related to the unique ageing of *A. islandica*, a comparison was made with 63 mollusk species (30 bivalves; Fig. 6. 5a-h). We present the parameters as a function of the ultimate structural length to correct for size. For most parameters examined, *A. islandica* had values within the range of other bivalves, though visually at the edge (Fig. 6. 5a-h). Only its ageing acceleration factor ($\ddot{h}_a$; Fig. 5e) strongly deviated, being the lowest of all the mollusks within the DEB collection (Amp, 2017). *Tridacna gigas* (the giant clam) had parameters values that were more outside the norm than those of *A. islandica*.

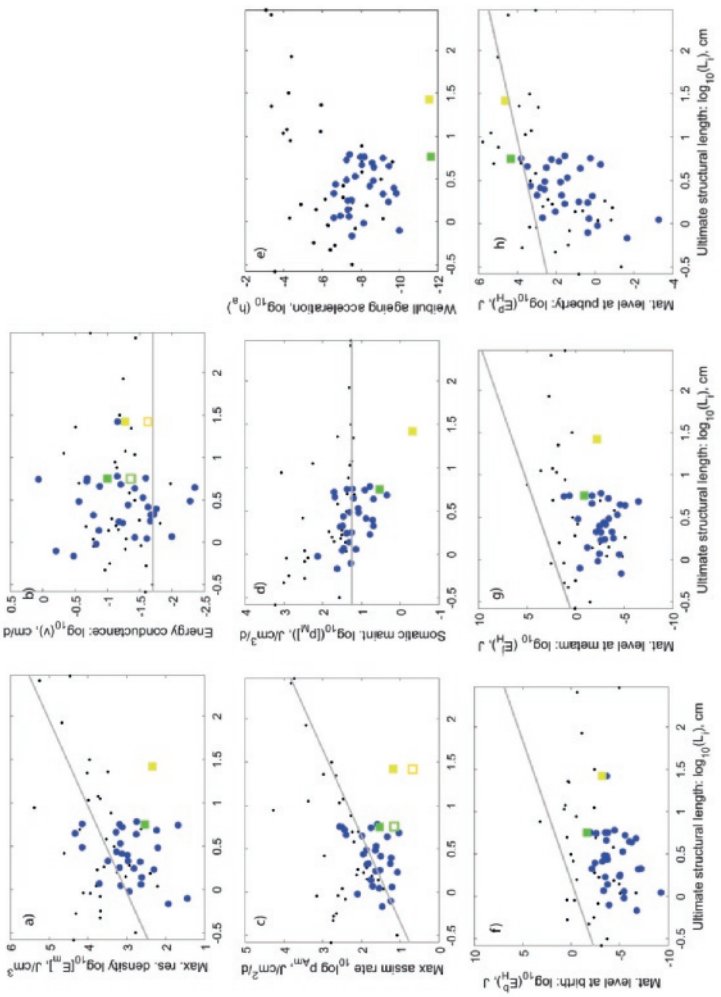

Fig. 6. 5: Comparison of DEB parameters as functions of ultimate structural length in mollusks. Small (black) dots: All Mollusca; large (blue) dots: only Bivalvia; green square: *A. islandica*; and yellow square: *T. gigas* (full square before metamorphosis, empty square after metamorphosis). Grey line: expectation of the DEB generalized animal. The parameters are: a) maximum energy density (E_m), b) energy conductance ($\dot{v}$), c) maximum specific assimilation $\{\dot{p}_{Am}\}$, d) specific somatic maintenance cost $[\dot{p}_M]$, e) ageing acceleration $(\ddot{h}_a)$, f) maturity at birth (E_H^b), g) maturity at metamorphosis (E_H^j), and f) maturity at puberty (E_H^p).

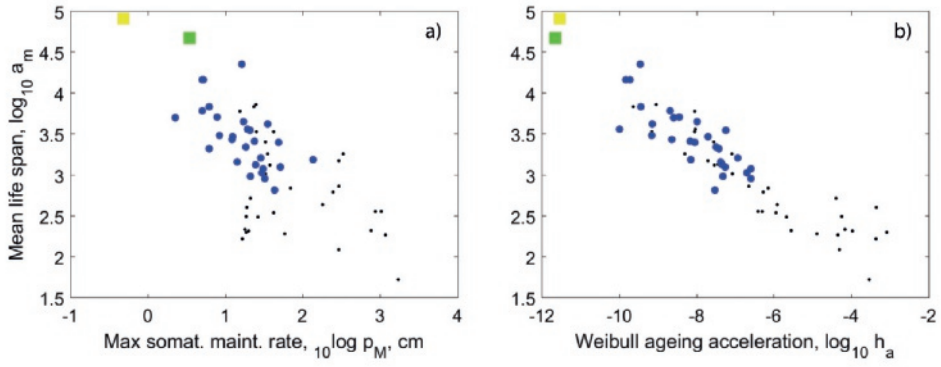

Fig. 6. 6: Mean life span (at abundant food) as function of a) maximum somatic maintenance ($[\dot{p}_M]$, J/cm^3/d), and b) ageing acceleration $\ddot{h}_a$. Small (black) dots: Mollusca; large (blue) dots: Bivalvia; green square: *A. islandica*; and yellow square: *T. gigas*. Values are calculated at reference temperature (20 °C).

Next, we investigated how life span is calculated under the DEB theory. According to Kooijman (2010), the mean life span of a species at abundant food conditions can be approximated by:

$$1.62 \left(\frac{\kappa\{\dot{p}_{Am}\}s_M}{\ddot{h}_a \dot{v}[\dot{p}_M]}\right)^{1/3}$$ (see supplementary material Box 6D for more details)

We see from this expression that the maximum specific assimilation $\{\dot{p}_{Am}\}$, energy conductance $\dot{v}$, specific somatic maintenance $[\dot{p}_M]$, and ageing acceleration $\ddot{h}_a$, are involved in determining longevity. *A. islandica* has one of the lowest $[\dot{p}_M]$ and highest mean life span of all mollusks within the DEB collection at the typical temperature for each species (Fig. 6. 5d; Amp 2017). When we computed the mean life span at abundant food of all species at the same reference temperature (20°C), the tropical species *T. gigas* , however, had higher mean life span than *A. islandica*'s (223 vs. 129 years, respectively; Fig. 6. 6a). The same happened with the parameter ageing acceleration (Fig. 6. 6b) . It appeared that mean life span scales negatively with maintenance $[\dot{p}_M]$ and ageing acceleration $\ddot{h}_a$ (Fig. 6. 6a, b). Our data suggest that the extreme longevity of both species is related to the low value of these two parameters (Fig. 6. 6a, b).

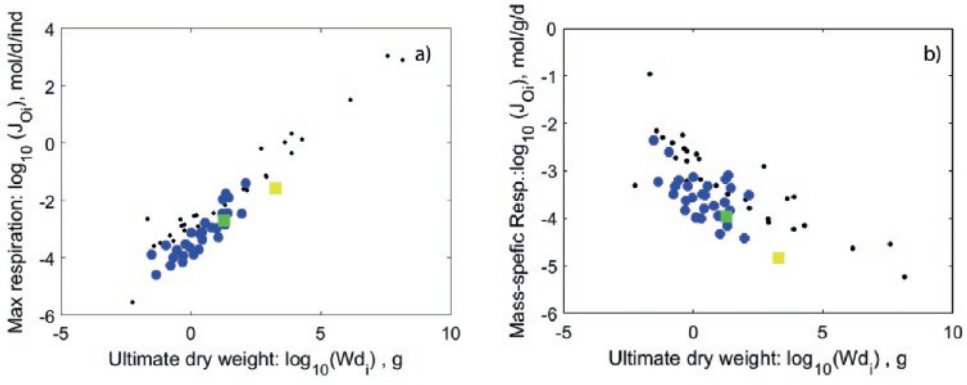

Fig. 6. 7: a) Maximum respiration rate as function of ultimate dry weight (weight at ultimate length) b) mass-specific oxygen consumption of a fully grown individual. Small (black) dots: Mollusca; large (blue) dots: Bivalvia; green square: *A. islandica*; and yellow square: *T. gigas*. NOTE: Values at the reference temperature (20 °C) for each species.

Begum et al. (2009) found that the weight-specific respiration of *A. islandica* was significantly below the average of 59 bivalve species (when compared at the same temperature). Within the DEB framework, the general pattern across species is that respiration of fully grown individuals increases with maximum body weight with a scaling coefficient around 0.75 (Fig. 6. 7a). This implies that mass-specific respiration of adult individuals is negatively related to the maximum body weight with a scaling coefficient around -0.25 (Fig. 6. 7b). In line with the finding of Begum et al. (2009), we found that the expected respiration of fully grown *A. islandica* was lower than the mean for bivalves of the same size (Fig. 6. 7a, b). Begum et al. (2009) also stated that individuals of *A. islandica* of almost the same size, but of quite different ages, had on average the same respiration, indicating that aging in itself does not play a role on the respiration of the species (at least the first 100 year of its life; Begum et al., 2009). However, ageing had a negative effect on respiration in shorter lived bivalves such as *Mytilus edulis* (Begum et al., 2009).

Box 6D: Mean life span

Section 6.1.1 of Kooijman (2010) specifies the mean age at death as : $a_m = \Gamma\left(\frac{4}{3}\right)/\dot{h}_W$ where Γ is the gamma function and $\dot{h}_W = (\frac{\ddot{h}_a e\, \dot{v}}{6\, L})^{1/3}$. e is the scaled reserve density ($e = \frac{E}{V[E_m]}$) and $[E_m] = \frac{\{\dot{p}_{Am}\}}{\dot{v}}$ is the maximum reserve density (J/cm^3). We refer the reader to that chapter for the full derivation and underlying assumptions which is outside the scope of this appendix.

The mean life span at abundant food ($e = 1$) and at maximum size, i.e. $L = L_\infty = \kappa \frac{\{\dot{p}_{Am}\}}{[\dot{p}_M]} s_{\mathcal{M}}$ is derived from this expression:

$$a_m = \frac{\Gamma\left(\frac{4}{3}\right)}{\dot{h}_W} = \Gamma\left(\frac{4}{3}\right) (\frac{6L}{\ddot{h}_a e\, \dot{v}})^{1/3}) \approx 1.62\, (\frac{L}{\ddot{h}_a e\, \dot{v}})^{1/3}$$

$L = L_\infty$ and $e = 1$ is substituted into the expression above which gives:

$$a_m = 1.62\, (\frac{L_\infty}{\ddot{h}_a\, \dot{v}})^{1/3} = 1.62\, (\frac{\kappa\, \{\dot{p}_{Am}\} s_{\mathcal{M}}}{\ddot{h}_a\, v[\dot{p}_M]})^{1/3}$$

Scaled functional responses

Laboratory data

The DEB scaled functional response *(f) f*or the highest food level within the laboratory growth experiment (Ballesta-Artero et al., 2018) had a value of 0.81 (Table 6. 3). For the estimation of *A. islandica* DEB parameters, we only included laboratory growth data which were derived at the highest food level (Ballesta-Artero et al., 2018). Medium food level data were not included because growth was not statistically different from growth at the highest food level (Ballesta-Artero et al., 2018).

At first, we included all the food treatments (high, medium, low, and no food ([15, 5, 0.5, ~ 0 x 10^6 cells/L], respectively) from Ballesta-Artero et al. (2018) into the AmP estimation procedure. After a number of unsuccessful attempts, however, to obtain reasonable parameter estimates (due to the very high number of parameters), we decided to only include the data from the high

food level for estimating *A. islandica* DEB parameters (see data doi: 10.4121/uuid:39f23dd7-bc2e-495b-a693-4ba70aa5ed75). One likely needs to proceed in a modular manner. First: obtain parameters for the standard DEB model under non-starvation conditions. Second: treat those parameters as given and estimate parameters of a starvation module which incorporates assumptions about how the organism responds (e.g. shrinking and/or modulating its maintenance).

It is known that *A. islandica* can reduce its metabolism to 10% of its normal rate (Strahl and Abele, 2010). Thus, it could be interesting to incorporate this behavior into DEB models. For instance, how the specific somatic maintenance $[\dot{p}_M]$, might be modulated during a starvation response. The parameters from this study will be helpful for that purpose.

Table 6. 3: Lifespan and scaled functional response estimates for the different locations. Maximum longevity (Long.) recorded indicated higher maximum longevities found in previous studies. Maximum longevity estimated was calculated with DEB parameters (Table 6. 1).

Location	f	Prim. Prod	Prim. Prod	Long. recorded	Long.	T	Depth
		mean gC m^{-2} yr^{-1}	estimates g C m^{-2} yr^{-1}	years	estimated years	°C	m
Fladen Gr.	0.59	124	110-138 [1, 1985-1994]	122 [7]	449	7.3	140
Faroe	0.72	60	60 [2, 1990-2003]	303 [8]	420	7.9	134-177
Fisher Bank	0.77	140	90-109, 119, 200 [1,3 (1988-1989), 4 (1988-2013)]	98 [7]	476	6.7	61
Lab. Exp.	0.81	-	-	-	-	-	-
Oyster Gr.	0.81	249	126-204, 199, 382 [1,3,4]	112 [7]	340	10	37-41
Silver Pit	0.87	89	97-117, 79, 82 [1,3,4]	155 [7]	343	9.9	40-68
Ingøya	0.98	160	120-200 [5,1981-2004]	290 [9]	507	6.0	10
Iceland	1	250	200-300 [6, 1958-1982]	507 [10]	562	4.7	5-7
Monkey Bank	1	271	171-225, 261, 354 [1,3,4]	88 [7]	439	7.4	52

Note: numbers between square brackets denotes references and years of estimates: [1] Skogen and Moll 2000,[2] Steingrund and Gaard 2005; [3] Joint and Pomroy1993, [4] Capuzzo et al.2017, [5] Skogen et al. (2007), [6] Astthorsson et al. (2007), [7] Witbaard et al. 1996,1999,2003, [8] Bonitz et al. 2018, [9] Mette et al. 2016, [10] . Butler et al., 2013. Comas separate the data of the different studies.

Field data

Monkey Bank, Iceland, and Ingøya had the highest estimated values of scaled functional response *'f'* of all the localities (Table 6. 3). Fladen Ground, in contrast, had the lowest. Our finding are in agreement with the food ranking of populations from Witbaard et al (1999). These rankings are not in agreement with those of average primary productivity estimates (Fig. 6. 8; r=0.6, p-value>0.05). For instance, Silver Pit population had a high *f* but a very low primary productivity (Table 6. 3).

Shell measurements used here came from specimens that were live-collected between 1993 and 2016. In the analyses, we did not make a distinction between the exact periods the animals were sampled. Therefore, part of the discrepancy between food availability estimates could result by multidecadal or higher frequency variations in primary production (see Table 6. 3). Witbaard et al. (1999) demonstrated, however, that the relative differences in growth between localities remain equal when comparing the same or different periods of time, implying that *A. islandica* growth rates reflect long-term systematic differences in site-specific environmental variability.

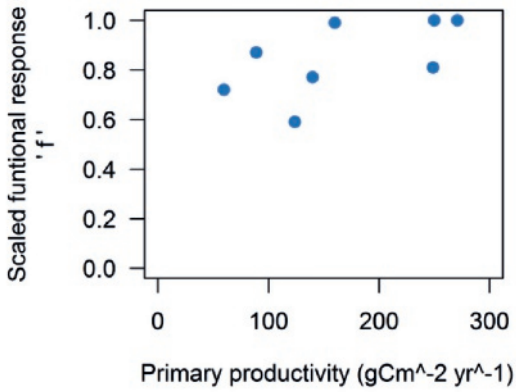

Fig. 6. 8: Scaled functional response as a function of primary production (average of estimates Table 6. 3).

Furthermore, although primary productivity at the surface can be an indicator for food availability at the seafloor, these two measurements may differ substantially (Fig. 6. 8). Depth of

the population under study is an important factor to consider (Witbaard and Duineveld, 1990; Witbaard et al., 1999). The deeper a population lives, the longer the time it takes for phytoplankton to sink to the seafloor. During this time, the phytoplankton is grazed by zooplankton and degraded by bacteria. Thus, depth will affect both the quantity and quality of the food available to benthos. Therefore, using the scaled functional response may be a more accurate tool to describe food availability for benthic organisms because it integrates decades and even centuries of information from the benthic zone. Moreover, for some locations, f could be the only source of information.

Lifespan versus food availability

We investigated the relationship between *A. islandica* lifespan and food availability (*f*) at the different North Atlantic localities, but, did not find a clear trend between these two variables (Table 6. 3). The Iceland and Ingøya localities contain specimens with the highest longevity (≥ 300 years) and exhibit the highest food availability. Yet, the Monkey Bank population, also exhibited one of the highest levels of food availability, whereas the oldest individual recorded was only about 88 years old (Table 6. 3). We must also consider that maximum age observed and recorded could differ from the actual maximum lifespan of a population (Beukema, 1989).

Under DEB theory, lower food levels for a population are associated with longer life-spans of its individuals (at the same temperature; Kooijman 2010). Other studies using various taxa have also reported that caloric restriction increases organism's lifespans, probably due to a reduction in its metabolic rate (Fontana et al., 2010; Moss et al., 2016). Therefore, A*. islandica's* self-induced metabolic rate depression (MRD) periods, varying between 1-30 days (Taylor, 1976, Abele et al., 2008; Ballesta-Artero et al., 2017), may be a factor involved in its extreme longevity. Another factor can be its high antioxidant capacity (Abele et al., 2008), captured in our DEB model by the extremely low ageing acceleration parameter $\ddot{h}_a$ (Fig. 6. 5d), i.e., a low accumulation of the waste that provokes ageing (Kooijman, 2010). Those factors together increase the species longevity because they reduce the generation of reactive oxygen species (ROS), which damages cells structures and deteriorate the physiological functions of the organism (Philipp et al. 2005; Philipp

and Abele, 2010). Our data, however, suggest no direct relationship between food availability and longevity of the studied *A. islandica* populations (Table 6. 3).

CONCLUSIONS

We constructed the first DEB model for the long-living bivalve *Arctica islandica***.** Our results indicate that: (1) *A. islandica's* extreme longevity arises from low somatic maintenance costs $[\dot{p}_M]$ and a low ageing acceleration ($\ddot{h}_a$), (2) food availability estimates based on the DEB's scaled functional response may be a more accurate estimates than primary productivity for *A. islandica* localities because it integrates decades, and even centuries, of food information from the benthic zone. Moreover, we could not find a direct relationship between *A. islandica* lifespan and food availability in the studied North Atlantic populations.

Compliance with Ethical Standards

The authors declare that they have no conflict of interest. All applicable international, national, and/or institutional guidelines for the care and use of animals were followed.

Acknowledgments

We thank all who contributed to the AmP collection. This work was funded by the EU within the framework (FP7) of the Marie Curie Initial Training Network ARAMACC (604802). SA and MLC were supported by the Research Council of Norway ("FRamework for integrating Eco-physiological and Ecotoxicological data into marine ecosystem-based management tools" NFR 255295; and "Reconstruction of Environmental Histories Using Long-Lived Bivalve Shells in the Norwegian Arctic (RELIC)" NFR-227048E10, respectively). AJW and MJM were supported by U.S. National Science Foundation grant #1417766, "Exploring the role of oceanic and atmospheric forcing on Arctic marine climate from newly developed annual shell based records in coastal Norway."

Chapter 7

Discussion

This thesis examined the feeding behavior and growth of the long-living bivalve *Arctica islandica* in relation to the main driving environmental factors (Chapters 2, 4, and 6). This semi-sessile organism incorporates into its annually deposited shell bands information from the local environment (Witbaard, 1997). The environmental archive recorded in its shell can be unlocked through different techniques, such as trace elements and microstructure analyses (Chapters 3 and 5). This enables the retrospective assessment of environmental change. The various chapters deciphered diverse aspects of the biology and ecology of this unique organism, and the results may stimulate further proxy development for this species. In this final chapter, I discuss the main findings of my research and point out some future lines of investigation.

Main findings and future lines of research

1. The field experiment in northern Norway (Chapter 2 and Box 7A) reported for the first time the *in situ* biological activity of *A. islandica* at a fine temporal scale. Valve gape in this *A. islandica* population exhibited a highly synchronized and well-defined seasonal pattern that was mainly driven by the concentration of chlorophyll-a. During each of the four years of the study, the main period of active gaping lasted eight months (between February and September). Therefore, a paleoclimatic reconstruction based on shells from this population should take into account that the specimens record the environment only during 8 of the 12 months of the year.

To confirm and expand our results, the next step would be to record *A. islandica* seasonal gaping activity at various other populations. Then, we could check if chlorophyll-a also drives the rhythm of those populations. Moreover, combining biological and geochemical techniques to study *A. islandica's* growing season should be the next step to get reliable results about this proxy species (Ballesta-Artero et al., in preparation (b)).

2. The study of the *A. islandica* shell microstructure (Chapters 3 and 5) indicated that scanning electron microscopy (SEM) could not detect changes in temperature, food source, or food concentration from the deposited carbonated shell. Confocal Raman microscopy (CRM) could, however, quantify significant changes of the orientation of microstructural units reared at different temperatures (Chapter 3). These results suggest that the crystallographic orientation of biomineral units of *A. islandica* shells may serve as an alternative proxy for seawater temperature.

The pigment composition of *A. islandica* shells were also studied by CRM, but it seemed that they are not altered by the studied diets (Chapter 3).

Additional work is required to confirm crystallographic orientation as a new temperature proxy. Moreover, subsequent studies with CRM, and/or with other advanced methods as Electron Backscatter Diffraction (EBSD; Milano et al., 2017a), may identify physical properties of microstructures as proxies for palaeo-environmental reconstructions.

3. Water temperature and both food type and concentration influence the growth rate of *A. islandica* (Chapters 3 and 4). Higher growth rates were found at the most biodiverse diet, i.e. the one composed of different phytoplankton species (*Isochrysis sp., Tetraselmis sp., Paulova sp., Thalassiosira sp. and Nannochloropsis spp*). When the food diet was kept constant, the concentration of algal food was the main factor driving siphon activity and with that, shell and tissue growth. Thus, these experimental outcomes support the results from the *in situ* field study (Chapter 2), where gaping activity was mainly driven by the concentration of chlorophyll-a and to a lesser degree by seawater temperature.

Although our results suggest that temperature within the range from 3 to 13 °C had a limited effect on shell and tissue growth when compared to the role of food availability, future experiments at a broader temperature range (0–20 °C) will better elucidate the effect of temperature on *A. islandica* growth.

4. Physiological processes seem to play a dominant role in the incorporation of elements into *A. islandica* shells (Chapter 5). Shell growth rate exerts a large control on the incorporation of Sr, Mg, Ba, and Na. The effect of temperature and food on the shell chemistry seems overarched by shell growth. Although element-to-calcium ratios in *A. islandica* shells contain environmental information, this information cannot be easily distinguished from physiological controls (mainly shell growth rate). Further studies are needed before these ratios can be used as reliable environmental proxies. Specifically, the pathways that these elements follow from the water and the food into the shell need further attention.

Box 7A: *Arctica islandica* gaping activity 2014-2017

Valve gape measurements over the four calendar years also showed a well-defined activity cycle in *A. islandica* (Fig. 7A. 1). The distinct types of gaping activity levels were consistent between years as well as among individuals. We discerned two levels of activity, i.e. "active" with an average valve gape > 0.2, and "inactive" with an average valve gape ≤ 0.2 (Fig. 7A. 1).

On average, the sample population of *A. islandica* individuals was inactive from the beginning of October to the end of January (with an average daily gape < 0.3 %; Fig. 7A. 1). Only the winter 2016/2017 was slightly different, the specimens started to be active already at the end of December (Fig. 7A. 1). In all years monitored, a consistent transition from low valve gape to high started between February and March. The daily mean valve gape then increased considerably between the months of March and April, from 0.41 to 0.63 in 2014, from 0.36 to 0.56 in 2015, from 0.39 to 0.56 in 2016, and from 0.44 to 0.64 in 2017 (Fig. 7A. 1). During the four years, the highest, continuous level of activity occurred in late spring to early summer. Valve gape monthly means reached their maximum in May 2014 (0.84) and in July 2015, 2016 and 2017 (0.78, 071, 0.70 respectively; Fig. 7A. 1).

Table 7A. 1: Correlation between the daily average gaping activity of the specimens (AvgGape) versus the different environmental variables (left bottom). The top right shows the P-values of the corresponding correlations. The highest correlation with AvgGape is shown in bold

	AvgGape	Temperature	Salinity	Light	Sea level	log_[Chla]	log_Turb
AvgGape		<0.001	0.02	<0.001	<0.001	<0.001	<0.001
Temperature	0.18		<0.001	0.06	<0.001	<0.001	<0.001
Salinity	0.07	-0.22		<0.001	<0.001	0.43	<0.001
Light	0.53	-0.05	0.13		<0.001	<0.001	<0.001
Sea level	-0.45	-0.12	-0.14	-0.36		<0.001	<0.001
log_[Chla]	**0.73**	0.55	-0.02	0.23	-0.45		<0.001
log_Turb	0.39	0.34	-0.15	-0.08	-0.21	0.68	

When average valve gape activity was compared with daily means of the different environmental variables, [Chl-a] was the variable with the highest correlation (r=0.7; P-value <0.01), followed by light, sea level, turbidity, temperature, and salinity (Table 7A. 1). The periods with the highest valve gape coincided with the highest levels of [Chl-a] (Fig. 7A. 1a). It is also apparent that the seasonal change in valve gape activity was temporally offset from temperature, with higher valve gape values leading the temperature pattern by 2–3 months (Fig. 7A. 1b).

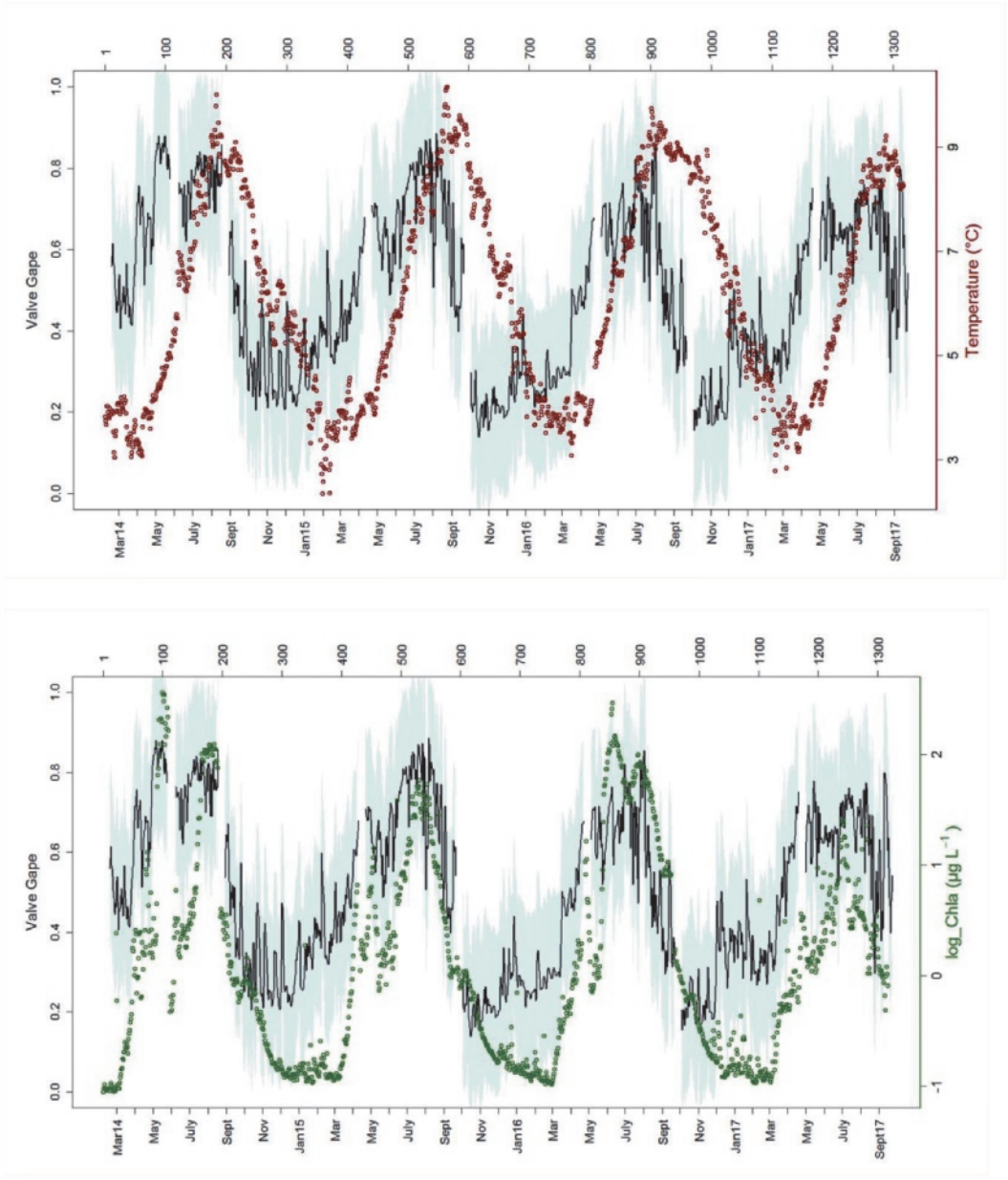

Fig. 7A. 1: Valve gape daily mean (black line) and SD (grey shadow) by month from all available specimens per unit of time (n=7–15) a) with temperature (red dots) and b) with chlorophyll-a concentration (green dots)**.** Top axis indicates experimental days

5. The DEB model for *Arctica islandica* (Chapter 6) helped to understand *A. islandica's* extreme longevity. We found that the low somatic maintenance costs $[\dot{p}_M]$ and the low accumulation of waste that provokes ageing ($\ddot{h}_a$) were key processes allowing this organism to survive for centuries. Moreover, the DEB's scaled functional response may be a more accurate indicator of food conditions than primary productivity estimates, because it integrates feeding conditions over long periods and thus can provide centuries of information on food availability in the benthic zone.

The present DEB model can be extended in order to model the response of the species to starvation. The possibility to considerably reduce metabolism, as observed in mollusks, is an interesting issue to incorporate into DEB models. Future studies could model, for instance, how $[\dot{p}_M]$ is modulated during a starvation response. Moreover, the reproduction buffer of *A. islandica* could also be taken into account whenever there is more information about the species reproductive behavior (Box 7B). Within DEB, species-specific reproduction buffer handling rules are needed in order to specify when reproduction occurs and what triggers it (Saraiva et al., 2012; Gourault et al 2018). The DEB parameters estimated in Chapter 6 will be helpful for those purposes.

Shell-based chronologies and proxy development within the ARAMACC project

Arctica islandica's annual increments provide a precise temporal framework that allows to study environmental change from areas where instrumental records are lacking. Within the ARAMACC project new shell-based chronologies were developed at locations such as Faroe and North West France (Bonitz et al. 2018; Featherstone et al. 2017), and are still being developed for the Scotland coast, the North Sea, and the Irish Sea (North Sea; Alexandroff et al., in preparation; Estrella-Martinez et al., in preparation). Not only *A. islandica* specimens were studied, but also potential proxy species as *Glycymeris glycymeris, Glycymeris pilosa, and Callista chione* (Peharda et al. 2016; Purroy et al., 2017, 2018; Featherstone et al., 2017). Moreover, climate model simulations were evaluated using environmental paleoclimatic reconstructions based on *A. islandica* shells (Pyrina et al., 2017).

Proxy development was the goal of the following studies: Trofimova et al. (2018), who evaluated the reproducibility of stable oxygen isotopes in relation to the microstructural organization of *A. islandica* shells; Milano et al. (2017a, b), who found microstructural characteristics that can be used as novel proxies in bivalve species such as *Cerastoderma edule* and *A. islandica*; and Zhao et al. (2017a, b, c), who helped to decipher the complexity of element incorporation into bivalve shells by means of various laboratory experiments. Up-to-date information and new publications about ARAMACC findings can be found on the web page: www.aramacc.com.

Box 7B: *Arctica islandica* reproduction in Ingøya (northern Norway)

Arctica islandica is a boreal species with an optimal thermal range between 6-16 °C (Golikov and Scarlato, 1973; Cargnelli et al., 1999; Zettler et al., 2001; Begum et al., 2009), but tolerates temperatures between 0 and 20 °C (Kraus et al., 1992; Witbaard et al., 1997a; Hippler et al., 2013; Fig. 7B. 1). Its larval stages (trochopore, veliger, and pediveliger) have a more restricted optimal temperature range, between 8 and 16 °C, than adults (Fig. 7B. 1; Cargenilli et al., 1999). Fertilized eggs of ocean quahogs hatch into planktonic trochophore larvae, which first turns into veliger larvae, and then to a pediveliger one, a transitional larval stage which develops a foot for burrowing (Fig. 7B. 1; Cargenilli et al., 1999). The length of the larval development period ranges from 32 to 60 days, mainly depending on the water temperature (Lutz et al., 1982; Cargenilli et al., 1999). Larval stages disperse with the local currents until they metamorphose into semi-sesile juveniles, which settle at the sea-bottom (Fig. 7B. 1).

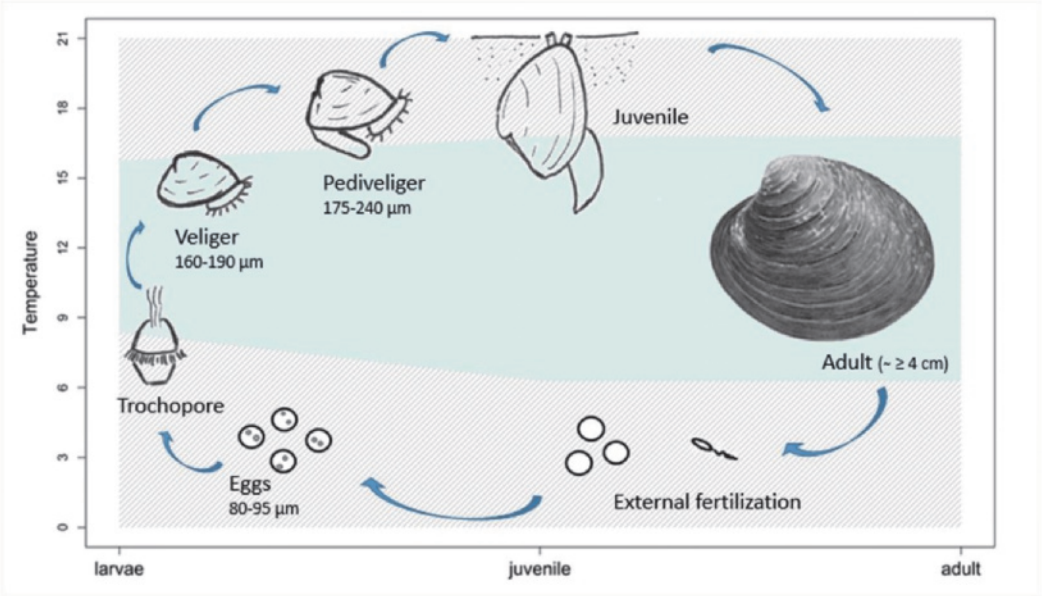

Fig. 7B. 1: *Arctica islandica* life cycle and range of temperature (based on Carneglii et al., 1999). Blue shadow represents optimal temperature range at the different life stages, and grey dash background shows tolerance range for the species

Age and length at which *A. islandica* become an adult vary between populations (Thórarinsdóttir and Einarsson, 1996). It is usually assumed than specimens bigger than 4 cm length are sexually mature (Thompson et al. 1980; Thórarinsdóttir and Einarsson, 1996), with ages between 10 and 13 years old (Thompson et al. 1980). We investigated the monthly investment into soma and gonads related to sex and size from the population in Ingøya (Ballesta-Artero et al., in preparation (a)), and we found that sexual differentiation was evident in 336 of the 423 specimens analyzed. We used splash samples to determine sex and gonad developmental stage. Male gametes were difficult to differentiate from immature stages (Fig. 7B. 2a, b). Females' gametes, on the contrary, were quite conspicuous (Fig. 7B. 2c).

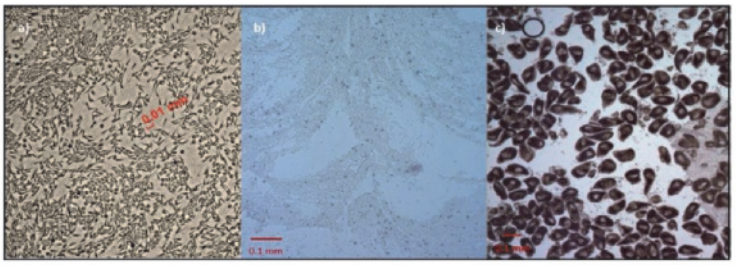

Fig. 7B. 2: a) Male gonadal tissue of *Arctica islandica*, b) no celular structures definable as male or female c) female oocytes (October 2015)

We also checked the sex of the larger individuals of the population at Ingøya (>85 mm, n = 42) and we found that 63 % of them were females. However, we cannot conclude that *A. islandica* females live longer, as Muraswski et al. (1980) hypothesized, because we did not check the age of all those individuals. The smallest and the biggest female individual which could be sexed were 49-mm and 91-mm length, respectively (total range: 18.8-95.9 mm). We found ripe oocytes in all the monthly samples taken between May 2014 and January 2016. The total body mass (soma+ gonads) had a clearer seasonal pattern than the gonadal mass, even when we splitted the sample by sex (Fig. 7B. 3). Gonadal and body mass indexes seem to indicate two reproduction peaks in 2014 (July and October) and one extended peak in 2015 (from June to October; Fig. 7B. 3). Our findings support *A. islandica* reproduction overall its life span (Thompson et al. 1980; Thorarinsdottir, 2000). Timing and duration of events in *A. islandica* gametogenic cycle seem variable between years, possibly due to variable environmental conditions (Thorarinsdottir 2000).

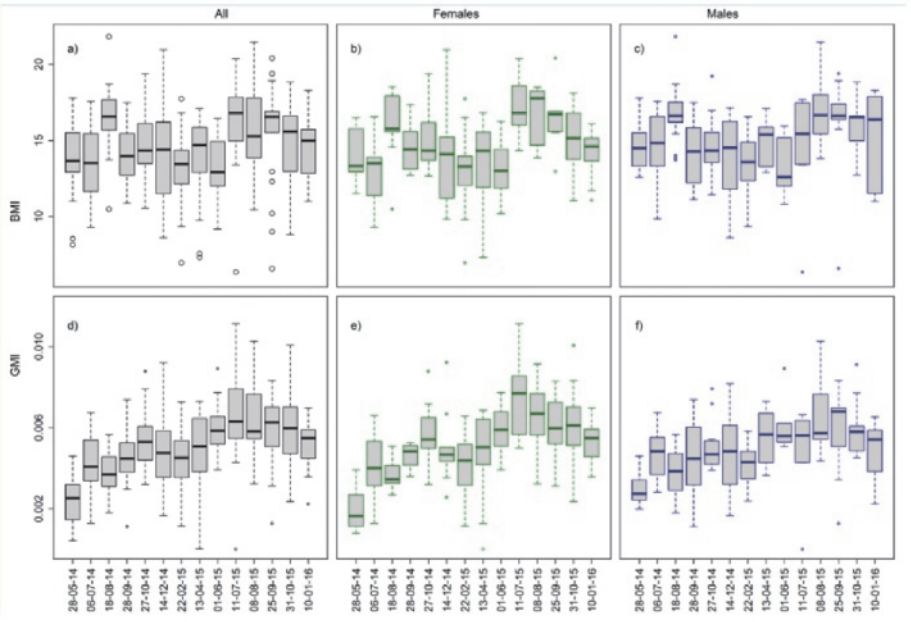

Fig. 7B. 3: a) Body Mass Index (BMI = total AFDW/Height3 *1000 , mg/mm3) of all *A. islandica* specimens per month b) females BMI c) males BMI d) gonadal mass index of all *A. islandica* specimens per month e) females GMI c) males GMI. NOTE: AFDW= ash free dry weight (dry weight-ash weight).

References

A

Abele and Puntarulo, 2004. Formation of reactive species and induction of antioxidant defence systems in polar and temperate marine invertebrates and fish. Comp. Biochem. Physiol. Mol. Integr. Physiol. 138: 405–415. doi: 10.1016/j.cbpb.2004.05.013

Abele et al., 2009. Bivalve models of aging and the determination of molluscan lifespans. Exp. gerontol. 44: 307–315. doi: 10.1016/j.exger.2009.02.012

Abele et al., 2008. Imperceptible senescence: ageing in the ocean quahog *Arctica islandica*. Free Radical Res. 42: 474–480. doi: 10.1080/10715760802108849

Abele et al., 2002. Temperature–dependence of mitochondrial function and production of reactive oxygen species in the intertidal mud clam *Mya arenaria*. J. Exp. Biol. 205: 1831–1841. doi: 10.1016/j.ecolind.2011.04.007

Aizenberg et al., 2005. Skeleton of *Euplectella sp.*: structural hierarchy from the nanoscale to the macroscale. Science 309 (5732): 275–278. doi: 10.1126/science.1112255

Ambrose et al., 2012. Growth line deposition and variability in growth of two circumpolar bivalves *(Serripes groenlandicus*, and *Clinocardium ciliatum*). Polar Biol. 35:345–354. doi: 10.1007/s00300–011–1080–4

AmP, online database of DEB parameters, implied properties and referenced underlying data. bio.vu.nl/thb/deb/deblab/add_my_pet. Last accessed: 2017/12 /14

Andrus, 2011. Shell midden sclerochronology. Quat. Sci. Rev. 30(21–22): 2892–2905, doi: 10.1016/j.quascirev.2011.07.016

Astthorsson et al., 2007. Climate variability and the Icelandic marine ecosystem. Deep Sea Research Part II: Topical Studies in Oceanography 54: 2456–2477. doi: 10.1016/j.dsr2.2007.07.030

B

Baker et al., 1998. Selective feeding and biodeposition by zebra mussels and their relation to changes in phytoplankton composition and seston load. J. Shellfish Res. 17: 1207–1213.

Ballesta-Artero et al., 2018. Interactive effects of temperature and food availability on the growth of *Arctica islandica* (Bivalvia) juveniles. Mar. Environ. Res. 133: 67–77. doi: 10.1016/j.marenvres.2017.12.004

Ballesta-Artero et al., in preparation (a). Reproductive investment of the bivalve *Arctica islandica* in Northern Norway.

Ballesta-Artero et al., in preparation (b). Combining biological and geochemical techniques to study the growing season of the bivalve *Arctica islandica.*

Ballesta-Artero et al., 2017. Environmental factors regulating gaping activity of the bivalve *Arctica islandica* in Northern Norway. Mar. Biol. 164: 116. doi: 10.1007/s00227–017–3144–7

Bayne, 1998. The physiology of suspension feeding by bivalve molluscs: an introduction to the Plymouth "TROPHEE" workshop. J. Exp. Mar. Biol. Ecol. 219: 1–9. doi: 10.1016/S0022–0981(97)00172–X

Begum, 2009. Environmental constraints on growth, age and lifetime metabolic budgets of the bivalve *Arctica islandica* (Doctoral dissertation, PhD Thesis) Universität Bremen

Begum et al., 2010. Growth and energy budget models of the bivalve *Arctica islandica* at six different sites in the Northeast Atlantic realm. J. Shellfish Res. 29: 107–115. doi: 10.2983/035.029.0103

Begum et al., 2009. A metabolic model for the ocean quahog *Arctica islandica*—effects of animal mass and age, temperature, salinity, and geography on respiration rate. J. Shellfish Res. 28: 533–539. doi: 10.2983/035.028.0315

Beierlein et al., 2015. Confocal Raman microscopy in sclerochronology: A powerful tool to visualize environmental information in recent and fossil biogenic archives. Geochem. Geophys. Geosystems 16: 325–335. doi: 10.1002/2014GC005547

Beirne et al., 2012. Experimental validation of environmental controls on the $\delta^{13}C$ of *Arctica islandica* (ocean quahog) shell carbonate. Geochim. Cosmochim. Acta 84: 395–409. doi: 10.1016/j.gca.2012.01.021, 2012.

Berman et al. 1993. Biological control of crystal texture: a widespread strategy for adapting crystal properties to function. Science 259(5096): 776–779. doi: 10.1126/science.259.5096.776

Beukema, 1988. Bias in estimates of maximum life span, with an example of the edible cockle, *Cerastoderma edule*. Neth. J. Zool. 39: 79–85. doi: 10.1163/156854289X00048

Black et al., 2008. Establishing highly accurate production–age data using the tree–ring technique of crossdating: a case study for Pacific geoduck (*Panopea abrupta*), Can. J. Fish. Aquat. Sci. 65: 2572–2578. doi: 10.1139/F08–158

Black et al., 2016. The value of crossdating to retain high–frequency variability, climate signals, and extreme events in environmental proxies. Glob. Chang. Biol. 22: 2582–2595. doi: 10.1111/gcb.13256

Bøggild, 1930. The shell structure of the mollusks, in Det Kongelige Danske Videnskabernes Selskabs Skrifter, Natruvidenskabelig og Mathematisk, pp. 231–326, Afdeling.

Bonitz et al., 2018. Links between phytoplankton dynamics and shell growth of *Arctica islandica* on the Faroe Shelf. J. Mar. Syst. 179: 72–87. doi: 10.1016/j.jmarsys.2017.11.005

Borcherding, 2006. Ten years of practical experience with the Dreissena–monitor, a biological early warning system for continuous water quality monitoring Hydrobiologia 556: 417–426. doi: 10.1007/s10750–005–1203–4

Brey et al., 1990. *Arctica (Cyprina) islandica* in Kiel Bay (Western Baltic): growth, production and ecological significance. J. Exp. Mar. Biol. Ecol. 136: 217–235. doi: 10.1016/0022–0981(90)90162–6

Bricelj and Malouf, 1984. Influence of algal and suspended sediment concentrations on the feeding physiology of the hard clam *Mercenaria mercenaria*. Mar. Biol. 84: 155–165. doi: 10.1007/BF00393000

Butler et al., 2009. Accurate increment identification and the spatial extent of the common signal in five *Arctica islandica* chronologies from the Fladen Ground, northern North Sea. Paleoceanography 24: PA2210. doi: 10.1029/2008pa001715

Butler et al., 2013. Variability of marine climate on the North Icelandic Shelf in a 1357–year proxy archive based on growth increments in the bivalve *Arctica islandica*. Palaeogeogr. Palaeoclimatol. Palaeoecol. 373: 141–151. doi: 10.1016/j.palaeo.2012.01.016

Butler et al., 2010. Marine climate in the Irish Sea: analysis of a 489–year marine master chronology derived from growth increments in the shell of the clam *Arctica islandica*. Quat. Sci. Rev. 29: 1614–1632. doi: 10.1016/j.quascirev.2009.07.010

C

Capuzzo et al., 2017. A decline in primary production in the North Sea over 25 years, associated with reductions in zooplankton abundance and fish stock recruitment. Glob. Change Biol. 24: e352-e364. doi: 0.1111/gcb.13916

Cargnelli et al., 1999. Ocean quahog, *Arctica islandica*, life history and habitat characteristics. NOAA Tech Memo NMFS–NE–148.

Carnes and Slade, 1988. The use of regression for detecting competition with multicollinear data. Ecology 69: 266–274. doi: 10.2307/1941282

Carroll et al., 2009. Bivalves as indicators of environmental variation and potential anthropogenic impacts in the southern Barents Sea. Mar. Pollut. Bull. 59: 193–206. doi: 10.1016/j.marpolbul.2009.02.022

Carroll et al., 2011. Climatic regulation of *Clinocardium ciliatum* (bivalvia) growth in the northwestern Barents Sea. Palaeogeogr. Palaeoclimatol. Palaeoecol. 302: 10–20. doi: 10.1016/j.palaeo.2010.06.001

Carter, 1980. Environmental and biological controls of bivalve shell mineralogy and microstructure. Skeletal Growth of Aquatic Organisms (Topics in Geobiology), edited by D. C. Rhoads and R. A. Lutz, pp. 69–113, Plenum, N. Y. doi: 10.1007/978–1–4899–4995–0_3

Carter and Clark, 1985. Classification and phylogenetic significance of molluscan shell microstructure. Studies in Geology, Notes for a Short Course 13: 50–71, edited by T. W. Broadhead.

Carter et al., 2012. Illustrated glossary of the Bivalvia. Treatise Online: 1–209.

Carter et al., 1998. Thermal potentiation and mineralogical evolution in the Bivalvia (Mollusca). J. Paleontol. 72: 991–1010.

Checa et al., 2006. Organization pattern of nacre in Pteriidae (Bivalvia: Mollusca) explained by crystal competition. Proc. Biol. Sci. 273: 1329–37. doi: 10.1098/rspb.2005.3460

Clarke, 2003. Costs and consequences of evolutionary temperature adaptation. Trends Ecol. Evol. 18: 573–581. doi: 10.1016/j.tree.2003.08.007

Currey, 1999. The design of mineralised hard tissues for their mechanical functions. J. Exp. Biol. 202: 3285–3294.

Cusack et al., 2008. Oxygen isotope composition in *Modiolus modiolus* aragonite in the context of biological and crystallographic control. Mineral. Mag. 72: 569–577. doi: 10.1180/minmag.2008.072.2.569

D

Dahlgren et al., 2000. Phylogeography of the ocean quahog (*Arctica islandica*): influences of paleoclimate on genetic diversity and species range. Mar. Biol. 137: 487–495. doi: 10.1007/s002270000342

Dauphin et al., 2003. In situ chemical speciation of sulfur in calcitic biominerals and the simple prism concept, J. Struct. Biol. 142: 272–280. doi: 10.1016/S1047–8477(03)00054–6.

DEB wiki. 17–May–2018. http://www.debtheory.org/wiki

Deith, 1985. The composition of tidally deposited growth lines in the shell of the edible cockle, *Cerastoderma edule*. J. Mar. Biol. Assoc. UK 65: 573–581. doi: 10.1017/S0025315400052425

DeLong KL, Quinn TM, Taylor FW, Shen CC, Lin K (2013) Improving coral–base paleoclimate reconstructions by replicating 350 years of coral Sr/Ca variations. Palaeogeogr. Palaeoclimatol. Palaeoecol. 373: 6–24. doi: 10.1016/j.palaeo.2012.08.019

Dodd, 1965. Environmental control of strontium and magnesium in *Mytilus*. Geochim. Gosmochim. Acta 29: 385–398. doi: 10.1016/0016–7037(65)90035–9

Dunca et al. (2009) Using ocean quahog (*Arctica islandica*) shells to reconstruct palaeoenvironment in Öresund, Kattegat and Skagerrak, Sweden. Int. J. Earth Sci. 98: 3–17. doi: 10.1007/s00531–008–0348–6

Duncan, 2011. Healthcare risk adjustment and predictive modeling. Actex Publications.

E

Elliot et al., 2009. Profiles of trace elements and stable isotopes derived from giant long–lived *Tridacna gigas* bivalves: potential applications in paleoclimate studies. Palaeogeogr. Palaeoclimatol. Palaeoecol. 280: 132–142. doi: 10.1016/j.palaeo.2009.06.007

Epifanio, 1979. Growth in bivalve molluscs: nutritional effects of two or more species of algae in diets fed to the American oyster *Crassostrea virginica* (Gmelin) and the hard clam *Mercenaria mercenaria* (L.). Aquaculture 18: 1–12. doi: 10.1016/0044-8486(79)90095-4

Epplé et al., 2006. Sclerochronological records of *Arctica islandica* from the inner German Bight. The Holocene 16: 763–769. doi: 10.1191/0959683606hl970rr

Epstein et al., 1953. Revised carbonate–water isotopic temperature scale. Bull. Geol. Soc. Am., 64, 1315–1326.

Evans et al. 2009. Heritability of shell pigmentation in the Pacific oyster, *Crassostrea gigas*. Aquaculture 286: 211–216. doi: 10.1016/j.aquaculture.2008.09.022

F

Featherstone et al., 2017. Influence of riverine input on the growth of *Glycymeris glycymeris* in the Bay of Brest, North–West France. PloS One 12(12): p.e0189782. doi: 10.1371/journal.,pone.0189782

Fitzer et al., 2015. Ocean acidification alters the material properties of *Mytilus edulis* shells, J. R. Soc. Interface 12(103): 20141227. doi: 10.1098/rsif.2014.1227

Fitzer et al., 2014. Ocean acidification reduces the crystallographic control in juvenile mussel shells. J. Struct. Biol. 188: 39–45. doi: 10.1016/j.jsb.2014.08.007

Fontana et al., 2010. Extending healthy life span—from yeast to humans. Science 328: 321–326. doi: 10.1126/science.1172539

Foster et al., 2008. Mg in aragonitic bivalve shells: Seasonal variations and mode of incorporation in *Arctica islandica*. Chem. Geol. 254: 113–119. doi: /10.1016/j.chemgeo.2008.06.007

Foster et al., 2009. Strontium distribution in the shell of the aragonite bivalve *Arctica islandica*. Geochem. Geophys. Geosyst. 10(3). doi: 10.1029/2007GC001915

Freitas et al., 2009. Reconstruction of food conditions for Northeast Atlantic bivalve species based on Dynamic Energy Budgets. J. Sea Res. 62: 75–82. doi: 10.1016/j.seares.2009.07.004

Freitas et al., 2006. Environmental and biological controls on elemental (Mg/Ca, Sr/Ca and Mn/Ca) ratios in shells of the king scallop *Pecten maximus*. Geochim. Gosmochim. Acta 70: 5119–5133. doi: 10.1016/j.gca.2006.07.029

Freitas et al., 2005. Mg/Ca, Sr/Ca, and stable-isotope (δ18O and δ13C) ratio profiles from the fan mussel *Pinna nobilis*: Seasonal records and temperature relationships. Geochem. Geophys. Geosyst. 6(4). doi: 10.1029/2004GC000872

Frenzel et al., 2012. Nanostructure and crystallography of aberrant columnar vaterite in *Corbicula fluminea* (Mollusca). J. Struct. Biol. 178: 8–18. doi: 10.1016/j.jsb.2012.02.005

Fryda et al., 2009. Crystallographic texture of Late Triassic gastropod nacre: Evidence of long–term stability of the mechanism controlling its formation. Bull. Geosci. 84: 745–754, doi: 10.3140/bull.geosci.1169

G

Galley et al., 2010. Optimisation of larval culture of the mussel *Mytilus edulis* (L.), Aquac. Int. 18: 315–325. doi: 10.1007/s10499–009–9245–7

García–March et al., 2016. In situ biomonitoring shows seasonal patterns and environmentally mediated gaping activity in the bivalve, *Pinna nobilis*. Mar. Biol. 163: 1–2. doi: 10.1007/s00227–016–2812–3

García–March et al., 2008. Shell gaping behaviour of *Pinna nobilis* L., 1758: circadian and circalunar rhythms revealed by in situ monitoring. Mar. Biol. 153: 689–698. doi: 10.1007/s00227–007–0842–6

Geeza et al., 2018. Controls on magnesium, manganese, strontium, and barium concentrations recorded in freshwater mussel shells from Ohio. Chem. Geol. doi: 10.1016/j.chemgeo.2018.01.001

Gillikin et al., 2008. Synchronous barium peaks in high–resolution profiles of calcite and aragonite marine bivalve shells. Geo–Mar. Lett. 28: 351–358. doi: 10.1007/s00367–008–0111–9

Gillikin et al., 2006. Barium uptake into the shells of the common mussel (*Mytilus edulis*) and the potential for estuarine paleo–chemistry reconstruction. Geochim. Gosmochim. Acta 70: 395–407. doi: 10.1016/j.gca.2005.09.015

Gillikin et al., 2005a. Assessing the reproducibility and reliability of estuarine bivalve shells (*Saxidomus giganteus*) for sea surface temperature reconstruction: Implications for paleoclimate studies, Palaeogeogr. Palaeoclimatol. Palaeoecol. 228: 70–85. doi: 10.1016/j.palaeo.2005.03.047

Gillikin et al., 2005b. Strong biological controls on Sr/Ca ratios in aragonitic marine bivalve shells. Geochem. Gosmochim. Acta 6 (5). doi: 10.1029/2004GC000874

Golikov and Scarlato, 1973. Method for indirectly defining optimum temperatures of inhabitancy for marine cold–blooded animals. Mar. Biol. 20: 1–5. doi: 10.1007/BF00387667.

Goodkin et al., 2007. A multicoral calibration method to approximate a universal equation relating Sr/Ca and growth rate to sea surface temperature. Paleoceanography 22. doi: 10.1029/2006PA001312

Gordon and Carriker, 1978. Growth lines in a bivalve mollusk: subdaily patterns and dissolution of the shell. Science 202: 519–521. doi: 10.1126/science.202.4367.519

Gourault et al., 2018. Modeling reproductive traits of an invasive bivalve species under contrasting climate scenarios from 1960 to 2100. J. Sea Res. doi: 10.1016/j.seares.2018.05.005

Graham, 2003. Confronting multicollinearity in ecological multiple regression. Ecology 84: 2809–2815. doi: 10.1890/02–3114

Griesshaber et al., 2010. The application of EBSD analysis to biomaterials : microstructural and crystallographic texture variations in marine carbonate shells. Semin. Soc. Esp. Miner. 7: 22–34.

Grossman and Ku, 1986. Oxygen and carbon isotope fractionation in biogenic aragonite: Temperature effects. Chem. Geol. 59: 59–74. doi: 10.1016/0168-9622(86)90057-6

H

Hahn et al., 2012. Marine bivalve shell geochemistry and ultrastructure from modern low pH environments: environmental effect versus experimental bias. Biogeosciences 9: 1897–1914. doi: 10.5194/bg–9–1897–2012

Hart and Blusztajn, 1998. Clams as recorders of ocean ridge volcanism and hydrothermal vent field activity. Science 280: 883–886. doi: 10.1126/science.280.5365.883

Hatch et al., 2013. Ba/Ca variations in the modern intertidal bean clam *Donax gouldii*: An upwelling proxy. Palaeogeogr. Palaeoclimatol. Palaeoecol. 373: 98–107. doi: 10.1016/j.palaeo.2012.03.006

Hedegaard et al., 2006. Molluscan shell pigments: An in situ resonance Raman study, J. Mollus. Stud. 72: 157–162. doi: 10.1093/mollus/eyi062

Hiebenthal et al., 2013. Effects of seawater pCO2 and temperature on shell growth, shell stability, condition and cellular stress of Western Baltic Sea *Mytilus edulis* (L.) and *Arctica islandica* (L.). Mar. Biol. 160: 2073–2087. doi: 10.1007/s00227–012–2080–9

Hiebenthal et al., 2012. Interactive effects of temperature and salinity on shell formation and general condition in Baltic Sea *Mytilus edulis* and *Arctica islandica*. Aquat. Biol. 14: 289–298. doi: 10.3354/ab00405

Higgings, 1980. Effects of food availability on the valve movements and feeding behavior of juvenile *Crassostrea virginica* (Gmelin). I. Valve movements and periodic activity. J. Exp. Mar. Biol. Ecol. 45: 229–244. doi: 10.1016/0022–0981(80)90060–X

Hippler et al., 2013. Exploring the calcium isotope signature of *Arctica islandica* as an environmental proxy using laboratory– and field–cultured specimens. Palaeogeogr. Palaeoclimatol. Palaeoecol. 373: 75–87. doi: 10.1016/j.palaeo.2011. 11.015.

Holmes et al., 2003. Phenotypic and genotypic population differentiation in the bivalve mollusc *Arctica islandica*: results from RAPD analysis. Mar. Ecol. Prog. Ser. 254: 163–176. doi: 10.3354/meps254163

Hopkins and Farrow, 1985. Raman microprobe determination of local crystal orientation. J. Appl. Phys. 59: 1103–1110. doi: 10.1063/1.336547

I

Ieno and Zuur, 2015. A beginner's guide to data exploration and visualization with R. Highland Statistics Ltd., Newburgh, United Kingdom

Izumida et al., 2011. Biological and water chemistry controls on Sr/Ca, Ba/Ca, Mg/Ca and $\delta^{18}O$ profiles in freshwater pearl mussel *Hyriopsis* sp. Palaeogeogr. Palaeoclimatol. Palaeoecol. 309: 298–308. doi: 10.1016/j.palaeo.2011.06.014

James FC, McCulloch CE (1990) Multivariate analysis in ecology and systematics: panacea or Pandora's box? Annu. Rev. Ecol. Syst. 21: 129–166. doi: 10.1146/annurev.es.21.110190.001021

Jochum et al., 2012. Accurate trace element analysis of speleothems and biogenic calcium carbonates by LA–ICP–MS. Chem. Geol. 318–319, 31–44. doi: 10.1016/j.chemgeo.2012.05.009

Jochum et al., 2011. Determination of reference values for NIST SRM 610–617 glasses following ISO guidelines. Geostand. Geoanal. Res. 35: 397–429. doi: 10.1111/j.1751–908X.2011.00120.x

Jochum et al., 2005. GeoReM: a new geochemical database for reference materials and isotopic standards. Geostand. Geoanal. Res. 29: 87–133. doi: 10.1111/j.1751–908X.2005.tb00904.x

Joint and Pomroy, 1993. Phytoplankton biomass and production in the southern North Sea. Mar. Ecol. Prog. Ser. 99: 169–182.

Jones et al., 2009. High–resolution palaeoclimatology of the last millennium: a review of current status and future prospects. The Holocene 19: 3–49. doi: 10.1177/0959683608098952

Jones, 1983. Sclerochronology: reading the record of the molluscan shell: annual growth increments in the shells of bivalve molluscs record marine climatic changes and reveal surprising longevity. Am. Sci., 71: 384–391.

Jones, 1980. Annual cycle of shell growth increment formation in two continental shelf bivalves and its paleoecologic significance. Paleobiology 6: 331–340. doi: 10.1017/S0094837300006837

Jorgensen, 1996. Bivalve filter feeding revisited. Mar. Ecol. Prog. Ser. 142: 287–302. doi: 10.3354/meps142287

Jou et al., 2013. Synthesis and measurement of valve activities by an improved online clam–based behavioral monitoring system. Comput. Electron. Agric. 90: 106–118. doi: 10.1016/j.compag.2012.09.008

Joubert et al., 2014. Temperature and food influence shell growth and mantle gene expression of shell matrix proteins in the pearl oyster *Pinctada margaritifera*. PloS One, 9(8), p.e103944. doi: 10.1371/journal.pone.0103944

K

Kaartvedt, 2008. Photoperiod may constrain the effect of global warming in arctic marine systems J. Plankton Res. 30: 1203–1206. doi: 10.1093/plankt/fbn075

Karampelas et al., 2009: Role of polyenes in the coloration of cultured freshwater pearls, Eur. J. Mineral. 21: 85–97. doi: 10.1127/0935–1221/2009/0021–1897

Karney et al., 2011. Identification of growth increments in the shell of the bivalve mollusc *Arctica islandica* using backscattered electron imaging. J. Microsc. 241: 29–36. doi: 10.1111/j.1365–2818.2010.03403.x.

Kennish et al., 1994. In situ growth rates of the ocean quahog*, Arctica islandica* (Linnaeus, 1767) in the Middle Atlantic Bight. J. Shellfish Res. 13: 473–478.

Kilada et al., 2007. Validated age, growth, and mortality estimates of the ocean quahog (*Arctica islandica*) in the western Atlantic. ICES J. Mar. Sci. 64: 31–38. doi: 10.1093/icesjms/fsl001

Klein et al., 1996. Sr/Ca and $^{13}C/^{12}C$ ratios in skeletal calcite of *Mytilus trossulus*: Covariation with metabolic rate, salinity, and carbon isotopic composition of seawater. Geochim. Gosmochim. Acta 60: 4207–4221. doi: 10.1016/S0016–7037(96)00232–3

Klünder et al., 2008. Laser ablation analysis of bivalve shells – archives of environmental information. Geol. Surv. Denm. Greenl. Bull. 15: 89–92.

Kooijman, 2014. Metabolic acceleration in animal ontogeny: An evolutionary perspective. J. Sea Res. 94: 128–137. doi: 10.1016/j.seares.2014.06.005

Kooijman, 2010. Dynamic energy budget theory for metabolic organisation. Cambridge university press. doi: 10.1017/CBO9780511805400

Kraus et al., 1992. A comparison of growth rates in *Arctica islandica* (Linnaeus, 1767) between field and laboratory populations. J. Shellfish Res. 11: 289–294

L

Langton and McKay, 1976. Growth of *Crassostrea gigas* (Thunberg) spat under different feeding regimes in a hatchery. Aquaculture 7: 225–233. doi: 10.1016/0044–8486(76)90141–1

Langton et al., 1977. The effect of ration size on the growth and growth efficiency of the bivalve mollusc *Tapes japonica*. Aquaculture 12: 283–292. doi: 10.1016/0044–8486(77)90207–1

Lika and Kooijman, 2003. Life history implications of allocation to growth versus reproduction in Dynamic Energy Budgets. Bull. Math. Biol. 5: 809–834. doi: 10.1016/S0092–8240(03)00039–9

Lika et al., 2011. The "covariation method" for estimating the parameters of the standard Dynamic Energy Budget model I: philosophy and approach. J. Sea Res. 66: 270–277. doi: 10.1016/j.seares.2011.07.010

Lika et al., 2018. Body size as emergent property of metabolism. J. Sea Res. doi: 10.1016/j.seares.2018.04.005

Linard et al., 2011. Calcein staining of calcified structures in pearl oyster *Pinctada margaritifera* and the effect of food resource level on shell growth. Aquaculture 313: 149–155. doi: 10.1016/j.aquaculture.2011.01.008

Lohmann and Schöne, 2013. Climate signatures on decadal to interdecadal time scales as obtained from mollusk shells (*Arctica islandica*) from Iceland. Palaeogeogr. Palaeoclimatol. Palaeoecol. 373: 152–162. doi: 10.1016/j.palaeo.2012.08.006

Lorens and Bender, 1980. The impact of solution chemistry on *Mytilus edulis* calcite and aragonite. Geochim. Gosmochim. Acta. 44: 1265–1278. doi: 10.1016/0016–7037(80)90087–3

Lorrain et al., 2005. Strong kinetic effects on Sr/Ca rations in the calcitic bivalve *Pecten maximus*. Geology 33: 965–968. doi: 10.1130/G22048.1

Lowenstam, 1954. Factors affecting the aragonite: calcite ratios in carbonate–secreting marine organisms. J. Geol. 62: 284–322.

Lowenstam and Weiner, 1989. On biomineralization, Oxford University Press, New York. pp.324.

Lutz, 1984. Paleoecological implications of environmentally controlled variation in molluscan shell microstructure, Geobios 17: 93–99. doi: 10.1016/S0016–6995(84)80161–8

Lutz et al., 1983. Growth of experimentally cultured ocean quahogs (*Arctica islandica* L.) in north temperate embayments. J. World Aquacult. Soc. 14: 185–190. doi: 10.1111/j.1749–7345.1983.tb00074.x

Lutz et al., 1982. Larval and early post–larval development of *Arctica islandica*. J. Mar. Biol. Assoc. U. K. 62: 745–769. doi: 10.1017/S0025315400070314

M

Maire et al., 2007. Relationship between filtration activity and food availability in the Mediterranean mussel *Mytilus galloprovincialis*. Mar. Biol. 152: 1293–1307. doi: 10.1007/s00227–007–0778–x

Mann, 1982. The seasonal cycle of gonadal development in *Arctica islandica* from the southern New England shelf. Fish. Bull. 80: 315–26.

Marali and Schöne, 2015. Oceanographic control on shell growth of *Arctica islandica* (Bivalvia) in surface waters of Northeast Iceland—Implications for paleoclimate reconstructions. Palaeogeogr. Palaeoclimatol. Palaeoecol. 420: 138–149. doi: 10.1016/j.palaeo.2014.12.016

Marali et al., 2017a. Reproducibility of trace element time–series (Na/Ca, Mg/Ca, Mn/Ca, Sr/Ca, and Ba/Ca) within and between specimens of the bivalve *Arctica islandica*–A LA–ICP–MS line scan study. Palaeogeogr. Palaeoclimatol. Palaeoecol. 484: 109–128. doi: 10.1016/j.palaeo.2016.11.024

Marali et al., 2017b. Ba/Ca ratios in shells of *Arctica islandica*—Potential environmental proxy and crossdating tool. Palaeogeogr. Palaeoclimatol. Palaeoecol. 465: 347–361. doi: 10.1016/j.palaeo.2015.12.018

Marchitto et al., 2000. Precise temporal correlation of Holocene mollusk shells using sclerochronology. Quatern. Res. 53:236–246. doi: 10.1006/qres.1999.2107

Markich, 2003. Influence of body size and gender on valve movement responses of a freshwater bivalve to uranium. Environ. Toxicol. 18: 126–136. doi: 10.1002/tox.10109

Marques et al., 2018a. The AmP project: Comparing Species on the Basis of Dynamic Energy Budget Parameters. doi: 10.1371/journal.pcbi.1006100.

Marques et al., 2018b. Fitting Multiple Models to Multiple Data Sets. J. Sea Res. doi: 10.1016/j.seares.2018.07.004

Massabuau et al., 2015. Environmental monitoring of Arctic waters with unmanned bivalve biosensor technology: one year of background data acquisition in the Barents Sea. Paper presented at the InSPE Russian Petroleum Technology Conference, Moscow, Russia, 26–28 October. doi: 10.2118/176681–MS

Mat et al., 2012. Evidence for a plastic dual circadian rhythm in the oyster *Crassostrea gigas*. Chronobiol. Int. 29: 857–867. doi: 10.3109/07420528.2012.699126

Merkel et al., 2007. Micromechanical properties and structural characterization of modern inarticulated brachiopod shells. J. Geophys. Res. 112(G02008). doi: 10.1029/2006JG000253

Mette et al., 2016. Linking large–scale climate variability with *Arctica islandica* shell growth and geochemistry in northern Norway. Limnol Oceanogr 61: 748–764. doi: 10.1002/lno.10252

Milano et al., 2017a. The effects of environment on *Arctica islandica* shell formation and architecture. Biogeosciences 14: 1577–1591. doi: 10.5194/bg–14–1577–2017

Milano et al., 2017b. Changes of shell microstructural characteristics of *Cerastoderma edule* (Bivalvia) – A novel proxy for water temperature. Palaeogeogr. Palaeoclimatol. Palaeoecol. 465: 395–406. doi: 10.1016/j.palaeo.2015.09.051

Milano et al., 2016a. Effects of cooking on mollusk shell structure and chemistry: Implications for archeology and paleoenvironmental reconstruction. J. Archaeol. Sci. Reports 7: 14–26. doi: 10.1016/j.jasrep.2016.03.045

Milano et al., 2016b. Impact of high pCO_2 on shell structure of the bivalve *Cerastoderma edule*, Mar. Environ. Res. 119: 144–155. doi: 10.1016/j.marenvres.2016.06.002

Møhlenberg and Riisgård, 1979. Filtration rate, using a new indirect technique, in thirteen species of suspension–feeding bivalves. Mar. Biol. 54: 143–147. doi: 10.1007/BF00386593

Mook, 1971. Paleotemperatures and chlorinities from stable carbon and oxygen isotopes in shell carbonate. Palaeogeogr. Palaeoclimatol. Palaeoecol. 9: 245–263, doi: 10.1016/0031–0182(71)90002–2

Morton, 2011. The biology and functional morphology of *Arctica islandica* (Bivalvia: Arcticidae) – A gerontophilic living fossil. Mar. Biol. Res. 7: 540–553. doi: 10.1080/17451000.2010.535833

Moss et al., 2016. Lifespan, growth rate, and body size across latitude in marine Bivalvia, with implications for Phanerozoic evolution. Proc. R. Soc. London, Ser. B 283, No. 1836, p. 20161364. doi: 10.1098/rspb.2016.1364

Murawski et al., 1982. Growth of the ocean quahog, *Arctica islandica*, in the middle Atlantic Bight. Fish. Bull. 80: 21–34.

N

Nehrke and Nouet, 2011. Confocal Raman microscope mapping as a tool to describe different mineral and organic phases at high spatial resolution within marine biogenic carbonates: case study on *Nerita undata* (Gastropoda, Neritopsina). Biogeosciences 8: 3761–3769. doi: 10.5194/bg–8–3761–2011

Newell et al., 2001. The effects of velocity and seston concentration on the exhalant siphon area, valve gape and filtration rate of the mussel *Mytilus edulis*. J. Exp. Mar. Biol. Ecol. 261: 91–111. doi: 10.1016/S0022–0981(01)00285–4

Nishida et al., 2015. Thermal dependency of shell growth, microstructure, and stable isotopes in laboratory–reared *Scapharca broughtonii* (Mollusca: Bivalvia). Geochem. Geophys. Geosystems 16: 2395–2408. doi: 10.1002/2014GC005684

Nishida et al., 2012. Seasonal changes in the shell microstructure of the bloody clam, *Scapharca broughtonii* (Mollusca: Bivalvia: Arcidae). Palaeogeogr. Palaeoclimatol. Palaeoecol. 363: 99–108. doi: 10.1016/j.palaeo.2012.08.017

Nudelman et al., 2006. Mollusk shell formation: mapping the distribution of organic matrix components underlying a single aragonitic tablet in nacre. J. Struct. Biol. 153: 176–187. doi: 10.1016/j.jsb.2005.09.009

Nürnberg et al., 1996. Assessing the reliability of magnesium in foraminiferal calcite as a proxy for water mass temperatures. Geochim. Gosmochim. Acta 60: 803–814. doi: 10.1016/0016–7037(95)00446–7

Oertzen, 1972. Cycles and rates of reproduction of six Baltic Sea bivalves of different zoogeographical origin. Mar. Biol. 14: 143–149. doi: 10.1007/BF00373213

O'Neil and Gillikin, 2014. Do freshwater mussel shells record road–salt pollution? Sci. Rep. 4: 7168. doi: 10.1038/srep07168

P

Peharda et al., 2016. The bivalve *Glycymeris pilosa* as a multidecadal environmental archive for the Adriatic and Mediterranean Seas. Mar. Environ. Res. 119: 79–87. doi 10.1016/j.marenvres.2016.05.022

Pérez–Huerta et al., 2013 El Niño impact on mollusk biomineralization–implications for trace element proxy reconstructions and the paleo–archeological record. PLoS One, 8(2), e54274, doi: 10.1371/journal.pone.0054274

Pérez–Huerta et al., 2011. High resolution electron backscatter diffraction (EBSD) data from calcite biominerals in recent gastropod shells. Micron. 42: 246–51, doi: 10.1016/j.micron.2010.11.003

Philipp and Abele, 2010. Masters of longevity: lessons from long–lived bivalves–a mini–review. Gerontology 56: 55–65.

Philipp et al., 2005. Chronological and physiological ageing in a polar and a temperate mud clam. Mechanisms of ageing and Development, 126: 598–609.

Poulain et al., 2015. An evaluation of Mg/Ca, Sr/Ca, and Ba/Ca ratios as environmental proxies in aragonite bivalve shells. Chem. Geol. 396: 42–50. doi: 10.1016/j.chemgeo.2014.12.019

Prezant and Tan Tiu, 1986. Spiral crossed–lamellar shell growth in *Corbicula* (Mollusca: Bivalvia), Trans. Am. Microsc. Soc. 105: 338–347.

Purroy at al., 2017. Combined use of morphological and molecular tools to resolve species mis–identifications in the Bivalvia the case of *Glycymeris glycymeris* and *G. pilosa*. PloS One 11(9): p.e0162059.

Purroy et al., 2018. Drivers of shell growth of the bivalve, *Callista chione* (L. 1758)–Combined environmental and biological factors. Mar. Environ. Res. 134: 138–149. doi: 10.1016/j.marenvres.2018.01.011

Purton et al., 1999. Metabolism controls Sr/Ca ratios in fossil aragonitic mollusks. Geology 27: 1083–1086. doi: 10.1130/0091–7613(1999)027%3C1083:MCSCRI%3E2.3.CO;2

Pyrina et al., 2017. Pseudo–proxy evaluation of climate field reconstruction methods of North Atlantic climate based on an annually resolved marine proxy network. Clim. Past. 13(10): p.1339. doi: 10.5194/cp-13-1339-2017

R

Richardson, 2001. Molluscs as archives of environmental change. Oceanogr. Mar. Biol. an Annu. Rev. 39: 103–164.

Riisgård, 1991. Filtration rate and growth in the blue mussel, *Mytilus edulis* Linneaus, 1758: Dependence on algal concentration. J. Shellfish Res. 10.

Riisgård and Larsen, 2015. Physiologically regulated valve–closure makes mussels long–term starvation survivors: test of hypothesis. J. Molluscan Stud. 81: 303–307 doi: 10.1093/mollus/eyu087

Riisgård et al., 2006. Valve–gape response times in mussels (*Mytilus Edulis*)–Effects of laboratory preceding–feeding conditions and *in situ* tidally induced variation in phytoplankton biomass. J. Shellfish Res. 25: 901–911. doi: 10.2983/0730–8000(2006)25[901:vrtimm]2.0.co;2

Riisgård et al., 2003. Regulation of opening state and filtration rate in filter–feeding bivalves (*Cardium edule, Mytilus edulis, Mya arenaria*) in response to low algal concentration. J. Exp. Mar. Biol. Ecol. 284:105–127. doi: 10.1016/S0022–0981(02)00496–3

Rodland et al., 2006. A clockwork mollusc: Ultradian rhythms in bivalve activity revealed by digital photography. J. Exp. Mar. Biol. Ecol. 334: 316–323. doi: 10.1016/j.jembe.2006.02.012

Rodríguez–Navarro et al., 2006. Microstructure and crystallographic–texture of giant barnacle (*Austromegabalanus psittacus*) shell. J. Struct. Biol. 156: 355–362. doi: 10.1016/j.jsb.2006.04.009

Ropes, 1985. Modern methods used to age oceanic bivalves. The Nautilus 99: 53–57.

Ropes, 1984. Procedures for preparing acetate peels and evidence validating the annual periodicity of growth lines formed in the shells of ocean quahogs, *Arctica islandica*. Mar. Fish. Rev. 46: 27–35.

Ropes et al., 1984. Documentation of annual growth lines in ocean quahogs, *Artica islandica* Linne. Fish. Bull. 82: 1–19.

Rosenheim et al., 2004. High resolution Sr/Ca records in sclerosponges calibrated to temperature in situ. Geology 32: 145–148. doi: 10.1130/G20117.1

Rubenstein and Koehl, 1977. The mechanisms of filter feeding: some theoretical considerations. Am. Nat., 111, 981–994. doi: 10.1086/283227

Rucker and Valentine, 1961. Salinity response of trace element concentration in *Crassostrea virginica*. Nature 190: 1099. doi: 10.1038/1901099a0

S

Sager and Sammler, 1983. Mathematical investigations into the longevity of the ocean quahog *Arctica islandica* (Mollusca: Bivalvia). Int. Rev. Hydrobiol. 68: 113–120.

Saraiva et al., 2012. Validation of a Dynamic Energy Budget (DEB) model for the blue mussel *Mytilus edulis*. Mar. Ecol. Prog. Ser. 463: 141–158. doi: 10.3354/meps09801

Schaffer et al., 1991. Conjugation length dependence of Raman scattering in a series of linear polyenes: Implications for polyacetylene. J. Chem. Phys. 94: 4161. doi: 10.1063/1.460649

Schöne, 2013. *Arctica islandica* (Bivalvia): a unique paleoenvironmental archive of the northern North Atlantic Ocean, Glob. Planet. Change. 111: 199–225. doi: 10.1016/j.gloplacha.2013.09.013

Schöne, 2008. The curse of physiology—challenges and opportunities in the interpretation of geochemical data from mollusk shells, Geo–Marine Lett. 28: 269–285. doi: 10.1007/s00367–008–0114–6

Schöne and Gillikin, 2013. Unraveling environmental histories from skeletal diaries—advances in sclerochronology. Palaeogeogr., Palaeoclimatol., Palaeoecol. 373: 1–5. doi: 10.1016/j.palaeo.2012.11.026

Schöne and Surge, 2012. Treatise Online no. 46: Part N, Revised, Volume 1, Chapter 14: Bivalve sclerochronology and geochemistry. Treatise online. doi: 10.17161/to.v0i0.4297

Schöne et al., 2013. Crystal fabrics and element impurities (Sr/Ca, Mg/Ca, and Ba/Ca) in shells of *Arctica islandica*—Implications for paleoclimate reconstructions. Palaeogeogr. Palaeoclimatol. Palaeoecol. 373: 50–59. doi: 10.1016/j.palaeo.2011.05.013

Schöne et al., 2011. Sr/Ca and Mg/Ca ratios of ontogenetically old, long–lived bivalve shells (*Arctica islandica*) and their function as paleotemperature proxies. Palaeogeogr. Palaeoclimatol. Palaeoecol. 302: 52–64. doi: 10.1016/j.palaeo.2010.03.016

Schöne et al., 2010. Effect of organic matrices on the determination of the trace element chemistry (Mg, Sr, Mg/Ca, Sr/Ca) of aragonitic bivalve shells (*Arctica islandica*)—Comparison of ICP–OES and LA–ICP–MS data. Geochem. J. 44: 23–37. doi: 10.2343/geochemj.1.0045

Schöne et al. (2005a) Daily growth rates in shells of *Arctica islandica*: Assessing sub–seasonal environmental controls on a long–lived bivalve mollusk. Palaios 20: 78–92. doi: 10.2110/palo.2003.p03–101

Schöne et al. (2005b) Climate records from a bivalved Methuselah (*Arctica islandica*, Mollusca; Iceland). Palaeogeogr. Palaeoclimatol. Palaeoecol. 228: 130–148. doi: 10.1016/j.palaeo.2005.03.049

Schöne et al., 2004. Sea surface water temperatures over the period 1884–1983 reconstructed from oxygen isotope ratios of a bivalve mollusk shell (*Arctica islandica*, southern North Sea). Palaeogeogr. Palaeoclimatol. Palaeoecol. 212: 215–232. doi: 10.1016/j.palaeo.2004.05.024

Schöne et al., 2003. North Atlantic Oscillation dynamics recorded in shells of a long–lived bivalve mollusk. Geology 31: 1037–1040. doi: 10.1130/g20013.1

Schwartzmann et al., 2011. In situ giant clam growth rate behavior in relation to temperature: a one–year coupled study of high–frequency noninvasive valvometry and sclerochronology. Limnol Oceanogr 56: 1940– 1951. doi: 10.4319/lo.2011.56.5.1940

Seilacher, 1972. Divaricate patterns in pelecypod shells. Lethaia, 5: 325–343. doi: 10.1111/j.1502–3931.1972.tb00862.x

Sinclair, 2005. Toward a unified theory of caloric restriction and longevity regulation. Mech. Ageing Dev. 126: 987–1002. doi: 10.1016/j.mad.2005.03.019

Skogen and Moll, 2000. Importance of ocean circulation in ecological modeling: An example from the North Sea. J. Mar. Syst. 57: 289–300. doi: 10.1016/j.jmarsys.2005.06.002

Skogen et al., 2007. Interannual variability in Nordic seas primary production. ICES J. Mar. Sci. 64: 889–898. doi: 10.1093/icesjms/fsm063

Soldatov et al., 2013. Qualitative composition of carotenoids, catalase and superoxide dismutase activities in tissues of bivalve mollusc *Anadara inaequivalvis* (Bruguiere, 1789), J. Evol. Biochem. Phys. 49: 3889–398. doi: 10.1134/S0022093013040026

Sousa et al., 2008. From empirical patterns to theory: A formal metabolic theory of life. Phil. Trans. R. Soc. B 363: 2453–2464. doi: 10.1098/rstb.2007.2230

Stecher et al., 1996. Profiles of strontium and barium in *Mercenaria mercenaria* and *Spisula solidissima* shells. Geochim. Gosmochim. Acta 60: 3445–3456. doi: 10.1016/0016–7037(96)00179–2

Steingrund and Gaard, 2005. Relationship between phytoplankton production and cod production on the Faroe Shelf. ICES J. Mar. Sci. 62: 163–176. doi: 10.1016/j.icesjms.2004.08.019

Steinhardt et al., 2016. The application of long–lived bivalve sclerochronology in environmental baseline monitoring. Front. Mar. Sci. 3: 176. doi: 10.3389/fmars.2016.00176

Stemmer and Nehrke, 2014. The distribution of polyenes in the shell of *Arctica islandica* from North Atlantic localities: a confocal Raman microscopy study. J. Molluscan Stud. 80: 365–370. doi: 10.1093/mollus/eyu033

Stemmer et al., 2013. Elevated CO(2) levels do not affect the shell structure of the bivalve *Arctica islandica* from the Western Baltic. PLoS One 8:e70106. doi: 10.1371/journal.pone.0070106

Stott et al., 2010. The potential of *Arctica islandica* growth records to reconstruct coastal climate in north west Scotland, UK. Quat. Sci. Rev. 29: 1602–1613. doi: 10.1016/j.quascirev.2009.06.016

Strahl, 2011. Life strategies in the long–lived bivalve *Arctica islandica* on a latitudinal climate gradient–Environmental constraints and evolutionary adaptations. Doctoral dissertation. University of Bremen

Strahl and Abele, 2010. Cell turnover in tissues of the long–lived ocean quahog *Arctica islandica* and the short–lived scallop *Aequipecten opercularis*. Mar. Biol. 157 : 1283–1292. doi : 10.1007/s00227-010-1408-6

Strahl et al., 2011. Physiological responses to self–induced burrowing and metabolic rate depression in the ocean quahog *Arctica islandica*. J Exp. Biol. 214: 4223–4233. doi: 10.1242/jeb.055178

Strahl et al., 2007. Physiological aging in the Icelandic population of the ocean quahog *Arctica islandica*. Aquat. Biol. 1: 77–83. doi: 10.3354/ab00008

Strasser et al., 2008. Temperature and salinity effects on elemental uptake in the shells of larval and juvenile softshell clams *Mya arenaria*. Mar. Ecol. Prog. Ser. 370: 155–169. doi: 10.3354/meps07658

Strömgren and Cary, 1984. Growth in length of *Mytilus edulis* L. fed on different algal diets. J. Exp. Mar. Bio. Ecol. 76: 23–34. doi: 10.1016/0022–0981(84)90014–5

Surge and Walker, 2006. Geochemical variation in microstructural shell layers of the southern quahog (*Mercenaria campechiensis)*: Implications for reconstructing seasonality. Palaeogeogr. Palaeoclimatol. Palaeoecol. 237: 182–190. doi: /10.1016/j.palaeo.2005.11.016

T

Tan Tiu, 1988. Temporal and spatial variation of shell microstructure of *Polymesoda caroliniana* (Bivalvia: Heterodonta). Am. Malacol. Bull. 6: 199–206.

Tan Tiu and Prezant, 1989. Temporal variation in microstructure of the inner shell surface of *Corbicula fluminea* (Bivalvia: Heterodonta). Am. Malacol. Bull. 7: 65–71.

Tan Tiu and Prezant, 1987. Shell microstructural responses of *Geukensia demissa granosissima* (Mollusca: Bivalvia) to continual submergence. Am. Malacol. Bull. 5: 173–176.

Tang and Riisgård, 2016. Physiological regulation of valve–opening degree enables mussels *Mytilus edulis* to overcome starvation periods by reducing the oxygen uptake. Open J. Mar. Sci. 6:341–352. doi: 10.4236/ojms.2016.63029

Taylor, 1976. Burrowing behaviour and anaerobiosis in the bivalve *Arctica islandica* (L.). J. Mar. Biol. Assoc. UK 56: 95–109. doi: 10.1017/S0025315400020464

Taylor and Kennedy, 1969. The shell structure and mineralogy of *Chama pellucida* Broderip. Veliger 11: 391–398.

Thébault et al., 2009. Barium and molybdenum records in bivalve shells: Geochemical proxies for phytoplankton dynamics in coastal environments? Limnol. Oceanogr. 54: 1002–1014. doi: 10.4319/lo.2009.54.3.1002

Thompson et al., 1980a. Annual internal growth banding and life history of the ocean quahog *Arctica islandica* (Mollusca: Bivalvia). Mar. Biol. 57: 25–34. doi: 10.1007/BF00420964

Thompson et al., 1980b. Advanced age for sexual maturity in the ocean quahog *Arctica islandica* (Mollusca: Bivalvia). Mar Biol. 57: 35–39. doi: 10.1007/BF00420965

Thomsen et al., 2013. Food availability outweighs ocean acidification effects in juvenile *Mytilus edulis*: laboratory and field experiments. Global Change Biol. 19: 1017–1027. doi: 10.1111/gcb.12109

Thorarinsdottir, 2000. Annual gametogenic cycle in ocean quahog, *Arctica islandica* from north–western Iceland. J. Mar. Biol. Assoc. UK 80: 661–666.

Thórarinsdóttir and Einarsson, 1996. Distribution, abundance, population structure and meat yield of the ocean quahog, *Arctica islandica*, in Icelandic waters. J. Mar. Biol. Assoc. UK 76: 1107–1114. doi: 10.1017/S0025315400040996

Thorarinsdottir and Steingrimsson, 2000. Size and age at sexual maturity and sex ratio in ocean quahog, *Arctica islandica* (Linnaneus, 1767), off Northwest Iceland. J. Shellfish Res. 19: 943–947.

Thorin, 2000. Seasonal variations in siphonal activity of *Mya arenaria* (Mollusca) J. Mar. Biol. Assoc. UK 80: 1135–1136. doi: 10.1017/S0025315400003258

Toland et al., 2000. A study of sclerochronology by laser ablation ICP–MS. J. Anal., At. Spectrom. 15: 1143–1148. doi: 10.1039/b002014l

Tran et al., 2011. Field chronobiology of a molluscan bivalve: how the moon and sun cycles interact to drive oyster activity rhythms. Chronobiol. Int. 28: 307–317. doi: 10.3109/07420528.2011.565897

Trofimova et al., 2018. Oxygen isotope composition of *Arctica islandica* aragonite in the context of shell architectural organization-implications for paleoclimate reconstructions. Geochem. Geophy. Geosy. 19: 453–470. doi: 10.1002/2017GC007239

U

Urey et al., 1951. Measurement of paleotemperatures and temperatures of the Upper Cretaceous of England, Denmark, and the southeastern United States. Bull. Geol. Soc. Am. 62: 399–416. doi: 10.1130/0016–7606(1951)62[399:MOPATO]2.0.CO;2

V

Van der Meer, 2006. An introduction to Dynamic Energy Budget (DEB) models with special emphasis on parameter estimation. J. Sea Res. 56: 85–102. doi: 10.1016/j.seares.2006.03.001

Van der Veer et al., 2001. Intra–and interspecies comparison of energy flow in North Atlantic flatfish species by means of dynamic energy budgets. J. Sea Res. 45: 303–320. doi: 10.1016/S1385–1101(01)00061–2

Vander Putten et al., 2000. High resolution distribution of trace elements in the calcite shell layer of modern *Mytilus edulis*: Environmental and biological controls. Geochim. Gosmochim. Acta 64: 997–1011. doi: 10.1016/S0016–7037(99)00380–4

W

Walne, 1972. The influence of current speed, body size and water temperature on the filtration rate of five species of bivalves. J. Mar. Biol. Assoc. UK 52: 345–374. doi: 10.1017/S0025315400018737

Wanamaker and Gillikin, 2018. Strontium, magnesium, and barium incorporation in aragonitic shells of juvenile *Arctica islandica*: Insights from temperature controlled experiments. Chem. Geol. doi: 10.1016/j.chemgeo.2018.02.012.

Wanamaker et al., 2016. The potential for the long– lived bivalve *Arctica islandica* to contribute to our understanding of past AMOC dynamics. US CLIVAR Var. 14: 13–19.

Wanamaker et al., 2012. Surface changes in the North Atlantic meridional overturning circulation during the last millennium. Paleoceanography 3: 237–252. doi: 10.1038/ncomms1901, 2012.

Wanamaker et al., 2011a. Reconstructing mid–to high–latitude marine climate and ocean variability using bivalves, coralline algae, and marine sediment cores from the Northern Hemisphere. Palaeogeogr. Palaeoclimatol. Palaeoecol. 302: 1–9. doi: 10.1016/j.palaeo.2010.12.024

Wanamaker et al., 2011b. Gulf of Maine shells reveal changes in seawater temperature seasonality during the Medieval Climate Anomaly and the Little Ice Age. Palaeogeogr. Palaeoclimatol. Palaeoecol. 302: 43–51. doi: 10.1016/j.palaeo.2010.06.005

Wanamaker et al., 2009. A late Holocene paleo–productivity record in the western Gulf of Maine, USA, inferred from growth histories of the long–lived ocean quahog (*Arctica islandica*). Int. J. Earth Sci. 98: 19–29. doi: 10.1007/s00531–008–0318–z

Wanamaker et al., 2008a. Coupled North Atlantic slope water forcing on Gulf of Maine temperatures over the past millennium. Clim. Dyn. 31: 183–194. doi: 10.1007/ s00382–007–0344–8.

Wanamaker et al., 2008b. Very long–lived mollusks confirm 17th century ad tephra–based radiocarbon reservoir ages for North Icelandic shelf waters. Radiocarbon 50: 399–412. doi: 10.1017/S0033822200053510

Wanamaker et al., 2008c. Experimentally determined Mg/Ca and Sr/Ca ratios in juvenile bivalve calcite for *Mytilus edulis*: implications for paleotemperature reconstructions. Geo–Mar. Lett. 28: 359–368. doi: 10.1007/s00367–008–0112–8

Wanamaker et al., 2007. Experimental determination of salinity, temperature, growth, and metabolic effects on shell isotope chemistry of *Mytilus edulis* collected from Maine and Greenland, Paleoceanography, 22(2). doi: 10.1029/2006PA001352

Warton and Hui, 2011. The arcsine is asinine: the analysis of proportions in ecology. Ecology 92: 3–10. doi: 10.1890/10–0340.1

Weidman et al., 1994. The long–lived mollusc *Arctica islandica*: a new paleoceanographic tool for the reconstruction of bottom temperatures for the continental shelves of the northern North Atlantic Ocean. J. Geophys. Res. (C Oceans) 99: 18305–18314. doi: 10.1029/94jc01882

Weinberg et al., 2002. Influence of rising sea temperature on commercial bivalve species of the US Atlantic coast. In American Fisheries Society Symposium (pp. 131–140). Am. Fish. Soc.

Weiner and Addadi, 1991. Acidic macromolecules of mineralized tissues: the controllers of crystal formation, Trends Biochem. Sci. 16: 252–256. doi: 10.1039/a604512j

Widdows, 1991. Physiological ecology of mussel larvae. Aquaculture 94: 147–163. doi: 10.1016/0044–8486(91)90115–N

Williams and Pilditch, 1997. The entrainment of persistent tidal rhythmicity in a filter–feeding bivalve using cycles of food availability. J. Biol. Rhythms 12: 173–181. doi: 10.1177/074873049701200208

Winter, 1978. A review on the knowledge of suspension–feeding in lamellibranchiate bivalves, with special reference to artificial aquaculture systems. Aquaculture 13: 1–33. doi: 10.1016/0044–8486(78)90124–2

Winter, 1969. Uber den einflub der nahrungskonzentration und anderer faktoren auf filtrierleistung und nahrungsausnutzung der Muscheln *Arctica islandica* und *Modiolus modiolus*. Mar. Biol. 4: 87–137.

Winter and Langton, 1976. Feeding experiments with *Mytilus edulis* L. at small laboratory scale: 1. The influence of the total amount of food ingested and food concentration on growth. In: Persoone, G. et al. (Ed.) Proceedings of the 10th European Symposium on Marine Biology, Ostend, Belgium, Sept. 17–23, 1975: 1. Research in mariculture at laboratory– and pilot scale. pp. 565–581

Winter, 1969. Über den Einfluß der Nahrungskonzentration und anderer Faktoren auf Filtrierleistung und Nahrungsausnutzung der Muscheln *Arctica islan*dica und *Modiolus modiolus*. Mar. Biol. 4: 87–135, doi: 10.1007/BF00347037

Witbaard, 1997. Tree of the sea: The use of the internal growth lines in the shell of *Arctica islandica* (Bivalvia, Mollusca) for the retrospective assessment of marine environmental change (Doctoral dissertation, University of Groningen).

Witbaard and Hippler, 2009. Seasonal timing of shell and tissue growth in *Arctica islandica*. Paper presented at the Bivalve biomineralisation: archival potential and proxy incorporation, Brussels, Belgium, 4–5 May 2009.

Witbaard and Duineveld, 1990. Shell–growth of the bivalve *Arctica islandica* (L.), and its possible use for evaluating the status of the benthos in the subtidal North Sea. Basteria, 54(1/3): 63–74.

Witbaard et al., 2003. Copepods link quahog growth to climate. J. Sea Res. 50: 77–83. doi: 10.1016/ S1385–1101(03)00040–6

Witbaard et al., 1999. Geographical differences in growth rates of *Arctica islandica* (Mollusca: Bivalvia) from the North Sea and adjacent waters. J. Mar. Biol. Assoc. UK 79: 907–915. doi: 10.1017/S0025315498001076

Witbaard et al., 1997a. Growth of juvenile *Arctica islandica* under experimental conditions. Helgolaender Meeresun 51: 417–432. doi: 10.1007/BF02908724

Witbaard et al., 1997b. A long–term growth record derived from *Arctica islandica* (Mollusca, Bivalvia) from the Fladen Ground (northern North Sea). J. Mar. Biol. Assoc. UK 77: 801–816. doi: 10.1017/S0025315400036201

Witbaard et al., 1996. Growth variations in *Arctica islandica* L. (Mollusca): a reflection of hydrography–related food supply. ICES J. Mar. Sci. 53: 981–987. doi: 10.1006/jmsc.1996.0122

Witbaard et al., 1994. Verification of annual growth increments in *Arctica islandica* L. from the North Sea by means of oxygen and carbon isotopes. Neth. J. Sea Res. 33: 91–101. doi: 10.1016/0077–7579(94)90054–X

Z

Zettler et al., 2001. Distribution, abundance, and some population characteristics of the ocean quahog, *Arctica islandica* (Linnaeus, 1767), in the Meeklenburg Bight (Baltic Sea). J. Shellfish Res. 20: 161–170.

Zhao et al., 2017a. Insights from sodium into the impacts of elevated pCO2 and temperature on bivalve shell formation. J. Exp. Mar. Biol. Ecol. 486: 148–154. doi: 10.1016/j.jembe.2016.10.009

Zhao et al., 2017b. Controls on strontium and barium incorporation into freshwater bivalve shells (*Corbicula fluminea*). Palaeogeogr. Palaeoclimatol. Palaeoecol. 465: 386–394. doi: 10.1016/j.palaeo.2015.11.040

Zhao et al., 2017c. Delineating the role of calcium in shell formation and elemental composition of *Corbicula fluminea* (Bivalvia). Hydrobiologia 790: 259–272. doi: 10.1007/s10750–016–3037–7

Lists of publicacions

Peer reviewed publications:

Ballesta-Artero, I., Witbaard, R., Carroll, M.L. and van der Meer, J., 2017. Environmental factors regulating gaping activity of the bivalve *Arctica islandica* in Northern Norway. *Marine biology*, *164*(5), p.116. doi: 10.1007/s00227–017–3144–7

Milano, S., Nehrke, G., Wanamaker Jr, A.D., **Ballesta-Artero, I.**, Brey, T. and Schöne, B.R., 2017. The effects of environment on *Arctica islandica* shell formation and architecture. *Biogeosciences*, *14*, p.1577. doi: 10.5194/bg–14–1577–2017

Ballesta-Artero, I., Janssen, R., van der Meer, J. and Witbaard, R., 2018a. Interactive effects of temperature and food availability on the growth of *Arctica islandica* (Bivalvia) juveniles. *Marine environmental research*, *133*, pp.67-77. doi: 10.1016/j.marenvres.2017.12.004

Ballesta-Artero, I., Zhao, L., Milano, S., Mertz-Kraus, R., Schöne, B.R., van der Meer, J. and Witbaard, R., 2018b. Environmental and biological factors influencing trace elemental and microstructural properties of *Arctica islandica* shells. Science of The Total Environment, 645, pp.913-923. doi: 10.1016/j.scitotenv.2018.07.116

Submitted manuscript:

Ballesta-Artero, I., Agustine , S., Witbaard, R., Carroll, M. L., Mette M. J. , Wanamaker A. D., van der Meer, J. 2018. Energetics of the extremely long-living bivalve *Arctica islandica* based on a Dynamic Energy Budget model. Journal of Sea Research.

Manuscripts in preparation:

Ballesta-Artero, I., Mette M. J. , Wanamaker A. D., Carroll, M. L., van der Meer, J., and Witbaard, R. Combining biological and geochemical techniques to study the growing season of the bivalve *Arctica islandica.*

Ballesta-Artero, I., Carroll, M.L., van der Meer, J., and Witbaard, R. Reproductive investment of the bivalve *Arctica islandica* in Northern Norway.

Authors affiliations

1. Augustine, Starrlight:
   Akvaplan-niva, FRAM - High North Centre for Climate and the Environment, 9296 Tromsø, Norway.

2. Carroll, Michael L.:
   Akvaplan-niva, FRAM - High North Centre for Climate and the Environment, 9296 Tromsø, Norway.

3. Janssen, Reneé:
   Helicon MBO Den Bosch, Postbus 2279 5202 CG ’s-Hertogenbosch, The Netherlands.

4. Mette, Madelyn J.:
- Department of Geological and Atmospheric Sciences, Iowa State University, Ames, 50011 Iowa, USA.
- Uni Research Climate, 5008 Bergen, Norway (Present address).

5. Mertz-Kraus, Regina:
   Institute of Geosciences, University of Mainz, Joh.-J.-Becher-Weg 21, 55128 Mainz, Germany.

6. Milano, Stefania:
- Institute of Geosciences, University of Mainz, Joh.-J.-Becher-Weg 21, 55128 Mainz, Germany
- Department of Human Evolution, Max Planck Institute for Evolutionary Anthropology, Leipzig, Germany (Present address).
-

7. Nehrke, Gernot:
   Alfred Wegener Institute for Polar and Marine Research, Am Handelshafen 12, 27570 Bremerhaven, Germany.

8. Brey, Thomas:

   Alfred Wegener Institute for Polar and Marine Research, Am Handelshafen 12, 27570 Bremerhaven, Germany.

9. Schöne, Bernd R.:

   Institute of Geosciences, University of Mainz, Joh.-J.-Becher-Weg 21, 55128 Mainz, Germany.

10. van der Meer, Jaap:

- NIOZ; Netherlands Institute for Sea Research and Utrecht University, Department of Coastal Systems, PO Box 59, 1790 AB Den Burg, Texel, The Netherlands.
- Department of Animal Ecology, VU University Amsterdam, The Netherlands.

11. Witbaard, Rob:

    NIOZ; Netherlands Institute for Sea Research and Utrecht University, Department of Estuarine and Delta Systems, PO Box 140, 4400 AC Yerseke, The Netherlands.

12. Wanamaker Jr., Alan D.:

    Department of Geological and Atmospheric Sciences, Iowa State University, Ames, 50011 Iowa, USA.

13. Zhao, Liqiang:

- Institute of Geosciences, University of Mainz, Joh.-J.-Becher-Weg 21, 55128 Mainz, Germany.
- Department of Atmosphere and Ocean Research Institute, University of Tokio, Japan (Present address).

Acknowledgements

Thank you to all the people that supported me these four years of my life.

Particularly, I would like to thank:

Rob Witbaard and Jaap van der Meer for guiding me all this way. I was very lucky to have your support.

Michael Carroll for acting more as one of my PhD supervisors.

Thorleif Hansen and Ann Hansen for making my research possible and at the same time making me feel at home.

All the great people that helped me during fieldwork (Dmitri Barjitsi, Odd Fjelde, Erlend Hesten, Al Wanamaker, Maddie Mette, Aubrey Foulk, Mike Retelle, Will Ambrose, Julie Retelle, Dan Frost, Randall Hyman) as well as during the analysis and writing periods of this PhD thesis (especially to Susanne van Donk, Starrlight Augustine, and Ghadeer Shubassi).

All ARAMACC members for sharing with me the ups and downs of this intense period of my life.

NIOZ and principally to all members of the MEE/COS department.

All the good friends made on Texel that made our life much easier, even during the darkest days of Texel winters: Marta, Ramón, Anuar, Jorge, Santi, Johan, Andreas, Tristan, Maram, Yvonne, Martina, Gio, Jan Bakker, Wilma, Bas, Levina, Susanne, Emma, Kiki, Ginny, Eva, Roeland, Eelke, Julia, Eldar, Jan van Gils, Jaime, Clara, Zeynep, Michelle, Alejandro, Diana, and many others who we shared great moments with.

My family for encouraging me all these years.

Andrés, this degree would have been impossible without you.


Hyman
Hyman
ARAMACC